

**APPLICATION OF PHOTOCHEMICAL AND BIOLOGICAL
APPROACHES FOR COST-EFFECTIVE ALGAL BIOFUEL
PRODUCTION**

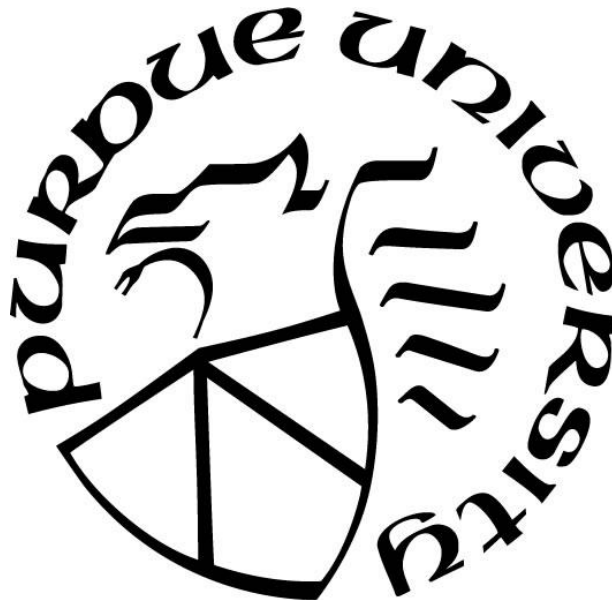
by
Zhe Sun

A Dissertation

Submitted to the Faculty of Purdue University

In Partial Fulfillment of the Requirements for the degree of

Doctor of Philosophy



Lyles School of Civil Engineering

West Lafayette, Indiana

May 2019

**THE PURDUE UNIVERSITY GRADUATE SCHOOL
STATEMENT OF COMMITTEE APPROVAL**

Dr. Zhi Zhou, Chair

Lyles School of Civil Engineering

Division of Environmental and Ecological Engineering

Dr. Ernest R. Blatchley III

Lyles School of Civil Engineering

Division of Environmental and Ecological Engineering

Dr. Loring F. Nies

Lyles School of Civil Engineering

Division of Environmental and Ecological Engineering

Dr. Jiqin Ni

Agricultural and Biological Engineering Department

Approved by:

Dr. Dulcy M. Abraham

Head of the Graduate Program

Dedicated to My Family

ACKNOWLEDGMENTS

First of all, I would like to thank my committee chair, Dr. Zhi Zhou, for his continuous support and motivation throughout my Ph.D. study and research. I would also like to thank Dr. Ernest R. Blatchley III, for his outstanding scientific guidance, constructive criticism and stimulated enlightenment in the past five years. I greatly appreciate countless conversation and discussion with Dr. Blatchley, which carried me through difficult times, in both my study and life. I am also grateful to Dr. Loring F. Nies and Dr. Jiqin Ni for serving in my Ph.D. committee as well as for their insightful inputs and suggestions on my research projects. This dissertation would not have been possible without valuable feedback from all my committee members.

Many thanks to the faculty and staff members of the Lyles School of Civil Engineering at Purdue University for their support and assistance. I would like to thank also the following organizations for financially supporting my graduate study and research: NSF International, US EPA, United States Geological Survey and Purdue Research Foundation Fellowship. Special thanks are given to Dr. Karl V. Wood, director of Mass Spectrometry Center at Purdue, for his wise suggestions on GC-MS analysis. I also thank my graduate student fellows and friends: Mian Wang, Xiangyu Li, Xiangning Huang, Kun Huang, Ran Chen, Yuanqi Wang, Chenxing Niu, Ziduan Han, and all my wonderful lab mates for their cooperation, encouragement and friendship.

Last, but obviously not least, I would express the deepest gratitude to my parents and my wife. Thanks for their trust, understanding and sacrifices during my long journey of academic growth. I would never reach here without their endless love and support.

TABLE OF CONTENTS

LIST OF TABLES	viii
LIST OF FIGURES	ix
ABSTRACT	x
CHAPTER 1. INTRODUCTION	1
1.1 Algal Biofuel as an Alternative to Fossil Fuels	1
1.2 Approaches and Challenges in Current Algal Cultivation and Lipid Extraction.....	2
1.2.1 Approaches and Challenges in Microalgae Cultivation	3
1.2.2 Approaches and Challenges in Lipid extraction	4
1.2.3 Approaches and Challenges in Cell Disruption	5
1.3 Application of UV irradiance to control invading organisms.....	6
1.4 Application of Algal Viruses for Cell Disruption.....	7
1.5 Objectives	8
CHAPTER 2. <i>TETRASELMIS</i> AS A CHALLENGE ORGANISM FOR VALIDATION OF UV SYSTEMS TO CONTROL INVADING ORGANISMS	10
2.1 Abstract.....	10
2.2 Introduction.....	11
2.3 Materials and Methods.....	16
2.3.1 Chemicals and Algae Culture	16
2.3.2 Analytical Methods.....	17
2.3.3 MPN Assay	17
2.3.4 Collimated Beam Reactor	17
2.3.4.1 UV ₂₅₄ dose-response behavior of <i>Tetraselmis</i> sp.	18
2.3.4.2 Effects of repeated UV exposure on <i>Tetraselmis</i> sp.....	18
2.3.4.3 Action spectrum of <i>Tetraselmis</i> and absorbance spectrum of extracted DNA.....	18
2.4 Results and Discussion	19
2.4.1 MPN Method Validation	20
2.4.2 UV ₂₅₄ Dose-response Behavior of <i>Tetraselmis</i> Cells Under a Collimated Beam	22
2.4.3 Effects of Repeated UV Exposure	26
2.4.4 Action Spectrum of <i>Tetraselmis</i> and Absorbance Spectrum of Extracted DNA.....	28

2.5	Conclusions.....	32
CHAPTER 3. UV INACTIVATION OF ALGAL VIRUSES TO PROTECT ALGAL PRODUCTIVITY		
		33
3.1	Abstract.....	33
3.2	Introduction.....	34
3.3	Materials and Methods.....	35
3.3.1	Microalgal Cultures and Growth Conditions.....	35
3.3.2	Plaque Assay and Algal Virus Isolation	36
3.3.3	Quantification of UV-induced Damage on Viral DNA with qPCR	37
3.3.4	Collimated Beam Reactor.....	38
3.3.5	UV ₂₅₄ Dose-response Behavior of Algal Virus PBCV-1	38
3.3.6	Action Spectrum of Algal Virus PBCV-1	38
3.4	Results and Discussion	39
3.4.1	Growth of <i>Chlorella</i> with and Without Algal Virus.....	40
3.4.2	UV ₂₅₄ Dose-response Behavior of PBCV-1 Under a LP Collimated Beam Reactor	41
3.4.3	Action Spectrum and Absorbance Spectrum of Extracted DNA.....	45
3.5	Conclusions.....	47
CHAPTER 4. NATURE-INSPIRED VIRAL DISRUPTION METHOD FOR COST-EFFECTIVE BIOFUEL PRODUCTION.....		
		49
4.1	Abstract.....	49
4.2	Introduction.....	49
4.3	Materials and Methods.....	52
4.3.1	Microalgae Cultivation and Quantification	52
4.3.2	Virus isolation and Quantification.....	52
4.3.3	Viral Infection and Dynamics.....	53
4.3.3.1	Transmission electron microscopy	53
4.3.3.2	Impact of viral infection on algal cell strength.....	54
4.3.3.3	Lipid extraction after viral infection.....	54
4.3.4	Lipid Transesterification and Quantification.....	54
4.3.5	Statistical Analysis.....	55
4.4	Results and Discussion	55

4.4.1	Virus isolation and Identification	55
4.4.2	Viral infection of <i>Chlorella</i> sp.....	56
4.4.2.1	Infection dynamics under different MOI.....	58
4.4.2.2	Reduction of algal cells' mechanical strength after viral infection	59
4.4.2.3	Lipid extraction after viral infection.....	61
4.4.2.4	Effect of viral disruption on composition of fatty acids	62
4.4.3	Economical Aspects.....	64
4.5	Conclusions.....	65
CHAPTER 5. CONCLUSIONS AND FUTURE WORK		66
5.1	Conclusions.....	66
5.2	Future Work.....	67
APPENDIX A. SUPPORTING INFORMATION FOR CHAPTER 2		69
APPENDIX B. SUPPORTING INFORMATION FOR CHAPTER 3		78
APPENDIX C. SUPPORTING INFORMATION FOR CHAPTER 4		81
REFERENCES		84

LIST OF TABLES

Table 1-1. Oil content in some microalgae (Satyanarayana et al., 2011).....	2
Table 2-1. Ballast water discharge regulations from the International Maritime Organization (IMO, 2008).	11
Table 2-2. Scoring of serially-diluted suspensions of <i>Tetraselmis</i> without UV treatment	21
Table 3-1. PCR primers to target algal viruses	37
Table 4-1. Composition and yield of fatty acids in extracted lipids.....	63
Table 4-2. Statistical analysis results of ANOVA analysis of individual fatty acids.....	64

LIST OF FIGURES

Figure 2-1. UV ₂₅₄ dose-response of <i>Tetraselmis</i> as measured with flat-plate collimated beam reactor	23
Figure 2-2. Responses of <i>Tetraselmis</i> cells to repeated UV ₂₅₄ irradiation	27
Figure 2-3. Viable <i>Tetraselmis</i> cell concentration as a function of UV dose	29
Figure 2-4. UV inactivation action spectrum for <i>Tetraselmis</i> cells and Absorption Spectrum of Extracted DNA.....	30
Figure 3-1. Pictures of plaque assay (left) and gel electrophoresis result (right)	39
Figure 3-2. TEM pictures of uninfected (a) and infected (b) <i>Chlorella</i> sp. Cells	40
Figure 3-3. Growth behavior of <i>Chlorella</i> sp. with and without virus inoculation	41
Figure 3-4. UV ₂₅₄ dose-response of PBCV-1 quantified by qPCR with PBCVs and 185R1 primer sets.....	42
Figure 3-5. UV ₂₅₄ dose-response of PBCV-1 measured by exposure under a LP UV collimated beam using a culture-based plaque assay and DNA damage by qPCR	43
Figure 3-6. Concentration of active PBCV-1 as a function of UV dose at each of nine wavelengths.	46
Figure 3-7. Normalized UV inactivation action spectrum for PBCV-1, MS2, Adenovirus 2, and DNA absorption.	46
Figure 4-1. Pictures of <i>Chlorella</i> cells before and after viral infection.....	57
Figure 4-2. Infection of algal cells under different MOI	59
Figure 4-3. Improvement of cell lysis efficiency after viral infection.	60
Figure 4-4. FAMES extracted from algal cells with various disruption methods.....	62

ABSTRACT

Author: Sun, Zhe. PhD

Institution: Purdue University

Degree Received: May 2019

Title: Application of Photochemical and Biological Approaches for Cost-effective Algal Biofuel Production

Committee Chair: Zhi Zhou

Rapid growth of energy consumption and greenhouse gas emissions from fossil fuels have promoted extensive research on biofuels. Algal biofuels have been considered as a promising and environmentally friendly renewable energy source. However, several limitations have inhibited the development of cost-effective biofuel production, which includes unstable cultivation caused by invading organisms and high cost of lipid extraction. This dissertation aims to investigate photochemical approaches to prevent culture collapse caused by invading organisms and biological approaches for the development of cost-effective lipid extraction methods.

As a chemical-free water treatment technology, ultraviolet (UV) irradiation has been widely applied to inactivate pathogens but has not been used in algal cultivation to control invading organisms. To evaluate the potential of using UV irradiation to control invading algal species and minimize virus predation, *Tetraselmis sp.* and *Paramecium bursaria* *Chlorella virus 1* (PBCV-1) were examined as challenge organisms to evaluate effectiveness of UV disinfection. The concentration of viable (reproductively/infectively active) cells and viruses were quantified by a most probable number (MPN) assay and a plaque assay. A low-pressure collimated-beam reactor was used to investigate UV₂₅₄ dose-response behavior of both challenge organisms. A medium-pressure collimated-beam reactor equipped with a series of narrow bandpass optical filters was used to investigate the action spectra of both challenge organisms. Both challenge organisms showed roughly five log₁₀ units of inactivation for UV₂₅₄ doses over 120 mJ/cm². The most effective wavelengths for inactivation of *Tetraselmis* were from 254 nm to 280 nm, in which the inactivation was mainly attributed to UV-induced DNA damage. On the contrary, the most effective wavelength for inactivation of PBCV-1 was observed at 214 nm, where the loss of infectivity was mainly attributed to protein damage. These results provide important information for design of UV reactors to minimize the impact of invading organisms in algal cultivation systems.

Additionally, a virus-assisted cell disruption method was developed for cost-effective lipid extraction from algal biomass. Detailed mechanistic studies were conducted to evaluate infection behavior of *Chlorovirus* PBCV-1 on *Chlorella sp.*, impact of infection on mechanical strength of algal cell wall, lipid yield, and lipid distribution. Viral disruption with multiplicity of infection (MOI) of 10^{-8} completely disrupted concentrated algal biomass in six days. Viral disruption significantly reduced the mechanical strength of algal cells for lipid extraction. Lipid yield with viral disruption increased more than three times compared with no disruption control and was similar to that of ultrasonic disruption. Moreover, lipid composition analysis showed that the quality of extracted lipids was not affected by viral infection. The results showed that viral infection is a cost-effective process for lipid extraction from algal cells as extensive energy input and chemicals required by existing disruption methods are no longer needed.

Overall, this dissertation provides innovative approaches for the development of cost-efficient algal biofuels. Application of UV disinfection and viral disruption significantly reduces chemical consumption and improves sustainability of algal biofuel production.

CHAPTER 1. INTRODUCTION

1.1 Algal Biofuel as an Alternative to Fossil Fuels

Rapid growth of energy consumption and greenhouse gas emissions from fossil fuels have promoted extensive research on biofuels. Due to the depletion of fossil fuels and increases of carbon dioxide (CO₂) concentration in the atmosphere, sustainable and environmentally friendly energy source is in an urgent need (Chisti, 2008; Milano et al., 2016). Among all biofuel sources, microalgae have shown advantages of high growth rate, low arable land use, and high lipid content over other energy crops (Alam et al., 2012; Brennan et al., 2010; H. Chen et al., 2015; Kirrolia et al., 2013). Integration of waste treatment systems and algal biomass cultivation has been reported to be promising in terms of producing biofuel from wastes (Doucha et al., 2005; Gupta et al., 2016). Compared with traditional diesel, biodiesel produced from algae contains more oxygen along with less sulfur and nitrogen, which can reduce the emission of hazardous compounds, such as SO_x, NO_x, CO, benzene, and toluene after combustion (Al-lwayzy et al., 2014; Tica et al., 2010).

Microalgae are primeval unicellular organisms with simple cellular structures that survive individually or in groups in aquatic environments, serving as the base of the food chain (Kirrolia et al., 2013). Microalgae are capable of photosynthesis and have higher efficiency to utilize solar energy than higher plants, which is attributed to their simple cellular structures (Walker et al., 2005). Microalgal cells are rich in the precursors to produce biodiesel (fatty acid alkyl esters), such as triacylglycerols (TAGs), diacylglycerols (DAGs), free fatty acids (FFAs) and phospholipids (PLs) (Chen et al., 2012). Dry weight-based oil content of several microalgae is listed in Table 1-1.

Lipid accumulation in microalgal cells is affected by culture conditions, such as temperature and nutrient level. Lipid production can be enhanced in some stressed environments (Reitan et al., 1994; Zhang et al., 2015) and nitrogen or phosphorus limited conditions can increase lipid accumulation in freshwater strains of *Scenedesmus* sp., but accompanied by a sacrifice on biomass accumulation (Xin et al., 2010). Another study indicated that the optimal cultivation temperature for *Chlorella* sp. to accumulate lipids was in the range of 12-18°C (Zhang et al., 2015).

Table 1-1. Oil content in some microalgae (Satyanarayana et al., 2011).

Species	Oil content (% dry wt)	Reference
<i>Botryococcus braunii</i>	25–75	(Chisti, 2007; Meng et al., 2009)
<i>Chlorella sp.</i>	28–32	(Chisti, 2007)
<i>Chlorella emersonii</i>	63	(Li et al., 2008)
<i>Chlorella minutissima</i>	57	(Li et al., 2008)
<i>Chlorella protothecoides</i>	23	(Li et al., 2008)
<i>Chlorella sorokiniana</i>	22	(Li et al., 2008)
<i>Chlorella vulgaris</i>	40, 56.6	(Li et al., 2008)
<i>Cylindrotheca</i>	16–37	(Meng et al., 2009)
<i>Cryptocodinium cohnii</i>	20	(Meng et al., 2009)
<i>Dunaliella primolecta</i>	23	(Chisti, 2007)
<i>Isochrysis sp.</i>	25–33	(Chisti, 2007)
<i>M. Subterraneus</i>	39.3	(Li et al., 2008)
<i>Monallanthus salina</i>	>20	(Chisti, 2007)
<i>N. laevis</i>	69.1	(Li et al., 2008)
<i>Nannochloris sp.</i>	20–35	(Chisti, 2007)
<i>Nitzschia sp.</i>	45–47	(Chisti, 2007; Meng et al., 2009)
<i>P.incisa</i>	62	(Li et al., 2008)
<i>Phaeodactylum tricornutum</i>	20–30	(Chisti, 2007)
<i>Schizochytrium sp.</i>	50–77	(Chisti, 2007; Meng et al., 2009)
<i>Tetraselmis sueica</i>	15–23	(Chisti, 2007)

1.2 Approaches and Challenges in Current Algal Cultivation and Lipid Extraction

Although algal biofuel has been considered as a prospective alternative for fossil fuels, several limitations have inhibited the development of cost-effective biofuel production, including reduced productivity caused by invading organisms and high cost of lipid extraction.

1.2.1 Approaches and Challenges in Microalgae Cultivation

Invasion of unwanted organisms, such as bacteria, viruses, fungi, algae, and grazers, can lead to reduced biomass productivity or even culture collapse in algal cultivation systems (Bartley et al., 2013; Day et al., 2012; Lammers et al., 2017). Contamination by other types of algae can lead to competition for nutrients and space with the selected production strain and affect the quality of lipids (Belay, 1997; Mitchell et al., 1987). Another issue is the potential risk of "biofouling" caused by adhering algae (Day et al., 2012). These adhering algae (e.g., adhering cyanobacteria) can shade nearby algal cells to reduce the photosynthetic activity of the selected strains. Additionally, biofouling on paddlewheels and other devices can reduce mixing in the cultivation system and thus influence algal biomass productivity.

To date, the relationship between microalgae and bacteria has not been fully revealed (Yun et al., 2017). The presence of some bacteria can be beneficial for algal growth since these bacteria can release some biomolecules to promote algal growth (Gonzalez et al., 2000; B.-H. Kim et al., 2014). On the other hand, bacteria compete for nutrients, reduce light penetration, and can induce mortality of microalgae (Day et al., 2012). It has been reported that bacterium *Bacillus cereus* is capable of lysing a wide range of cyanobacteria and algae (Shunyu et al., 2006). Another plaque-forming bacterium was able to lyse diatom *Phaeodactylum tricornutum* (Z. Chen et al., 2015).

Grazing of microalgae by zooplankton is also a problem in algal cultivation. Insect larvae have been reported to be responsible for loss of algal biomass during *Spirulina* cultivation (Belay, 1997). It was reported that ciliates wiped out a well-established algal culture in a few days (Moreno-Garrido et al., 2001; Post et al., 1983).

Viruses are the most common biological entities in aquatic systems and are responsible for cell lysis within every major algal phylum (Day et al., 2012; Gachon et al., 2010; Lawrence, 2008). Mortality of microalgae related to viral infection has been observed in both natural environments and mesocosm systems (Larsen et al., 2008; Lawrence, 2008).

1.2.2 Approaches and Challenges in Lipid extraction

Lipids serve as the reservoir of carbon and energy in microalgae and are enveloped in lipid droplets within microalgae's cytoplasm that are protected by a rigid cell wall (Kirrolia et al., 2013). The location of lipids as well as the water content in microalgae make their extraction more complicated than conventional extraction methods applied in the oil extraction of oil seeds, and therefore mechanical pressing is no longer applicable (Chiaramonti et al., 2017; Lam et al., 2012; Tanzi et al., 2013).

Numerous methods have been investigated for microalgal lipid extraction; however, most methods evaluated to date have encountered technical constraints that hinder their development for industrial scale application. As a result of high cost and energy intensive steps, lipid extraction is one of the main barriers to algal biofuel production (Coons et al., 2014; Halim et al., 2012; Steriti et al., 2014). Various lipid extraction methods have been investigated to improve extraction efficiency and reduce costs (Chiaramonti et al., 2017; Joannes et al., 2015; Steriti et al., 2014). Based on the type of microalgae biomass applied in the extraction process, extraction techniques can be categorized into dry biomass and wet biomass-based extraction methods.

In dry biomass based extraction, organic solvents are applied to extract lipids from algal cells (Sander et al., 2010). Currently, dry biomass extraction is technologically mature, and high value-added co-products, such as protein-rich biomass residues, can help improve the economic performance and compensate the extraction cost (Chiaramonti et al., 2017). However, the energy input for microalgae drying could reach as high as 89% of total energy input (Sander & Murthy, 2010). Therefore the energy intensive drying/dehydration pretreatment step in dry biomass based extraction makes wet biomass based extraction a competitive alternative (Lam & Lee, 2012; Lardon et al., 2009; Xu et al., 2011).

In wet biomass based extraction, no energy is required for dehydration, but solvents are not able to pass the cell wall to extract lipids because of the surface charge of microalgal cells force themselves to remain in the water phase (J. Kim et al., 2013). Hence, cell disruption pretreatment is mandatory in wet extraction to allow sufficient contact between solvent phase and intracellular lipids.

1.2.3 Approaches and Challenges in Cell Disruption

Several cell disruption methods have been investigated to break down the rigid microalgal cell walls, which are characterized by high mechanical strength and chemical resistance (Steriti et al., 2014). Generally, current cell disruption methods can be classified into physical, chemical, and biological methods.

Physical disruption methods include bead-beating, high pressure homogenization (HPH), ultrasonication, microwave, and electroporation (Chiaramonti et al., 2017; Greenly et al., 2015; Joannes et al., 2015; Richmond, 2008; Steriti et al., 2014). Microwaves shock the cell wall with high-frequency waves that can break the cell wall and disrupt the cells (Lee et al., 2010). The effect of sonication on cell disruption is attributable to cavitation and bubble collapse in water adjacent to cells, which can crack the cell wall (Adam et al., 2012). Bead-beating applies tiny beads to rupture cell wall by high-speed spinning and has been used widely (Harrison, 1991). Electroporation utilizes an electromagnetic field to generate dipole moments on the cell wall and can disrupt the formation of pores within the cell wall (J. Kim et al., 2013). Electroporation has been applied extensively to transport DNA through cell envelopes but the envelope can be destroyed when a sufficient electromagnetic field is added (Joannes et al., 2015). High pressure homogenization destroys cells by a hydraulic shear force generated from the high pressure employed on the algal slurry through a fine tube (Halim et al., 2012). Generally speaking, most physical disruption methods are difficult to scale up due to the continuous demand of intensive energy for thermal, electrical, or mechanical input (M. Wang et al., 2014).

Chemical disruption methods depend on selective chemical reactions to lyse algal cell walls. Inorganic chemical methods, such as acid and base hydrolysis (Sathish et al., 2012) and osmotic shock (J. Kim et al., 2013), have been applied. Organic chemicals, such as lysine and acetone, methanol and dimethyl sulfoxide (DMSO), have been implemented to lyse cell walls (Richmond, 2008; Shoaf et al., 1976). In addition, ionic liquids have been used to disrupt microalgal cells for their ability to dissolve tough biopolymers, such as the building blocks of cell wall (Orr et al., 2015). Hydroxyl radicals generated by the photocatalyst titanium dioxide and solar energy was also validated for algal cell disruption (Shwetharani et al., 2016). Although chemical disruption methods are less energy intensive and easier to scale-up as compared to physical disruption

methods, great demands of chemicals, need of chemical waste treatment and disposal, and potential equipment corrosion request economic and practical challenges for these processes (J. Kim et al., 2013).

Biological disruption methods are based on enzymatic degradation of a cell wall, which can be processed under mild reaction conditions with high selectivity as compared to chemical and physical methods (J. Kim et al., 2013). Actually, various types of microalgae even with very resistant layers can be lysed by specific mixtures of enzymes at relatively low energy cost (Chen et al., 2016; Taher et al., 2014), although the cost of enzymes is usually high (Chiaramonti et al., 2017).

Combinations of different methods can be applied as well. A combination of microwave and ionic liquids was proven to have higher lipid extraction efficiency as compared to conventional lipid extraction methods (Pan et al., 2016). In another study, efficient extraction from wet algal biomass (88% of total lipids) was achieved without applying organic solvent when thermal lysis and enzymatic disruption were collectively employed (Chen et al., 2016). Despite the improvement in efficiency, the inherent constraints of disruption methods still exist. Therefore, innovative disruption techniques are needed to reduce biofuel production cost.

1.3 Application of UV irradiance to control invading organisms

Invasion of unwanted organisms in algal cultivation systems and infections of human digestive systems by microbial pathogens share some common features. Strategies to prevent invasion or infection can be classified in two ways: 1) preventing the invading or infecting organisms from entering its new host (i.e., cultivation pond or human); 2) preventing the invading or infecting organisms from reproducing within the new host (Tsolaki et al., 2010).

UV radiation is known to cause damage to nucleic acids, lipids, and proteins in various organisms and has been viewed as a broad-spectrum antimicrobial agent (Hijnen et al., 2006). UV-induced damage may not lead to death of an individual organism, but sufficient exposure of UV-irradiation can prevent the organisms from reproducing (Blatchley et al., 2001), which is an important endpoint for water treatment in algal cultivation system since reproduction is required for a

successful invasion of algal cultivation systems. The idea behind the use of UV irradiation to prevent invasion is that the unwanted invading organisms that cannot reproduce will not be able to establish a population, so competition with highly efficiently algal strains in cultivation ponds will be significantly reduced. UV disinfection has been applied in water and wastewater treatment to reduce pathogenic microorganisms effectively but has not been used in disinfecting competing algal strains for biofuel production. The application of UV in algal cultivation can help reduce the likelihood of invasions by invading organisms that may be introduced into the system along with the water collected from natural water system.

1.4 Application of Algal Viruses for Cell Disruption

To explore additional methods on cell disruption, algal viruses can be considered since they are able to naturally lyse cyanobacteria and eukaryotic algae (Van Etten, Burbank, et al., 1985; Van Etten, Burbank, Xia, et al., 1983; Van Etten, Van Etten, et al., 1985). In fact, algal viruses have been reported to play important roles in structuring algal communities, such as their participation in the termination of algal blooms (Fuhrman, 1999; Gachon et al., 2010; Van Etten et al., 2012). This natural phenomenon suggests the potential of using algal viruses for disruption of microalgal cells.

Generally, viruses infecting eukaryotic algae have huge dsDNA genomes (up to 560 kb) that contain up to several hundred protein-encoding genes (Van Etten & Dunigan, 2012). The lysis cycle of *Chlorovirus* PBCV-1 was illustrated by Van Etten (Van Etten & Dunigan, 2012). At the beginning, *Chlorovirus* attaches to the host cell and the cell wall is degraded enzymatically. Then the internal viral membrane fuses with the host membrane and injects viral DNA as well as viral proteins, leaving the empty capsid outside (Meints et al., 1984). Viral DNA enters the host nucleus about 5-10 minutes post infection, then the host transcription system is reprogrammed to transcribe viral DNA. The assemblage of viral capsids initiates in the cytoplasm 2-3 hours post infection and the cytoplasm will be filled with virus particles 5-6 hours post infection. Finally, the host cell is lysed and virus particles are released at 6-8 hours post infection (Meints et al., 1986; Van Etten & Dunigan, 2012).

During the infection by an algal virus, the host's metabolic pathway can be reprogrammed. For example, *E. huxleyi* have been reported to have more triacylglycerides (TAGs) synthesis after viral infection (Malitsky et al., 2016), which is favorable in biodiesel production. Algal viruses themselves could also be a source of lipid. For example, *Chlorovirus* PBCV-1 has been reported to contain lipid membrane and another virus EhV that can infect *E. huxleyi* was reported to possess high content of TAGs (Malitsky et al., 2016; Van Etten & Dunigan, 2012).

The distribution of algal virus is global and no environmental and health risks have been reported for them. Algal viruses are wide spread throughout the world (e.g., *Chlorovirus* is widely detected with a concentration of 1-100 plaque forming units PFU/mL in freshwater) so they can be easily collected (Van Etten & Dunigan, 2012). On the other hand, algal viruses have been found at very high concentrations (e.g., *Chlorovirus* up to 100,000 PFU/mL) in some aquatic environments (Long et al., 2016; Short, 2012). Some studies revealed that the concentration of algal viruses is seasonally dependent and the decay rate of algal viruses is rapid in the natural environment (Long & Short, 2016). Additionally, most algal viruses are host specific and some *Chloroviruses* have been reported to only infect indigenous *Chlorella* strains (Yamada et al., 1991). Considering the above characteristics, such as highly host specific, large quantity in environment, and the rapid naturally decay rate, and low adverse effects on ecosystem and human health, algal viruses could be promising agents for natural decay of algae to release lipids for biofuel production.

1.5 Objectives

The main objective of this dissertation is to optimize current algal biofuel production process by controlling invading organisms for algal cultivation and involving a virus-assisted disruption method for cost-effective lipid extraction. The influence of UV irradiation on inactivating challenge invading organisms was explored. Additionally, a nature-inspired biological approach that utilizes viruses for algal cell disruption was proposed and examined as a new solution for cost-effective lipid extraction from microalgae.

The specific objectives of this dissertation are:

- 1) To investigate the feasibility of using *Tetraselmis* as an appropriate challenge alga for validation of UV reactors for inflow water treatment in algal cultivation system.
- 2) To examine the performance of UV radiation on controlling of invading virus with PBCV-1 as a challenge virus.
- 3) To provide a comprehensive and in-depth study to use viruses in algal lipid extraction.

CHAPTER 2. *TETRASELMIS* AS A CHALLENGE ORGANISM FOR VALIDATION OF UV SYSTEMS TO CONTROL INVADING ORGANISMS

This chapter has been published on *Water Research* and the main objective was to use a marine alga *Tetraselmis sp.* as a challenge organism for validation of UV systems (Sun et al., 2017). This study is well suited for the illustration of using UV systems to treat influent water for algal cultivation to control the contamination caused by invading alga.

2.1 Abstract

Tetraselmis is a widely distributed alga in seawater throughout the world. Transport and release of waterborne organisms as a result of ballasting and de-ballasting operations is widely acknowledged to represent an important mechanism for invasions by non-indigenous species. Regulatory requirements have been implemented globally to require treatment of ballast water before its release to the environment as a means of minimizing risks of invasion. UV-based processes represent an option for ballast water treatment; however, their use will require development of appropriate methods for reactor validation. To address this need, *Tetraselmis* was examined as challenge organism using a most probable number (MPN) assay for quantification of the concentration of viable (reproductively active) cells in suspension. A low pressure collimated-beam reactor was used to investigate UV₂₅₄ dose-response behavior of *Tetraselmis*. Based on the experimental conditions applied, *Tetraselmis* indicated 4.5-5 log₁₀ units of inactivation for UV₂₅₄ doses of approximately 120 mJ/cm², with no apparent change of resistance resulting from repeated exposure. A medium pressure UV collimated-beam reactor equipped with a series of narrow bandpass optical filters was used to investigate the action spectrum of *Tetraselmis* for wavelengths ranging from 228 nm – 297 nm. Radiation with wavelengths in the range 254-280 nm was observed to be most efficient for inactivation of *Tetraselmis*. Additionally, DNA was extracted from *Tetraselmis* to allow measurement of its absorption spectrum. These results indicated strong absorbance from 254 nm to 280 nm, thereby suggesting that damage to DNA plays an important role in the inactivation of *Tetraselmis sp.* However, deviations of the action spectrum shape from the shape of the DNA absorption spectrum suggest that UV-induced damage to biomolecules other than DNA may contribute to *Tetraselmis* inactivation at some wavelengths in the UVC range.

2.2 Introduction

Ballast water is carried by ships to ensure stability when they are empty. Ballasting and deballasting operations take place to offset changes of hull displacement associated with unloading and loading of cargo, respectively. However, the various biological materials contained in ballast water can pose threats to local aquatic systems after discharge, largely through invasions of non-indigenous species. Ballast water discharge-induced invasions have been reported worldwide (Carlton et al., 1993; Katsanevakis et al., 2013; Mead et al., 2011; Steichen et al., 2012). The International Maritime Organization has implemented requirements to treat ballast water prior to discharge as a means of reducing the risk of invasion (IMO, 2008). The IMO regulations are summarized in Table 2-1.

Table 2-1. Ballast water discharge regulations from the International Maritime Organization (IMO, 2008).

Organism Class	Acceptable Concentration
$d_m \geq 50 \mu\text{m}$	≤ 10 viable organisms/ m^3
$10 \mu\text{m} \leq d_m < 50 \mu\text{m}$	≤ 10 viable organisms/mL
Indicator Microbes	
<i>Vibrio cholerae</i> (serotypes O1 and O139)	≤ 1 cfu/100 mL
<i>E. coli</i>	≤ 250 cfu/100 mL
Intestinal <i>Enterococci</i>	≤ 100 cfu/100 mL

For practical purposes, the organism class defined by $d_m \geq 50 \mu\text{m}$ corresponds to zooplankton, whereas the organism class defined by $10 \mu\text{m} \leq d_m < 50 \mu\text{m}$ corresponds to phytoplankton. Therefore, ballast water treatment systems must be developed to properly manage the concentrations of these organism classes in treated water. In many applications, this implies that multiple treatment processes be applied. This approach is similar to the “multiple-barrier concept” that is the foundation of contemporary drinking water treatment. When properly implemented, multiple-barrier approaches have yielded potable water production systems that reliably and responsibly provide safe drinking water. It is reasonable to expect that application of the same principle to ballast water treatment will yield similarly positive results.

The United States Coast Guard (USCG) has responsibility for regulation of ballast water discharges in U.S. waters. As such, the Coast Guard has promulgated an analogous set of regulations to define acceptable discharges to U.S. waters. The USCG standards are numerically identical to the IMO standards listed in Table 2-1. However, the concentrations of organisms in the size classes $d_m \geq 50 \mu\text{m}$ and $10 \mu\text{m} \leq d_m < 50 \mu\text{m}$ are limited to ≤ 10 *living* organisms/ m^3 and ≤ 10 *living* organisms/mL, respectively. The substitution of the word *living* for the word *viable* has potentially important implications with respect to the treatment processes that are applied. This is especially true for UV-based ballast water treatment processes, largely because of the mechanisms by which UV-based treatment processes accomplish microbial inactivation.

Invasions of coastal waters by non-indigenous species and infections of human digestive systems by microbial pathogens share some common features. Successful prevention of an invasion or infection can be accomplished by several approaches (Tsolaki & Diamadopoulos, 2010), most of which involve preventing the invading or infecting organism from entering its new host (*i.e.*, a port or a human), providing conditions within the new host that prevent replication of the invading/infecting species, or treatment of the invading/infecting species to prevent subsequent reproduction.

Ultraviolet (UV) radiation is known to cause damage to nucleic acids, lipids, and proteins. As such, it represents a broad-spectrum antimicrobial agent (Hijnen et al., 2006). The damage caused by exposure to UV radiation may not lead to death of an individual organism; however, organisms that experience sufficient UV-induced damage may not be able to reproduce (Blatchley et al., 2001). Since reproduction is required for an invasion of a non-indigenous organism, it is hypothesized that the ability to reproduce can be used as an endpoint for ballast water treatment operations. In UV-based water treatment applications wherein disinfection is the objective (*e.g.*, disinfection of drinking water, wastewater, or wastewater reuse applications), loss of the ability to reproduce is viewed as an appropriate endpoint in that the affected organisms will not be able to cause infection.

UV photoreactors are commonly used in water treatment for disinfection, direct photolysis, and advanced oxidation process applications. UV dose (*aka* fluence), defined as the time-integral of

the UV fluence rate to which a photochemical target is exposed, represents the master variable in photochemical systems, in that it will govern the extent of any photoreaction. However, all contemporary, continuous-flow UV photoreactors deliver a distribution of UV doses; the performance of any photochemical reactor is determined by the dose distribution it delivers and the kinetics of the photochemical reaction(s) that take place within the system (Chiu et al., 1999). In turn, the dose distribution delivered by a UV photoreactor will be determined by the spatial distribution of electromagnetic radiation and fluid mechanical behavior within the irradiated zone of the reactor.

Given the complex nature of the spatial distributions of radiation energy and fluid mechanics within UV photoreactors, it is not possible to use on-line measurements to quantify the performance of these systems directly. Therefore, in many applications of UV-based treatment, validation protocols based on biosimetry have been developed to define the performance of a reactor over a range of operating conditions (NWRI, 2012; Sommer et al., 2004; USEPA, 2006). Biosimetry requires identification and use of a relevant challenge organism and an appropriate assay to measure (quantify) its response to UV irradiation. To date, no validation protocol has been standardized for ballast water treatment based on UV irradiation.

In general, the challenge organism used for biosimetry should be related to organisms that are believed to represent risk to the system in question, although the challenge organism itself should not represent a risk to the target system. A challenge organism should be relatively resistant to UV exposure; ideally, a challenge organism will be as resistant or more resistant than the organism(s) within an application that limit (govern) the application of the disinfection process being employed.

Algae tend to reproduce rapidly, with doubling times of one day or less being common. As such, they also have the potential to function as effective invaders when introduced to an ecosystem to which they are non-native, and where conditions favor their reproduction. Therefore, one or more algal species may have the potential to serve the function of an indicator or challenge organism in the development of ballast water management systems.

Algal cells rely on solar radiation to accomplish photosynthesis; therefore, they require an environment that provides access to this radiation. In aquatic systems, this means that photosynthetically-active algal cells must reside in the photic zone. However, by residing in this zone, algae may also be subjected to portions of the solar spectrum that can cause damage to biomolecules. For example, exposure to UVA radiation ($320 \text{ nm} \leq \lambda \leq 400 \text{ nm}$) is generally associated with indirect cellular damage caused by reactive oxygen species that are produced photochemically (McGuigan et al., 2012). In contrast, exposure to UVB radiation ($280 \text{ nm} \leq \lambda \leq 320 \text{ nm}$) is generally associated with damage to nucleic acids, which is mechanistically similar to the microbial inactivation processes that are associated with most UV-based disinfection systems, which typically rely on UVC radiation (Mbonimpa et al., 2012).

Algae have developed several functions or features to address this important conflict (Häder, 2011). First, they are often motile, which allows movement within the water column to locations that provide a favorable balance between photosynthetic activity and UV-induced damage. Algae tend to grow most effectively in environments that experience the lowest amounts of damaging solar UV exposure. Second, many species of algae have enzymatic (photolyase or protease) repair mechanisms that allow for damage to be identified and repaired. A third mechanism that is common among phytoplankton is the production of mycosporine-like amino acids (MAAs) which absorb in the UV range; in effect, these compounds function as a “sunscreen” for algal cells (Karentz et al., 1991; Ng et al., 2001).

As described above, biosimetric protocols require an appropriate challenge organism and a relevant response assay. The USCG regulations are based on the number concentration of live cells within each of two size (d_m) classes; they further prescribe that the live/dead distinction will be quantified using staining methods, typically based on the vital stains fluorescein diacetate and 5-chloromethylfluorescein diacetate (FDA and CMFDA, respectively).

Staining methods have been used in other treatment settings, such as chemical disinfection for drinking water, including chlorination and ozonation. In these applications, staining methods have been demonstrated to provide responses that are similar to those based on direct measurement of infectivity or reproduction for organisms such as *Cryptosporidium parvum* (Belosevic et al., 1997).

In such an application, indirect staining methods are appropriate in that the inclusion or exclusion of the dyes is governed by processes that are related to inactivation responses for chemical disinfectants like chlorine. However, these vital dyes have been demonstrated to be inappropriate and misleading for UV-based applications in that they are numerically and mechanistically dissimilar from the responses that result from UV exposure (Hargy et al., 2000).

FDA and CMFDA undergo biochemically-induced changes within organisms that are metabolically-active and that include intact membranes; the transformed molecules are fluorescent, thereby yielding an optical signal that can be used to discriminate live from dead cells. However, because a broad spectrum of physiological states exist among live and dead phytoplankton, there can be variability in the ability of staining methods based on FDA, CMFDA, or the two dyes in combination to accurately discriminate between live and dead cells. As an illustration, MacIntyre and Cullen compared responses of heat-treated and living cells based on these staining methods (MacIntyre et al., 2016). Among the 24 species of phytoplankton included in their study, only 8-10 displayed accurate discrimination by these staining methods.

Methods are also available to directly quantify changes in reproductive activity among treated microbes. One such method is based on the concept of the Most Probable Number (MPN) (McCrary, 1915). The foundation of the MPN method is serial dilution of a sample until a level of dilution is reached at which the diluted sample contains one or fewer viable cells. Each serially-diluted sample is incubated under conditions that favor the organisms' growth. The Poisson distribution is applied to the observed data, with diluted samples scored as "positive" (growth) or "negative" (no growth) at each dilution level after incubation to estimate the most probable concentration of viable organisms in the original sample. MPN tables for 3-tube tests and 5-tube tests can be found in *Standard Methods for the Examination of Water and Wastewater* (Clesceri et al., 2005; Gilcreas, 1966).

Olsen *et al.* (2015, 2016) examined the dose-response behavior of *Tetraselmis suecica* when subjected to polychromatic radiation from a medium-pressure Hg lamp. They quantified the responses of these algal cells using flow cytometry based on staining with 5-carboxyfluorescein diacetate acetoxymethyl ester (CFDA-AM). Parallel measurements were conducted by plate

counting and an MPN method. Their results indicated that culture-based methods yielded greater inactivation than the flow cytometry method. They also reported that UV doses of 400-800 mJ/cm² were required for effective treatment. However, there was some ambiguity in their method of quantifying applied dose, largely because of the polychromatic UV source they used in their experiments. Their data also indicated considerable variability between replicate experiments. A graphical summary of the data reported by Olsen *et al.* is presented in Figure A-1 in Appendix A.

In this study, *Tetraselmis* was examined as a prospective challenge organism for validation of UV reactors in ballast water treatment since they are ubiquitous in the marine environment and are therefore not likely to represent an invasive species in marine settings. Additionally, *Tetraselmis* are relatively easy to culture and assay, and preliminary data indicated that they are relatively resistant to UV radiation. The central hypotheses of this work were that *Tetraselmis* could represent an appropriate challenge organism for validation of UV reactors used in ballast water treatment, and that an MPN-based method would represent a relevant assay for quantification of the response of *Tetraselmis* to exposure to UV radiation.

2.3 Materials and Methods

2.3.1 Chemicals and Algae Culture

Tetraselmis (ATCC 50244) was used in all experiments. Once thawed, the culture was incubated under a 14-hour light, 10-hour dark cycle in an environmental chamber at 25°C in autoclaved (121°C for 15 minutes) ATCC Medium 1747 (Sodium glutamate: 1.7 g/L, Sodium glycerophosphate: 0.1 g/L, Cobalamin: 1 µg/L, Thiamine: 1 mg/L, EDTA: 4 mg/L, Iron(III) chloride hexahydrate: 0.196 mg/L, Manganese(II) sulfate monohydrate: 0.656 mg/L, Boric acid: 4.56 mg/L, Zinc sulfate heptahydrate: 88 µg/L, Cobalt(II) sulfate heptahydrate: 19.2 µg/L, Sea Salt: 26.96 g/L). Light was provided by suspending an IPOWERS Super HPS 600 W lamp in the environmental chamber at a distance of 1.1-2.1 m from all culture tubes and flasks in the chamber. The 14h:10h light:dark cycle was controlled using a circuit timer. The culture was maintained by transferring 1 mL of the active culture to 100 mL fresh, sterile growth medium every 3 weeks. The culture was incubated continuously under these conditions for the entire period of the experiments. All chemicals except sea salt were purchased from Sigma-Aldrich. Sea salt was purchased from

Instant Ocean and Reef Crystals. A PowerBiofilm[®] DNA Isolation Kit from MO BIO Laboratories, Inc. was used for extraction of DNA from *Tetraselmis*.

2.3.2 Analytical Methods

Cell concentrations were estimated using a hemocytometer (Hausser Scientific) and a microscope (Nikon Eclipse Ni with Plan Fluor x40 objective). A 96-well plate reader (Perkin Elmer) with 430 nm excitation filter and 680 nm emission filter was applied to quantify fluorescence responses of *Tetraselmis* cultures. Absorbance and transmittance measurements were carried out by a CARY 300 Bio UV-Visible Spectrophotometer and a NANODROP 2000c Spectrophotometer (Thermo Scientific). Incident UV irradiance was quantified using an IL 1700 Research Radiometer (International Light Technologies).

2.3.3 MPN Assay

Samples were serially diluted in autoclaved (121°C for 15 minutes) ATCC Medium 1747, then incubated as described above using the same environmental chamber, with the same lighting and temperature conditions that were used for preparation of the original cultures. Incubation was conducted for a period of up to four weeks, with scoring of individual tubes being performed intermittently during this incubation period. Both visual observation (*i.e.*, appearance of green color against a white background) and fluorescence measurements were applied for scoring of tubes in the MPN assay. The detection limit for the MPN assay was defined based on 0, 0, and 1 positive tubes in the last three dilutions of the series (Clesceri et al., 2005; Gilcreas, 1966). Since the exposed *Tetraselmis* suspensions for the repeated exposure experiments and action spectrum experiments were diluted 20 times and 30 times, respectively, the MPN and detection limit calculations for these two experiments were multiplied by 20 and 30, respectively.

2.3.4 Collimated Beam Reactor

Flat-plate collimated beams (Blatchley, 1997) built around low-pressure (LP) and medium-pressure (MP) mercury lamps were used to deliver UV radiation to aqueous suspensions of *Tetraselmis*. The LP lamp delivered almost monochromatic radiation ($\lambda = 254$ nm) to the samples. The output from the MP collimated beam was optically conditioned using a set of narrow bandpass (bandwidth at half-max ~ 10 nm) optical filters (Andover Corp). For all experiments with the

collimated beam systems, dose delivery was calculated following the approach described by (Bolton et al., 2003). Incident irradiance was measured using a radiometer (IL1700, International Light) that was calibrated for the wavelength of incident radiation. The wavelength chosen for calibration corresponded to the peak in the transmittance spectrum of the optical filter used in the experiment.

2.3.4.1 UV₂₅₄ dose-response behavior of *Tetraselmis* sp.

A *Tetraselmis* suspension in stationary phase was diluted to 200 mL to achieve a cell concentration of roughly 2×10^7 cells/L, as measured by a hemocytometer. This cell concentration represented a compromise between a high concentration of cells and high UV transmittance. The UVT₂₅₄ for cell suspensions at this concentration was approximately 89% through a 1.0 cm optical path. The diluted suspension was magnetically stirred during UV irradiation to keep the culture well-mixed. Each Petri dish (47 mm diameter) was filled with 8 mL diluted suspension prior to irradiation under the collimated beam. Following UV irradiation, the exposed suspensions were serially diluted and incubated according to the MPN assay.

2.3.4.2 Effects of repeated UV exposure on *Tetraselmis* sp.

A *Tetraselmis* suspension in stationary phase was diluted to 200 mL to achieve a cell concentration of roughly 2×10^7 cells/L, as measured by a hemocytometer. The initial concentration was also measured in triplicate using a three-tube MPN assay. Three 8 mL subsamples of the culture were then transferred to 47-mm Petri dishes. All UV exposures were performed based on the same procedure described in 2.3.4.1. Each of the three Petri dishes was exposed to UV₂₅₄ dose of 50 mJ/cm² at the beginning of the experiment, which was defined as day 0. Exposure to a UV₂₅₄ dose of 50 mJ/cm² was repeated once per day (24 hrs) for each of the subsequent 3 days. Between daily exposures, all Petri dishes were incubated under the defined condition described in 2.3.1. For each Petri dish, 0.10 mL samples were collected before and after daily exposure. These 0.10 mL samples were diluted to 2.0 mL, then subjected to the MPN assay to quantify viable cell concentrations.

2.3.4.3 Action spectrum of *Tetraselmis* and absorbance spectrum of extracted DNA

The UV dose-response behavior of *Tetraselmis* was quantified for wavelengths ranging from (nominally) 228 nm – 297 nm using the MP collimated beam with the optical filters described in Figure A-2.

Two 200 mL suspensions with cell concentration of approximately 10^8 cells/L were prepared. Suspension 1 was diluted with ATCC 1747 growth medium, which was applied at wavelengths \geq 254 nm. Suspension 2 was diluted with autoclaved 35 g/L NaCl solution (*i.e.*, a solution that contained no other organic or inorganic dissolved constituents), which was applied at wavelengths 228 nm and 239 nm to allow for workable UV transmittance (UVT) at these wavelengths. For each wavelength, 8 mL of the *Tetraselmis* suspension was exposed to the assigned wavelength based on the steps discussed in 2.3.4.1. Six 100 μ L samples were collected from the suspension before and during UV exposure after each had received a target UV dose. Each 100 μ L sample was diluted to 3.0 mL with ATCC medium 1747 and subjected to an MPN assay for quantification of dose-response behavior at the target wavelength. Given the time-consuming nature of the action spectrum experiment, a 5-tube MPN assay was implemented to improve statistical power over what could have been achieved using the 3-tube assay that was used on other experiments.

In parallel with the action spectrum experiments, DNA was extracted using a DNA Isolation Kit (PowerBiofilm[®], MO BIO Laboratories, Inc). The extracted solution was further purified by adding 1/10 volume of 3 M pH 5.2 sodium acetate and 2.5 volumes of 100% ethanol, followed by 2 hours' storage at -20 °C. The resulting suspension was then centrifuged at 18000 g for 30 min and 4°C, after which the supernatant was discarded. The pellet was resuspended in 1 mL 70% ethanol and spun at 18000 g for 15 min at 4°C. After the supernatant was removed, the pellet was dissolved in 50 μ L DI water and scanned from 400 nm - 200 nm with the Nanodrop spectrophotometer.

2.4 Results and Discussion

The growth behavior of *Tetraselmis* in ATCC Medium 1747 is illustrated in Figure A-3. The culture required roughly 14 days to reach a stationary phase. As a result, a procedure was established whereby 100 μ L of the cell suspension was transferred to 100 mL ATCC Medium 1747 every 2-3 weeks to maintain a robust culture.

Algal suspensions with actively growing cells could be identified visually by a bright green color against a white background; however, sample fluorescence was also used as a surrogate measure for scoring in MPN assay. The results of these measurements are summarized in Table A-1. A

fluorescence signal of 112.4 (arbitrary units) was defined as the upper 99.9% CI for the fluorescence measurements of ATCC Medium 1747 without inoculation. This value was used as the threshold fluorescence signal to discriminate positive (cell growth) from negative (no growth) samples. The numerical value of the threshold fluorescence signal will vary among instruments, but the method described above can be applied generally to determine this value.

2.4.1 MPN Method Validation

A sample of the *Tetraselmis* suspension from log phase growth (cell concentration quantified by hemocytometer with 95% CI: $7.35 \times 10^7 \pm 1.59 \times 10^7$ cells/L) was serially-diluted across a range of dilutions that should have yielded fewer than 1 viable cell per dilution tube. This test, which was conducted in triplicate, allowed for examination of the incubation time required to develop a positive response for samples under these conditions, as well as the validation of MPN assay.

Table 2-2 lists the fluorescence readings (430/680) and visual observation results as a function of time for this test.

The plate reader was able to identify the presence of *Tetraselmis* cells at lower concentration than was possible by visual observations with a naked eye. Therefore, positive tubes were identified earlier by fluorescence than by visual observations. However, the fluorescence measurements required more consumable supplies (pipette tips, 96-well plates) and labor. Therefore, while the plate-reader method offers benefits of improved sensitivity and objectivity in discrimination of positive and negative samples, it is a more costly method than the visual approach, both in terms of supplies and operator time. Ultimately, the results of scoring by use of the plate reader and visual observations yielded identical MPN estimates of the viable *Tetraselmis* cell concentration: 9.3×10^7 cells/L, with a 95% CI of 1.5×10^7 cells/L to 3.80×10^8 cells/L. The results from the hemocytometer method ($7.35 \times 10^7 \pm 1.59 \times 10^7$ cells/L) showed the similar estimates of concentration. Overall, the hemocytometer method yielded a smaller confidence interval, while the MPN method only quantified viable cells.

Table 2-2. Scoring of serially-diluted suspensions of *Tetraselmis* without UV treatment. Numerical values indicate fluorescence readings from the plate reader. Numerical values in **bold font** were scored positive, based on discrimination from background fluorescence of the growth medium. Values highlighted in grey were scored positive by visual inspection.

Dilution Series	Time (days)	Fluorescence counts (430/680) for each dilution factor								
		-1	-2	-3	-4	-5	-6	-7	-8	-9
#1	0	995	208	52	65	54	66	59	65	63
	5	1899	181	72	62	63	75	62	60	67
	14	24155	8887	3271	3325	1454	83	69	58	60
	20	25842	16640	9130	13309	5380	1487	92	101	101
	29	39431	22648	13979	22974	24809	12521	75	59	51
#2	0	1061	83	59	62	70	46	50	58	54
	5	1150	136	73	69	55	62	53	69	53
	14	16621	16621	16621	16621	16621	266	59	56	57
	20	21441	21441	21441	21441	21441	21441	108	97	81
	29	40977	40977	40977	40977	40977	40977	60	57	62
#3	0	984	169	78	60	58	61	50	65	69
	5	2175	175	91	60	56	53	63	45	64
	14	26815	26815	26815	26815	26815	77	71	60	60
	20	36024	36024	36024	36024	36024	95	83	96	103
	29	51668	51668	51668	51668	51668	59	50	64	52

The hemocytometer and MPN assay were also applied to *Tetraselmis* suspensions that were prepared for the UV₂₅₄ dose-response experiments. These results indicated cell concentration estimates based on hemocytometer of 1.97×10^7 cells/L (95% C.I. = $1.19 \times 10^7 - 2.67 \times 10^7$ cells/L) and by the MPN assay of 1.86×10^7 cell/L (95% C.I. = $3.00 \times 10^6 - 7.60 \times 10^7$ cells/L). Collectively, these findings suggest that the majority of *Tetraselmis* cells in suspension were cultivable for the conditions of incubation that were used in this work.

The result of the incubation time experiment suggested an incubation time of at least 3 weeks for untreated samples. However, the impact of UV exposure on cell growth was not incorporated into

this test. Therefore, incubations for UV-treated samples (described below) were conducted for a period of 4 weeks (28 days) to ensure that all samples had adequate time for growth to occur.

The MPN assay has the benefit of providing a direct measure of growth of the target microbe. Since growth (*i.e.*, reproduction) is required for an invasion, culture-based assays like MPN appear to be well-suited to UV-based treatment methods. However, other culture-based assays could be applied, such as plate counting.

Olsen *et al.* (Olsen et al., 2016) examined the use of MPN and plate counting (together with flow cytometry) for quantification of UV dose-response behavior of *Tetraselmis suecica* (see A-1). For UV doses ranging from 0-800 mJ/cm², the magnitudes of the errors associated with these three methods were similar. Error estimates by each of these methods can be reduced by inclusion of more replicates in the analysis.

2.4.2 UV₂₅₄ Dose-response Behavior of *Tetraselmis* Cells Under a Collimated Beam

In the quantification of UV₂₅₄ dose-response behavior of *Tetraselmis* with the collimated beam reactor, a three-tube MPN assay was applied. The UV₂₅₄ dose-response behavior of *Tetraselmis* cells, as measured with the collimated beam reactor is illustrated in Figure 2-1. More details are listed in Table A-2.

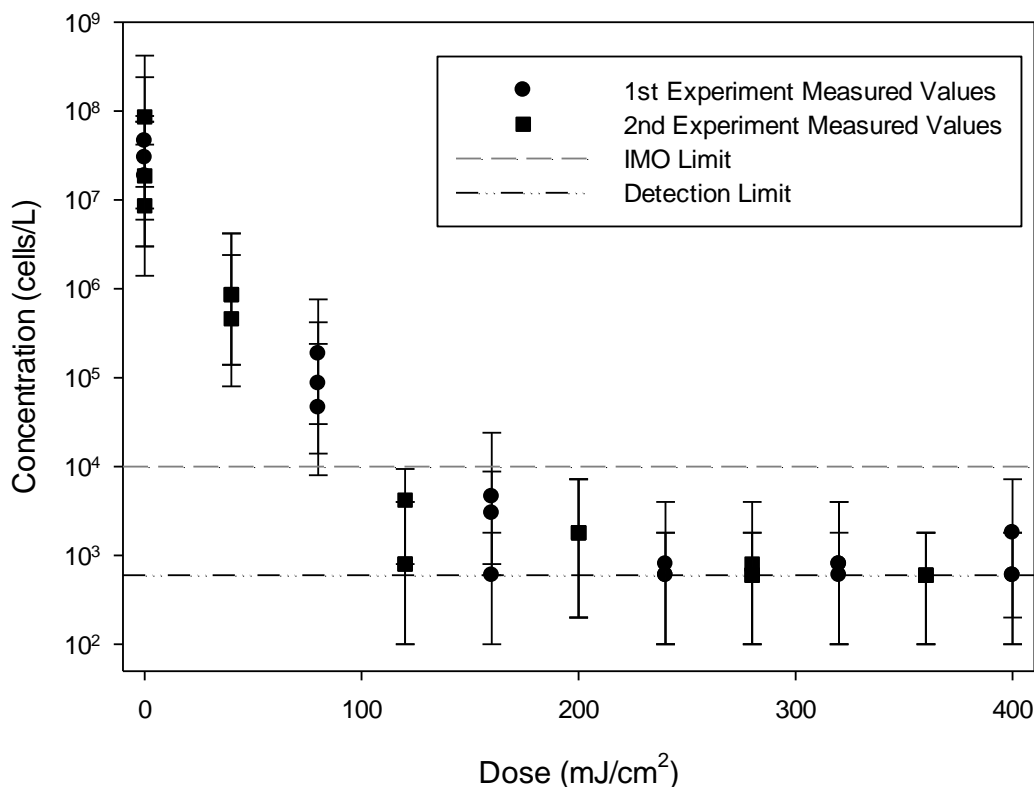


Figure 2-1. UV₂₅₄ dose-response of *Tetraselmis* as measured with flat-plate collimated beam reactor. Symbols represent the MPN for replicate measurements of each sample, while error bars represent the corresponding 95% CI. The horizontal, dash-dot line represents the limit of detection for the MPN method; the horizontal, dashed line indicates the regulatory limit for phytoplankton, as defined by the IMO.

The results of this test indicate roughly log-linear behavior for applied UV₂₅₄ doses up to approximately 120 mJ/cm². Dose values above this range yielded little or no change in the concentration of viable cells because all samples indicated viable cell concentrations at or below the limit of detection for the method.

The data in the UV₂₅₄ dose range 0-120 mJ/cm² indicated essentially first-order behavior, which is consistent with a single-event model:

$$\frac{dN}{dD} = -KN$$

N	=	concentration of viable cells (cells·L ⁻¹)
D	=	average UV dose received by the cell suspension (mJ·cm ⁻²)
K	=	inactivation constant (cm ² ·mJ ⁻¹)

The data from Figure 2-1, corresponding to doses ranging from 0-120 mJ/cm², were fitted to a single-event model using linear regression of the ln-transformed data, in the form of $\ln\left(\frac{N}{N_0}\right)$ vs. *Dose*. The result of this analysis was an inactivation constant (aka, germicidal factor) estimate of 0.0792 cm²/mJ ($R^2 = 0.924$). For perspective, Chevrefils *et al.* presented a critical review of UV dose-response behavior for common waterborne microbial pathogens and (non-pathogenic) indicator and challenge organisms (Chevrefils et al., 2006). Inactivation rate constants for common classes of waterborne microbes were as follows:

For viruses exposed to 254 nm radiation, reported inactivation constants ranged from 0.0122 cm²/mJ (Hepatitis IPNV) to 0.847 cm²/mJ (Reovirus T4) (Bohrerova et al., 2008; Liltved et al., 2006).

For bacteria, UV₂₅₄ dose-response behavior is strongly influenced by the form of the bacterial population, either as vegetative cells or spores. As an example, a representative inactivation constant for the spores of *Bacillus cereus* is 0.021 cm²/mJ (Clauß, 2006). In contrast, reported inactivation constant for vegetative *Bacillus cereus* cells was 0.306 cm²/mJ (Clauß, 2006). Additionally, reported inactivation constants for vegetative bacterial cells ranged from 0.017 cm²/mJ (*Deinococcus radiodurans*) to 1.41 cm²/mJ (*Vibrio cholerae*) (Clauß, 2006; Wilson, 1992). Given that *E. coli* and *Enterococci* are included in the IMO and USCG regulations, it is also relevant to consider their inactivation responses. Hijnen et al. reported an inactivation constant of 1.17 cm²/mJ for *E. coli* (Hijnen et al., 2006). The inactivation constant for *Enterococcus faecium* was reported to be 0.287 cm²/mJ (McKinney et al., 2012). Generally speaking, vegetative bacterial cells are effectively inactivated by UVC doses that are far lower than those required for inactivation of algal cells. Therefore, the use of UVC irradiation in ballast water treatment is likely

to be effective for control of bacteria in ballast water, including the target organisms *E. coli* and *V. cholerae* that are included in ballast water discharge regulations.

Protozoa have been reported to demonstrate a broad range of sensitivity to UV₂₅₄ irradiation. Reported inactivation constants for protozoa range from 0.031 cm²/mJ (*Acanthamoeba castellanii*) to 0.298 cm²/mJ (*Toxoplasma gondii*) (Cervero-Aragó et al., 2014; Ware et al., 2010).

Algae have been reported to be quite resistant to UV₂₅₄ irradiation. Reported inactivation constants for algae range from 0.0038 cm²/mJ (*Tetraselmis suecica*) to 0.055 cm²/mJ (*Microcystis aeruginosa*) (Olsen et al., 2015; Sakai et al., 2011).

The results presented in Figure 2-1 indicate that *Tetraselmis* cells are roughly 6X more sensitive to UV₂₅₄ irradiation than the most resistant virus (Hepatitis IPNV), at least 3X less sensitive than most vegetative bacterial cells included in the regulations, roughly 2X more sensitive than the most resistant protozoan species (*Acanthamoeba*), and roughly 20X more sensitive than the most resistant algae (*Tetraselmis suecica*). *Tetraselmis* cells are generally more resistant to UV₂₅₄ irradiation than most other microbes that are commonly used as challenge organisms in UV reactor validation studies. As such, *Tetraselmis* cells and the MPN assay may be appropriate for validation of UV reactor systems that are intended for ballast water treatment applications. However, the practical UV₂₅₄ dose range that will apply in the use of *Tetraselmis* will be limited to reduction equivalent dose (RED) of 120 mJ/cm² or less, unless other methods of culturing and exposing the algal cells to UV₂₅₄ irradiation are applied.

It is also relevant to consider the limit of detection for the MPN method in this experiment in the context of the IMO limit for phytoplankton cells. As illustrated in Figure 2-1, the limit of detection for the method is roughly an order of magnitude lower than the IMO limit for these cells. As such, measurements of viable phytoplankton concentrations by this method can reach well below the regulatory limit.

Another issue to consider is the starting cell concentration in this experiment, which was on the order of 10⁷-10⁸ cells/L. The range of applicable doses to which a *Tetraselmis* suspension can be

exposed to UV₂₅₄ radiation, while still yielding viable cells at a concentration above the detection limit for the MPN method, will be influenced by the starting cell concentration. As the initial cell concentration increases, a larger range of UV₂₅₄ doses can be applied before reaching the limit of detection. However, as the cell concentration increases, UVT₂₅₄ will decrease (UVT₂₅₄ as a function of *Tetraselmis* cell concentration is described in Figure A-4). For the conditions used in this experiment, UVT₂₅₄ was approximately 90% (1.0 cm optical path length), which represents a desirable attribute for UV-based water treatment applications. Lower transmittance values can be accommodated by UV systems, but the amount of UV power required to meet a given treatment objective will increase.

Also for perspective, it is relevant to consider the concentrations of algae that exist in the world's oceans and freshwater systems. The highest algal cells concentrations tend to be associated with algal bloom events. Reported cell concentrations in bloom events range from 10⁴-10⁶ cells/mL (10⁷-10⁹ cells/L) (Villacorte et al., 2015). The cell concentrations used in this research were in the middle of this range. Therefore, application of UV-based processes for control of *Tetraselmis* may be relevant, even when ballast water is taken from a body of water that is experiencing a bloom event. It is less clear that this generalization will apply to blooms of other algae, as information regarding UVT as a function of cell concentration is not available.

2.4.3 Effects of Repeated UV Exposure

One advantage of UV-based exposure is the opportunity it presents to accomplish repeated exposures of ballast water by employing a recirculating system or by ballasting and de-ballasting operations, either in a ship-based platform or on-shore, which could reduce the size of the UV system used for treatment. To examine this issue, an experiment was conducted to quantify the result of repeated exposures of *Tetraselmis* to UV₂₅₄ irradiation.

A *Tetraselmis* suspension with an initial cell concentration (counted by hemocytometer) of 1.41×10^8 cells/L \pm 1.81×10^7 cells/L (95% CI) was prepared. Before and after each exposure to UV₂₅₄ radiation, the suspension was sampled and subjected to a 3-tube MPN assay. The results are presented in Figure 2-2.

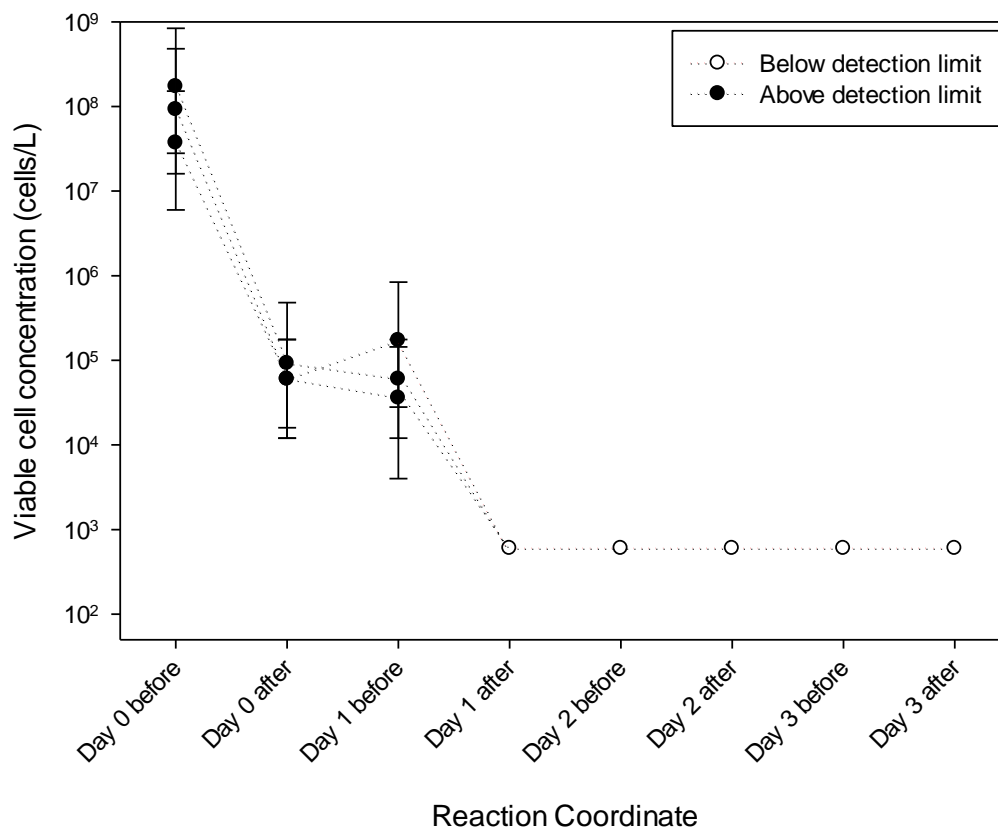


Figure 2-2. Responses of *Tetraselmis* cells to repeated UV₂₅₄ irradiation. Suspended *Tetraselmis* cells were subjected to a UV₂₅₄ dose of 50 mJ/cm² on each day of the experiment.

On day 0 of the experiment, the concentration of viable *Tetraselmis* cells was reduced by roughly 3 log₁₀ units in all three replicates as a result of UV₂₅₄ irradiation (UV₂₅₄ dose = 50 mJ/cm²). After one day of incubation, the MPN value from all replicates did not experience a statistically significant change from the preceding value. Following UV₂₅₄ irradiation on day 1 (second UV exposure of 50 mJ/cm²), no viable *Tetraselmis* cells were observed in the MPN assay, which indicates at least 2 additional log₁₀ units of inactivation (roughly 5 log₁₀ units total). From this point on in the experiment, the viable cell concentration was below the limit of detection.

Since *Tetraselmis* did not show apparent resistance to repeated UV exposure and little evidence of repair, repeated UV exposures, such as could be accomplished by recirculation during a voyage or by treating water during ballasting and de-ballasting operations, could yield relevant benefits for

control of phytoplankton. Additional data are needed to validate this strategy for waterborne microorganisms that are candidates for potential invasion via ballast water discharge.

MPN assay results are indicated for samples that were collected before and after UV₂₅₄ exposure on each day of the experiment. Solid symbols indicate samples where the viable cell concentration was above the limit of detection; open symbols indicate samples where the viable cell concentration was below the limit of detection.

2.4.4 Action Spectrum of *Tetraselmis* and Absorbance Spectrum of Extracted DNA

Nucleic acid damage caused by UV irradiation is most effective at wavelengths close the absorbance maximum of nucleic acids, usually in the vicinity of 265 nm (USEPA, 2006). Low-pressure Hg lamps are efficient generators of UV radiation at a characteristic wavelength of 254 nm, which makes them effective for inactivation of microbes by causing damage to nucleic acids. However, some organisms experience damage to other important biomolecules such as proteins and lipids (Santos et al., 2013). When combined with the fact that polychromatic UV sources (e.g., medium-pressure Hg lamps) are commonly used, there is interest in understanding the wavelength-dependence of UV dose-response behavior for microbes that could be used as challenge organisms in reactor validation experiments. The action spectrum of *Tetraselmis* was quantified for wavelengths ranging from (nominally) 228 nm – 297 nm. Two cell suspensions were developed as described in 2.3.4.3, the initial cell concentrations of suspension 1 and suspension 2 (95% CI) were 1.34×10^8 cells/L ($\pm 3.85 \times 10^7$ cells/L), and 1.34×10^8 cells/L ($\pm 3.37 \times 10^7$ cells/L), respectively. Figure 2-3 provides a graphical summary of the results of this experiment in the form of viable cell concentration as a function of UV dose for each wavelength applied.

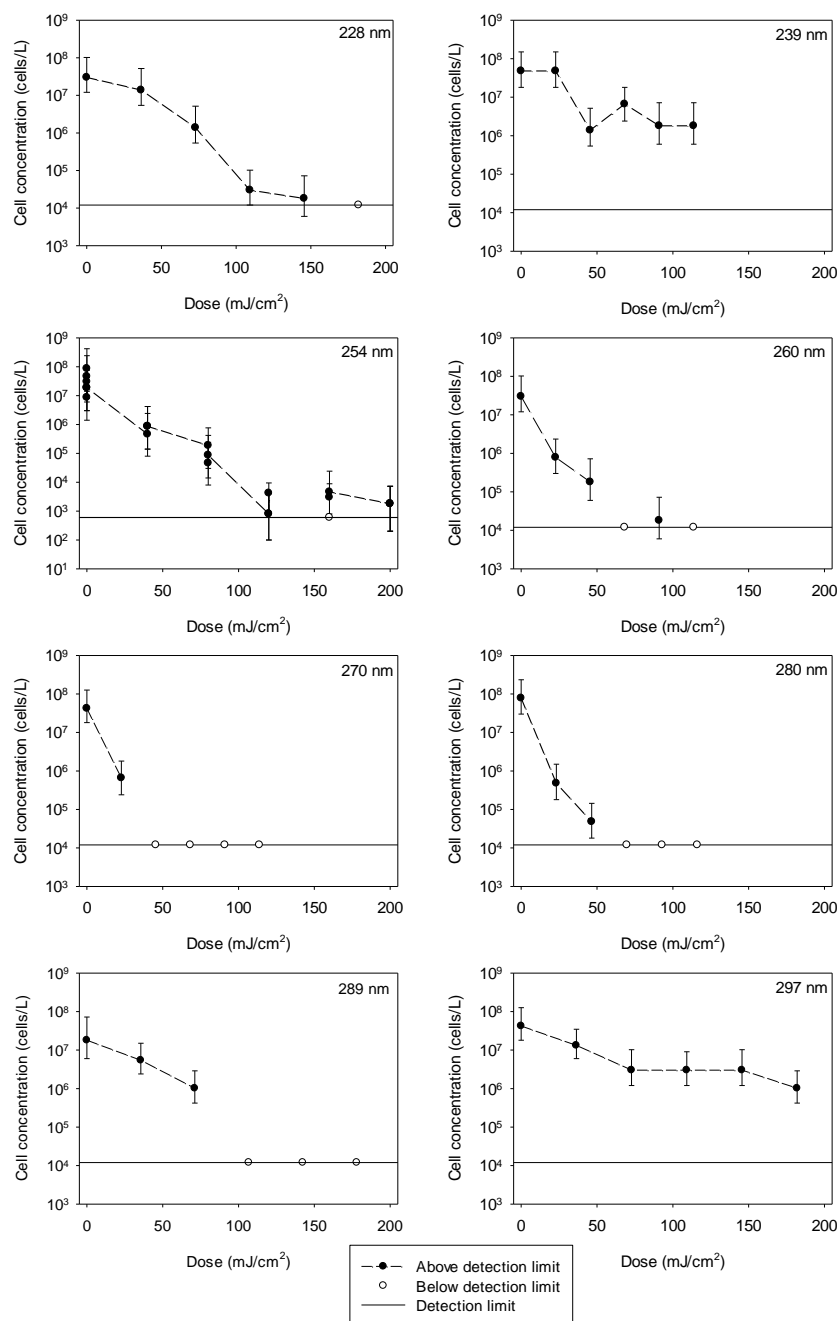


Figure 2-3. Viable *Tetraselmis* cell concentration as a function of UV dose. Data points indicate MPN for each condition; error bars represent the 95% CI for each measurement. The horizontal line indicates the limit of detection for the method. Open black circles indicate measurements that are below the limit of detection.

Measured values of viable *Tetraselmis* cell concentration up to the first data point below detection limit at each wavelength were fitted to a single-event model using linear regression of the

transformed data, in the form of $\ln\left(\frac{N}{N_0}\right)$ vs. *Dose*, as described in section 2.4.2. Figure 2-4 illustrates the inactivation constants as a function of wavelength; also included in this figure is the absorption spectrum of DNA extracted from *Tetraselmis*.

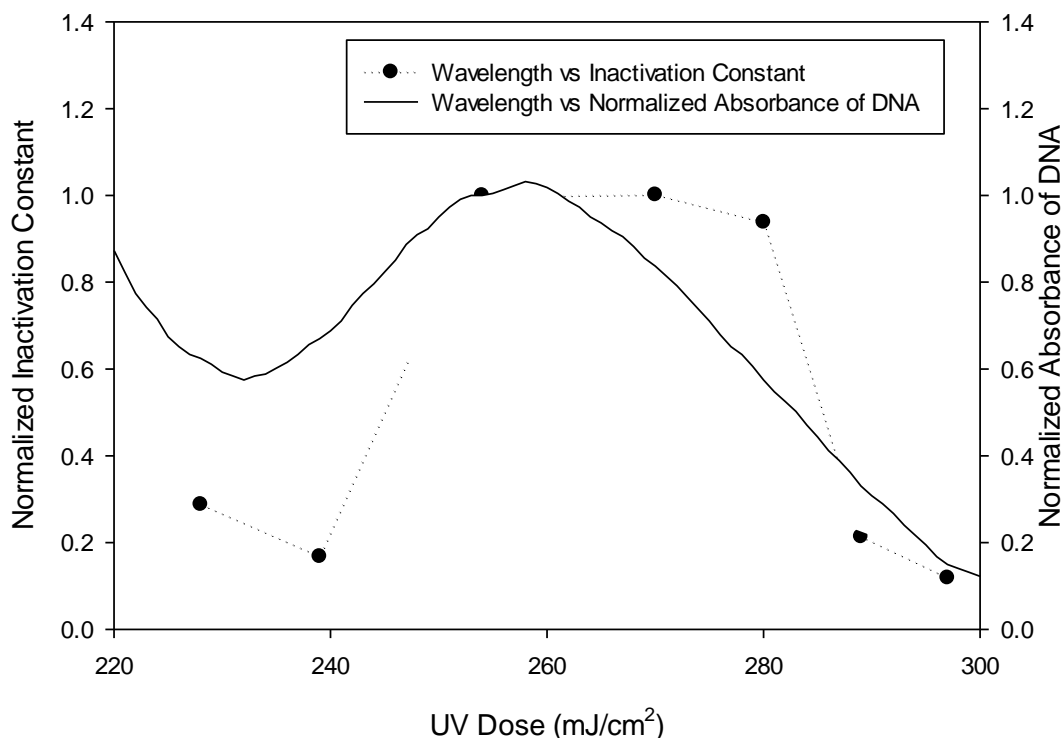


Figure 2-4. UV inactivation action spectrum for *Tetraselmis* cells and Absorption Spectrum of Extracted DNA. Both absorbance of DNA and inactivation constants were normalized to their corresponding values at 254 nm.

The action spectrum for *Tetraselmis* has a shape that is characteristic of inactivation responses for which the dominant mechanism of inactivation is DNA damage. The action spectrum had essentially flat behavior from 254 nm to 280 nm. The absorption spectrum for DNA showed a peak in the vicinity of 260 nm, with decreasing values at wavelengths above and below this wavelength. One possible explanation for the similar inactivation behavior at wavelengths from 260 nm to 280 nm was lack of resolution at these wavelengths. The sparse data sets obtained at these wavelengths are likely to introduce error in the estimation of a rate constant based on regression analysis. Further experiments with refinement of dose delivery at lower range may reduce this error. Also,

the nominal wavelengths applied in the action spectrum experiment were based on peak transmittance of the optical filters applied in this work which had a band width (at half-max) of approximately 10 nm, which yielded some overlap among the applied wavelengths.

The most effective wavelengths for inactivation of *Tetraselmis* were from 254 nm to 280 nm, which included the absorbance peak of DNA at around 260 nm. The inactivation constant generally decreased at wavelengths above or below this range; however, there was some evidence of an increase of inactivation efficiency at wavelengths below approximately 240 nm. These wavelengths have been associated with damage to both DNA and proteins. However, radiation at these short wavelengths is often poorly transmitted in aqueous media. Therefore, the transmittance of *Tetraselmis* suspension at different concentrations as well as the supernatant after centrifugation were scanned from 400 nm to 200 nm. Details are described in Figure A-5, and the results showed that a number of constituents in water absorb strongly at wavelengths below 240 nm.

The results of this action spectrum experiment indicate that UV sources that generate radiation in the range from 254 nm to 280 nm will be the most efficient for inactivation of *Tetraselmis*. On the other hand, it is not clear that the action spectrum for *Tetraselmis* will translate to other phytoplankton species. Additional work is needed to define the behavior of other phytoplankton species that could contribute to invasions in connection with ballast water management.

The deviations between the DNA absorption and action spectra may also be an indication that *Tetraselmis* inactivation involves photochemical damage to DNA and other critical biomolecules. Ou *et al.* (Ou et al., 2012; Ou et al., 2011) demonstrated that UV₂₅₄ radiation is capable of degrading chlorophyll-a and proteins that are critical to photosynthesis among *Microcystis aeruginosa*. However, the UV₂₅₄ doses required to cause this damage were 1-2 orders of magnitude greater than those applied herein. At UV₂₅₄ doses in the range of 0-120 mJ/cm², little or no damage to these biomolecules that are critical to photosynthesis was reported by Ou *et al.* (Ou et al., 2012; Ou et al., 2011). No measurements of damage to specific biomolecules were included in our work, but the data presented in Figure 2-4 suggests that photochemical damage to biomolecules other than DNA may have contributed to inactivation of *Tetraselmis*.

2.5 Conclusions

Tetraselmis and MPN assay appear to be well-suited for validation studies of UV systems. *Tetraselmis* is fairly resistant to UVC radiation, with UV₂₅₄ dose-response behavior that is intermediate to other organisms that are environmentally-relevant or that are used in validation of UV-based systems that are designed for other endpoints. The MPN assay provides a relevant measurement endpoint for quantification of the behavior of UV systems used in ballast water treatment, as it provides a direct indication of the ability of an organism to grow, a condition that will be required for an invasion to occur.

The UV₂₅₄ dose-response behavior of *Tetraselmis* cells followed a single-event (i.e., 1st order) kinetic model to the point where the limit of detection for the MPN assay was reached. For the experimental conditions used in this research, this corresponded to roughly 4.5-5 log₁₀ units of inactivation for UV₂₅₄ doses up to approximately 120 mJ/cm². These conditions yielded viable *Tetraselmis* cell concentrations that were roughly an order of magnitude lower than the IMO limit for phytoplankton. Additionally, repeated UV exposure, such as could be accomplished via application of a recirculating UV system, appears to have merit for control of *Tetraselmis*.

The UV inactivation action spectrum for *Tetraselmis* has a shape that is characteristic of inactivation being associated with damage to cellular DNA. However, the imperfect agreement in the shapes of the action and DNA absorption spectra of *Tetraselmis* suggest that biomolecules other than DNA may contribute to UV-induced inactivation. Optimum inactivation of *Tetraselmis* was achieved at wavelengths in the range from 254 nm to 280 nm. As such, there may be merit to the use of UV sources that emit predominantly in this wavelength range.

The behavior of *Tetraselmis* under exposure to UV in ballast water systems provides performance information of algal inactivation with UV. As contamination with unwanted algae is a serious problem for algal cultivation to maintain a stable culture of desired alga (Day et al., 2012; Lammers et al., 2017; Rodolfi et al., 2009), our results provided important information to use UV to control invading algae in algal cultivation systems.

CHAPTER 3. UV INACTIVATION OF ALGAL VIRUSES TO PROTECT ALGAL PRODUCTIVITY

3.1 Abstract

In addition to competing algal species, one of the main challenges in algal biofuel production is collapse of an algal culture caused by predators or parasites, which may enter the cultivation systems with water collected from natural water sources. Algal viruses, as one type of algal parasite, have been reported to be responsible for algal mortality in both natural algal blooms and mesocosm experiments. A considerable body of research has been conducted to isolate highly efficient strains or genetically modify algae to minimize the impact of parasites, but only limited studies have been done on controlling algal parasites in cultivation systems. In this study, UVC-irradiation that is commonly applied in water treatment was evaluated for its efficiency of inactivating algal viruses.

Algal virus PBCV-1, which can infect freshwater algal species *Chlorella sp.*, was selected as a challenge parasite. The concentration of infective algal virus was quantified by plaque assay and UVC-induced DNA damage was quantified by real-time quantitative PCR. UV₂₅₄ dose-response behavior of PBCV-1 was investigated using a collimated beam system equipped with a low-pressure Hg lamp. UV dose-response behavior at different UV wavelengths (*i.e.*, action spectrum) was quantified using a collimated beam device that used a medium-pressure Hg lamp as the radiation source, along with a series of narrow bandpass optical filters. The results showed that a UV₂₅₄ dose of 140 mJ/cm² results in roughly 5 log₁₀ units of inactivation of PBCV-1 and dose of 60 mJ/cm² is sufficient to inactivate all PBCV at environmental concentrations (1-100 PFU/mL). The inactivation constants of PBCV-1 under UV₂₅₄ were 0.040 cm²/mJ based on infectivity and 0.011 cm²/mJ based on DNA damage. The UV inactivation action spectrum for PBCV-1 indicated that the optimum inactivation wavelength for PBCV-1 was 214 nm. The results in this study indicated that UV irradiation is an effective approach for inactivation of algal viruses and suggested that UV irradiation can be leveraged to reduce potential culture collapse in algal cultivation systems and improve algal culture stability for biofuel production.

3.2 Introduction

The rapid depletion of fossil fuels and increase of CO₂ emissions motivate the development of alternative energy sources that are sustainable and environmentally friendly (Chisti, 2008). Among all the biofuel sources, microalgae have attracted much attention due to their high growth rate, low arable land use, and high lipid content, relative to other energy crops (Alam et al., 2012; Brennan & Owende, 2010; H. Chen et al., 2015; Kirrolia et al., 2013). However, one of the major limitations that impede the development of cost-effective biofuel production is maintaining a stable algal culture in open cultivating systems (Rodolfi et al., 2009). Invasion of unwanted organisms such as bacteria, viruses, fungi, algae, and grazers can lead to productivity decrease or even culture collapse in algal cultivation systems (Bartley et al., 2013; Day et al., 2012; Lammers et al., 2017).

Viruses have been reported to play important roles in the mortality of microalgae in both the natural environment and mesocosm systems (Larsen et al., 2008; Lawrence, 2008). Viruses, the most abundant biological entities in aquatic systems, are able to cause the lysis of every major algal phylum (Day et al., 2012; Gachon et al., 2010; Lawrence, 2008). It has been reported that viral lysis can account for up to 100% mortality of marine alga *Emiliana huxleyi* (Bratbak et al., 1993). One study on lytic viruses (PgV) and their infections on algal species *Phaeocystis globosa* indicated that viral infection played an important role in *P. globosa* dynamics and the diversity of both host and virus community (Baudoux et al., 2005). A study on the brown tide showed that viruses may be a major source of mortality for brown tide blooms in regional coastal bays of New Jersey and New York (Gastrich et al., 2004). Other studies have shown that viruses can control host algal populations and have significant impact on the life-and-death dynamics of algal blooms (Fuhrman, 1999; Gachon et al., 2010; Lehahn et al., 2014; Van Etten & Dunigan, 2012). As water used for algae cultivation are usually collected from natural water systems, invading viruses in natural water may invade algal cultivation systems and significantly reduce the yield of algal biomass.

So far, there are only few methods to prevent invasion of unwanted organisms in algal cultivation systems (Day et al., 2012). Becker proposed an approach to shift pH to prevent the invasion of rotifers and other zooplankton (Becker, 1994). Bartley *et al.* proposed a method to control invading organisms by adjusting salinity during the cultivation of *Nannochloropsis salina* (Bartley et al.,

2013). However, to the best of our knowledge, there is no effective strategy in the literature for preventing viral invasion in algal cultivation systems. As a result, there remains a critical need to manage algal culture contamination by invading organisms, especially viruses.

UV irradiation is a broad-spectrum disinfection technique since it can cause damage to various biomolecules, such as nucleic acids, lipids, and proteins (Hijnen et al., 2006). UV-induced damage may not be lethal to individual organisms but may stop them from reproducing (Blatchley et al., 2001), which is required for a successful invasion. UV radiation has been commonly applied in water treatment to inactivate bacteria, protozoa, viruses, and algae (Malayeri et al., 2016). Many previous studies have focused on the UV responses of pathogens and organisms that are ecologically harmful, while the UV dose-response behavior of algal viruses remains largely unknown. Therefore, it is necessary to investigate the responses of algal viruses to UV irradiation; the results of this investigation will promote the application of UV in algal cultivation systems.

The objective of this study was to examine the performance of UV irradiation as a process for control of invading algal viruses. PBCV-1 was used as a challenge organism for UV treatment, as it is widely spread throughout the world and can infect *Chlorella* sp. (Van Etten & Dunigan, 2012), which has been often used in biofuel production (Chisti, 2007; Zhang et al., 2015). The genome of PBCV-1 has been fully sequenced and thus molecular biotechnology tools could be applied to investigate the inactivation mechanisms (Etten, 2003). Furthermore, the UV-dose response behavior of PBCV-1 was investigated at various wavelengths to identify the most effective wavelength to inactivate the virus. The results of this study will be important for development of effective strategies for controlling invading organisms among algal cultivation systems.

3.3 Materials and Methods

3.3.1 Microalgal Cultures and Growth Conditions

The fresh water microalgal strain *Chlorella* sp. (ATCC 50258) was used as a representative algal strain and cultivated in ATCC 847 growth medium at 25 °C. ATCC medium 847 contains 1.0 g Proteose Peptone, 250 mg NaNO₃, 25 mg CaCl₂, 75 mg MgSO₄, 75 mg K₂HPO₄, 175 mg KH₂PO₄, 25 mg NaCl, and a drop of 1.0% FeCl₃ solution in 1.0 L distilled water. Algal growth was

quantified with a hemocytometer (Hausser Scientific) and a fluorescence microscope (Nikon Eclipse Ni with Plan Fluor x40 objective).

3.3.2 Plaque Assay and Algal Virus Isolation

A water sample containing *Chlorovirus* was collected from the Celery Bog Nature Area, West Lafayette, IN. The collected water sample was filtered through a syringe filter with a 0.2 μm PTFE membrane (Thermo Scientific) to remove non-viral particles. Then *Chloroviruses* in the filtrate were isolated by the modified plaque assay method (Van Etten, Burbank, Kuczmarski, et al., 1983). A mixture of 100 μL diluted filtrate (approximately 50 PFU per 100 μL), 300 μL *Chlorella* cells (2×10^8 to 4×10^8 cells/mL), 100 μL erythromycin stock (1000 mg/L) and 5 mL of soft-agar medium was poured onto a 1.5% agar plate. Agar medium (1.5%) and soft-agar medium (0.75%) were prepared with ATCC 847 medium for the plaque assay. After one week of incubation at 25°C, viral plaques that formed on the agar plate were counted. *Chlorovirus* from a single plaque on the algal lawn was isolated and enriched. To maintain algal viruses, 300 μL filtrate was added to 100 mL host microalgae culture (3×10^7 to 7×10^7 cells/mL). After three days' incubation, a new virus stock was prepared by filtering the virus-rich suspension through a 0.2 μm syringe filter. Viral rich filtrates were stored at 4°C for future use.

The type of *Chlorovirus* from a single plaque was identified by polymerase chain reaction (PCR). A freeze-thaw pretreatment procedure consisting of three cycles of heating at 95°C for 2 mins and freezing to solid was carried out to release viral DNA. Four *Chlorovirus*-specific primers listed in Table 3-1 (Short et al., 2011) were examined to identify the isolated *Chlorovirus*. Each 50 μL PCR reaction contained 2 μL of pretreated sample, 10 μM virus-specific PCR primers, DreamTaq DNA Polymerase, and 10X DreamTaq green buffer. Negative controls were used with DI water instead of sample, while all other conditions remained the same. All PCR reactions were performed in a Biorad 1000-Series Thermal Cycler with denaturation at 95°C for 2 min, followed by 39 cycles of heating at 95°C for 30s, annealing at primer-specific temperatures (Table 3-1) for 45s and extension at 72°C for 1 min. At the end of cycling, all PCR reactions were subjected to a final extension step at 72°C for 30 min. After PCR, 8 μL of the reaction product were loaded into 1.5% Bio-rad Certified™ agarose gel stained with SYBR safe stain and subject to electrophoresis in a

Bio-Rad electrophoresis cell. The electrophoresis results were obtained by Bio-Rad Gel Doc™ XR+ with Image Lab™ software.

Table 3-1. PCR primers to target algal viruses

Primer name	Forward primer	Reverse primer	Annealing temperature (C)	Amplicon size (bp)
CVMS	AAGAAGGGAGCAT ACTTCACGC	CAAATGTAAGGG TAATAGATCTTC	50	645
PBCVS	CTTATCGCAGCTCT CGATTTTG	GTTCGGTGCTCGGA AATCCTTC	44	600
ATCVS	AAGAAAGGTGCCTA CTTTGAAC	AGGTCGTTCCGGAGC TTTGTACT	48	610
CHLV	CCWATCGCACGWC TMGATTTTG	ATCTCVCCBGCVAR CCACTT	52	560+

The morphology of isolated virus PBCV-1 was observed under a Tecnai T12 transmission electron microscope (TEM). Samples were prepared by the Purdue Electron Microscopy Facility modified from a method described previously (Greiner et al., 2009). Target algal suspensions (infected or control) were centrifuged to obtain an algal pellet and fixed with a cacodylate-buffered (pH6.8) 2% glutaraldehyde and 2% formaldehyde solution. After washing in buffer, samples were post-fixed in the same buffer with 2% OsO₄. The samples were dehydrated in a series of graded acetone and then embedded in Embed 812 Resin. Diamond knives were used to acquire ultrathin sections. The ultrathin sections were stained with uranyl acetate and lead citrate for TEM observation.

3.3.3 Quantification of UV-induced Damage on Viral DNA with qPCR

In this study, two qPCR primer sets with different amplicon sizes were used. One primer set was PBCVs (600 bp) (Table 3-1) and the other primer set was designed in this study using PrimerQuest Tool from Integrated DNA Technologies. The genomic sequence of *Chlorovirus* PBCV-1 was obtained from NCBI and protein coding gene sequence of A185R was used. The forward and reverse sequences of this new primer set 185R1 (107 bp) are ACTACGCAATTCCTGACGATAAG and GAGAGCTGCGATAGGTGTAAAG.

Each 20 µL qPCR reaction contained 1 µL of the pretreated sample, 10 µL Biorad supermix, 1 µL qPCR primers, and 7 µL water. Negative controls were conducted with distilled water instead of a DNA sample. All qPCR reactions were performed in a Bio-Rad CFX96™ Real-Time System;

the reaction sequence began with denaturation at 95°C for 3 min, followed by 39 cycles of heating at 95°C for 5s, annealing and extension at 60 °C for 30s. Standard curves for qPCR were generated from a set of eight-fold serially diluted standards (ranging from 4.06×10^9 to 4.06×10^2 gene copies per μL).

3.3.4 Collimated Beam Reactor

Collimated beam reactors (Blatchley, 1997) equipped with low-pressure (LP) and medium-pressure (MP) mercury lamps were used to deliver UV radiation at various wavelengths to PBCV-1 solutions. UV radiation delivered by LP lamp was almost monochromatic at 254 nm. A collimated beam reactor equipped with a MP lamp was tuned by a set of narrow bandpass optical filters (Andover Corp) to deliver UV radiation at specific wavelengths ranging from 214 nm to 310 nm. The applied UV irradiance was measured by an IL 1700 Research Radiometer (International Light Technologies). The calculation of dose delivery was based on the approach described in a previous study (Bolton & Linden, 2003).

3.3.5 UV₂₅₄ Dose-response Behavior of Algal Virus PBCV-1

Virus stock was diluted in nanopure water to a virus concentration of approximately 3×10^7 PFU/mL, which was quantified by plaque assay. The UV transmittance of the diluted virus suspensions at 254 nm was around 97% with 1 mm optical pathlength. For each experiment, a Petri dish with 47 mm diameter was filled with 8 mL virus suspension and mixed by a magnetic stirrer. UV₂₅₄ irradiation was imposed on the samples using a LP collimated beam. Samples of 150 μL were collected from the suspension before and during UV exposure after each target UV dose was achieved. Then 50 μL sample was treated with freeze-thaw pretreatment and then quantified by qPCR. The remainder of the sample was serially diluted and quantified by plaque assay.

3.3.6 Action Spectrum of Algal Virus PBCV-1

UV dose behavior of PBCV-1 was examined for wavelengths from 214 nm to 310 nm using the MP collimated beam reactor equipped with optical filters. The transmittance spectra of the optical filters were characterized using a CARY 300 Bio UV-Visible Spectrophotometer, as illustrated in Figure B-1 in Appendix B. Virus suspensions were prepared with a concentration around 3×10^6 PFU/mL to maintain high transmittances for all wavelengths. The transmittance of virus

suspension was measured by a Nanodrop 2000c Spectrophotometer (Thermo Scientific). The exposure experiments for each wavelength were conducted based on the procedure described in 3.3.5.

3.4 Results and Discussion

The algal virus used in this study was isolated by plaque assay (Figure 3-1) and one single plaque on the algal lawn was harvested and examined by PCR with *Chlorovirus*-specific primer sets. According to the gel electrophoresis result (shown in Figure 3-1), two bands appeared at 600 bp that were consistent with the reported amplicon sizes (Short et al., 2011), which indicated the presence of PBCV-1.

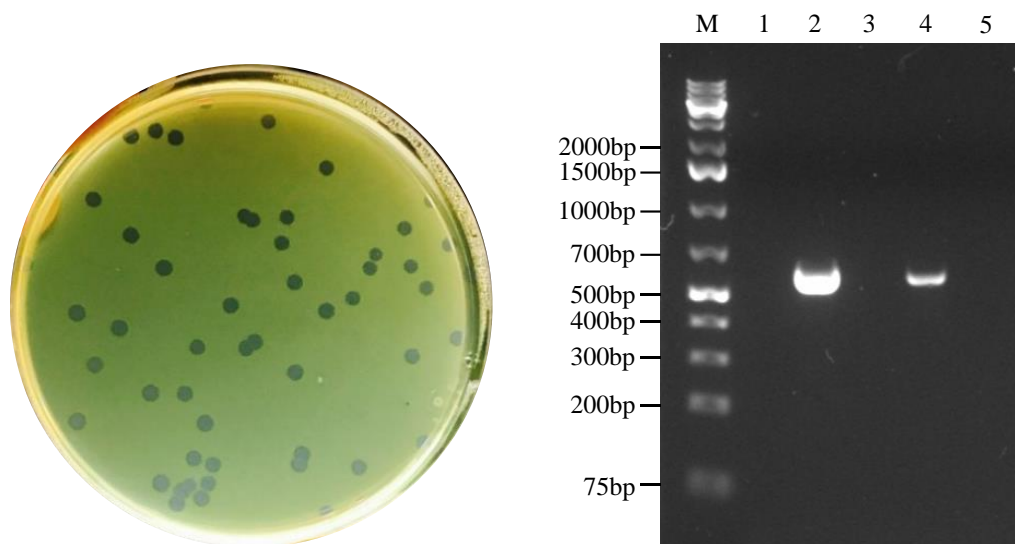


Figure 3-1. Pictures of plaque assay (left) and gel electrophoresis result (right). Lane M: DNA marker; lane 1: CVMs; lane 2: PBCVs; lane 3: ATCVs; lane 4: CHLVs; lane 5: negative control.

The morphology of healthy and infected *Chlorella* cells was observed by TEM (Figure 3-2). The virus particles with hexagonal shape identified with red arrows were easily identified in infected cells. The size of the virus particles was roughly 100 nm, which was in agreement with reported value in the literature (Meints et al., 1986).

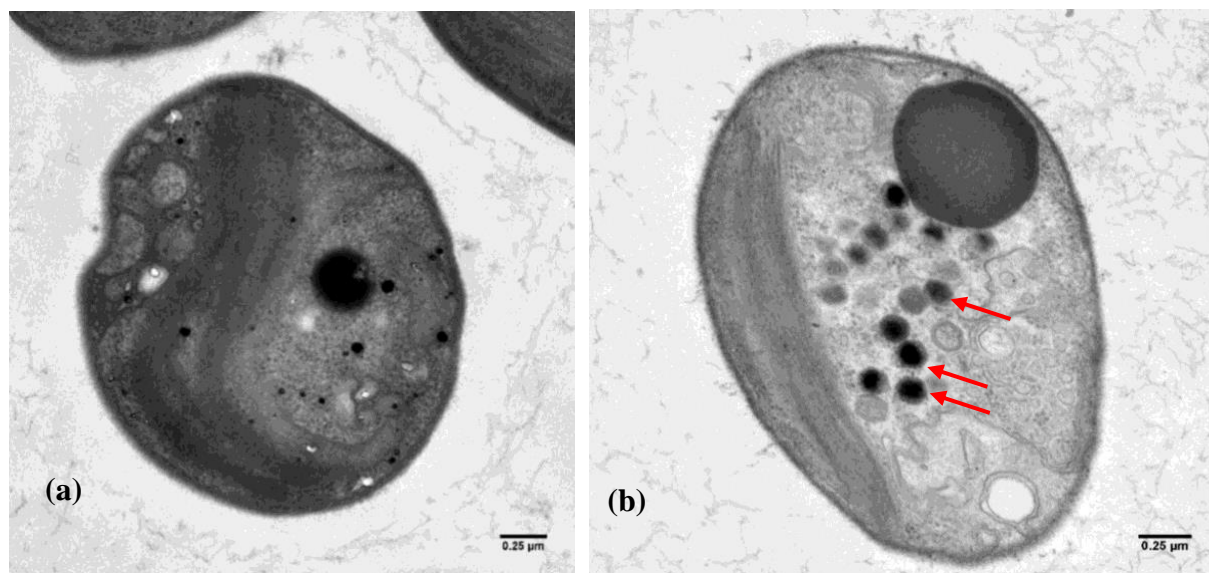


Figure 3-2. TEM pictures of uninfected (a) and infected (b) *Chlorella* sp. Cells

3.4.1 Growth of *Chlorella* with and Without Algal Virus

Although algal viruses are known to play important roles in the dynamics of algal cultures (Fuhrman, 1999; Gachon et al., 2010; Van Etten & Dunigan, 2012), the impact of viral infection (abundance at environmental level) on algae growth has not been investigated. In order to study the influence of virus on algal cultivation, four *Chlorella* suspensions were prepared in 150 mL ATCC 847 medium with final *Chlorella* concentration of $5.15 \times 10^3 \pm 1.14 \times 10^3$ cells/mL. Considering the environmental concentration of PBCV-1 can vary from 1-100 PFU/mL to 100,000 PFU/mL (Long & Short, 2016; Short, 2012; Van Etten & Dunigan, 2012), virus stock was inoculated to two of these samples resulting in a final virus concentration of 250 ± 90 PFU/mL. The other two samples were not inoculated with virus and served as controls. The growth behaviors of *Chlorella* sp. in all four samples were obtained by time-course cell counting during incubating at 25°C with a 14 h light and 10 h dark cycle.

The growth curves of *Chlorella* were presented in Figure 3-3. The virus free samples showed rapid growth from 5.15×10^3 cells/mL to 10^7 cells/mL in the first 10 days and then entered early stationary phase reaching approximately 2×10^7 cells/mL. By contrast, no algal growth was observed in the samples inoculated with virus until 19 days after inoculation. A peak of algal concentration

(roughly 10^6 cells/mL) occurred on day 21 but the algal culture then rapidly collapsed in 4 days to a value below the detection limit of cell counting by hemocytometer. According to this result, exposure of *Chlorella* to environmental level virus prevented algal growth during the first two weeks, then algal cells started to grow. Algae growth observed after 19 days may have been due to the low virus concentration at that time because of the fast decay of PBCV-1 (Short, 2012). As algae concentration reached a peak at 21 days, it is likely that the remaining undecayed virus particles triggered another mass infection, leading to the rapid collapse of the algal culture. This is because the initial mass infection was host density dependent and did not start until the host concentration reached a specific value (Brussaard, 2004; Short, 2012; Suttle et al., 1994). As such, the presence of virus could prevent algal growth and cause the collapse of the algal culture, which should be addressed in algal cultivation systems.

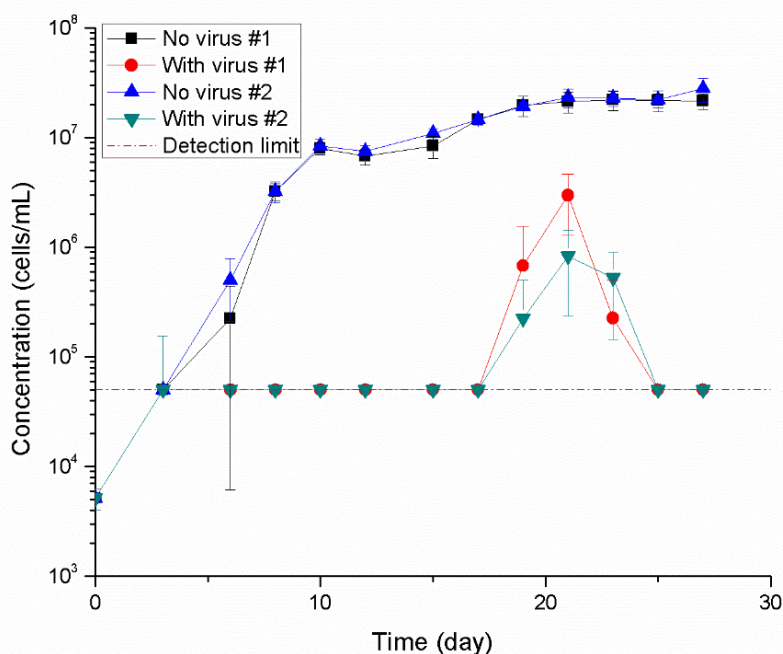


Figure 3-3. Growth behavior of *Chlorella* sp. with and without virus inoculation

3.4.2 UV₂₅₄ Dose-response Behavior of PBCV-1 Under a LP Collimated Beam Reactor

Since UV irradiance is effective for inactivation of pathogens in water treatment, it is also possible to apply UV irradiance to inactivate algal viruses. The UV₂₅₄ dose-response behavior of PBCV-1

was measured using a LP mercury collimated beam reactor. The overall loss of infectivity for PBCV-1 was quantified by a culture-based method—plaque assay. UV-induced damage to virus DNA was quantified by qPCR, since the damaged DNA could not be amplified by polymerase progression (Beck et al., 2013; Pecson et al., 2011). Two primer sets (PBCVs and 185R1) with different amplicon sizes were applied in this study for the qPCR test. The characteristics of these two primer sets including standard curves and melting curves are shown in Figure B-2. The UV₂₅₄ dose response of PBCV-1 based on these two primer sets is illustrated in Figure 3-4. Results obtained with PBCVs primer set (amplicon size of 600 bp) showed roughly log-linear behavior while the results with 185R1 primer set (amplicon size of 107 bp) did not show clear log-linear behavior.

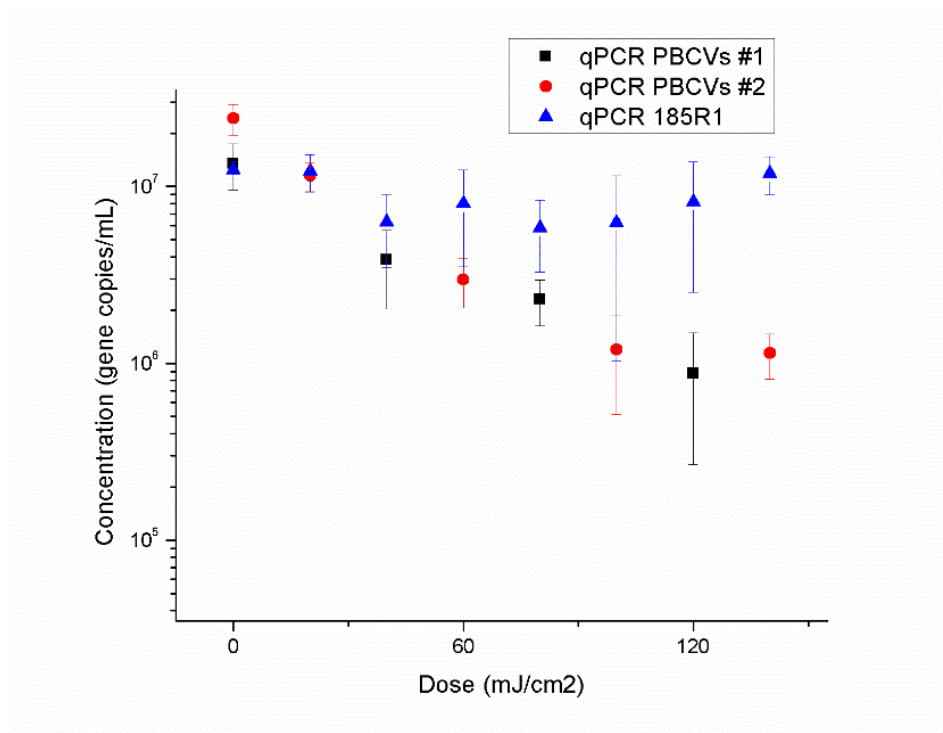


Figure 3-4. UV₂₅₄ dose-response of PBCV-1 quantified by qPCR with PBCVs and 185R1 primer sets.

The result is consistent with previous findings that large amplicon size is more sensitive to UV-induced damage (Pecson et al., 2011). Given the common assumption that UV induced damage has an equivalent chance to impose damage aiming all nucleotides on a genome, the longer amplicons are more sensitive to UV radiation than those of shorter ones (Pecson et al., 2011).

Therefore, the dose-response behavior of PBCV-1 with PBCVs primer set was used to compare with the results obtained by plaque assay.

The dose-response behavior of PBCV-1 is illustrated in Figure 3-5 and the detailed data were summarized in Table B-1. Results from both plaque assay and qPCR show roughly log-linear behavior for doses up to 120 mJ/cm². Both plaque assay and qPCR results were close to their detection of limit above this dose value (120 mJ/cm²).

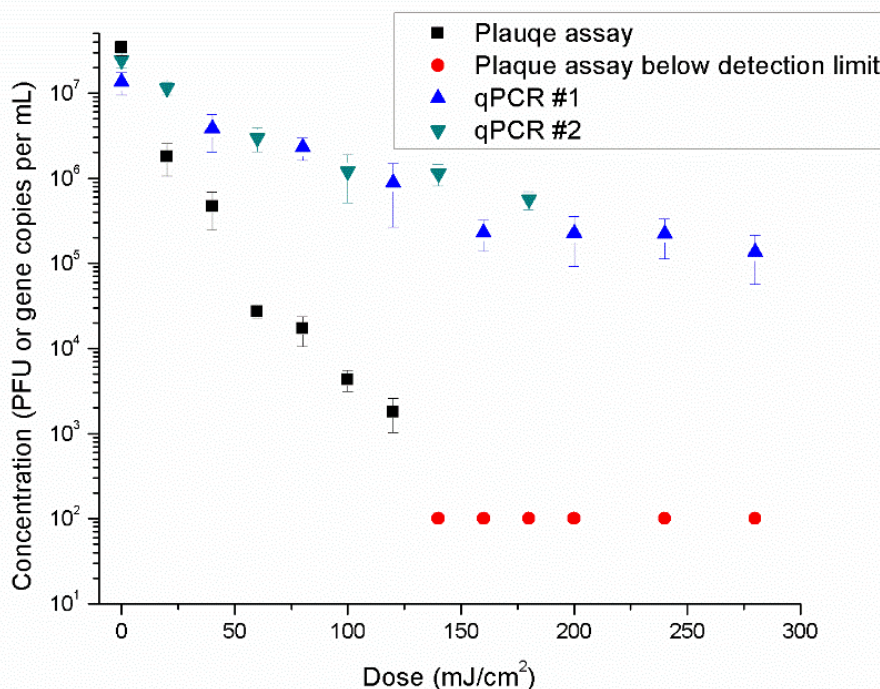


Figure 3-5. UV₂₅₄ dose-response of PBCV-1 measured by exposure under a LP UV collimated beam using a culture-based plaque assay and DNA damage by qPCR. Black symbols represent the results measured by plaque assay and red symbols indicate plaque assay measurements that were below detection limit. Blue and green symbols represent qPCR results.

The dose-response behavior of PBCV-1 measured by both plaque assay and qPCR in the dose range below 120 mJ/cm² were essentially first-order, which can be fitted to a single-event model:

$$\frac{dN}{dD} = -KN$$

N	=	concentration of viable cells ($\text{cells}\cdot\text{L}^{-1}$)
D	=	average UV dose received by the cell suspension ($\text{mJ}\cdot\text{cm}^{-2}$)
K	=	inactivation constant ($\text{cm}^2\cdot\text{mJ}^{-1}$)

The dose-response data in the dose range below $120 \text{ mJ}/\text{cm}^2$ were log-transformed and then fitted by linear regression in the form of $\ln(N/N_0)$ vs. dose. The calculated inactivation constant based on the results of plaque assay was $0.092 \text{ cm}^2/\text{mJ}$ ($R^2 = 0.84$), and the value was $0.025 \text{ cm}^2/\text{mJ}$ ($R^2 = 0.88$) for qPCR results. Due to the very limited studies on UV_{254} dose-response of algal virus, the UV_{254} inactivation constant obtained for PBCV-1 was compared with inactivation constants reported for some common waterborne viruses (Chevrefils et al., 2006; Malayeri et al., 2016). In this previous report, the most UV_{254} sensitive virus (Reovirus T4) showed an inactivation constant of $0.847 \text{ cm}^2/\text{mJ}$ and the inactivation constant for least UV_{254} sensitive virus (Hepatitis IPNV) was $0.0122 \text{ cm}^2/\text{mJ}$. The inactivation constant of PBCV-1 for UV_{254} is about 10 times more sensitive than that of the most sensitive virus and about 8 times less sensitive than that of the most resistant virus, which shows a moderate response to UV_{254} radiation.

PCR has been used to detect the UV induced damage to target organism genomes (Beck et al., 2013), but the inactivation constant obtained by qPCR was significantly underestimated (Pecson et al., 2011; Pecson et al., 2009). One explanation is that qPCR can only represent the damage on the target amplicon that is usually below 1000 bp, while the genome of virus is much larger than this size. UV induced lesions may occur on parts of the viral genome other than the target amplicon that could prevent replication but not qPCR amplification. Similarly, the likelihood of a DNA lesion detected by longer amplicon is higher than that detected by a shorter amplicon (Pecson et al., 2011). Although the result from qPCR cannot generate identical results measured by the culture-based method, the results from qPCR still showed good consistency when the same amplicon was applied. In this study, the dose-response behavior of PBCV-1 measured by qPCR showed consistent results when exposed to two independent UV_{254} exposures (Figure 3-5). Therefore, using qPCR to measure and interpret dose-response behavior is reasonable.

3.4.3 Action Spectrum and Absorbance Spectrum of Extracted DNA

It is known that UV induced damage to nucleic acids is wavelength dependent and the most efficient wavelength for DNA damage is located near 265 nm, which also corresponds with the maximum absorbance of nucleic acids (USEPA, 2006). The damage to DNA in this range of wavelength is attributed to the formation of cyclobutene dimers, which prevents the replication of DNA (Besaratina et al., 2011). Although LP mercury lamps can generate UV radiation at a wavelength of 254 nm that is efficient to damage nucleic acids in target organisms, it is not able to provide the UV radiation at other wavelengths that are effective to damage other important biomolecules (Santos et al., 2013). Proteins have been reported to have relatively high UV absorption at wavelengths below 240 nm, which is primarily attributed to the absorption of peptide bonds between amino acids (Harm, 1980). As such, it is interesting to investigate the UV dose-response behavior of PBCV-1 at UV wavelengths other than 254 nm. In this study, the action spectrum of PBCV-1 was measured for 9 specific wavelengths ranging from 214 nm - 310 nm. The UV dose-response behaviors of PBCV-1 for all nine wavelengths are presented in Figure 3-6. The measured concentration data of active PBCV-1 were ln-transformed to fit into the single-event model $\ln(N/N_0)$ vs. dose using linear regression. Figure 3-7 illustrates the relative absorption spectrum of DNA and the relative sensitivity of PBCV-1, calculated based on the ratio of the absorption or inactivation constant at specific wavelength to that of at 254 nm. Figure 3-7 also included the normalized action spectrum (normalized to the inactivation constant at 254 nm) of Adenovirus 2 (dsDNA) and MS2 coliphage (ssRNA), which were based on data from previous literature (Beck et al., 2013; Mamane-Gravetz et al., 2005). According to Figure 3-7, PBCV-1 was particularly sensitive to UV irradiation at wavelengths below 240 nm; the inactivation constant also demonstrated a local maximum at wavelengths between 260 nm to 280 nm.

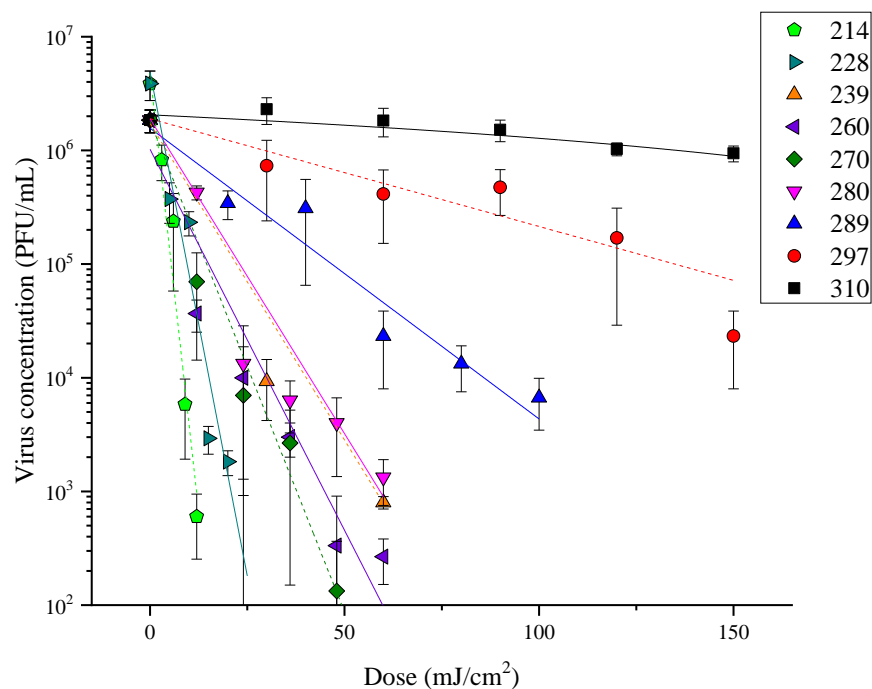


Figure 3-6. Concentration of active PBCV-1 as a function of UV dose at each of nine wavelengths.

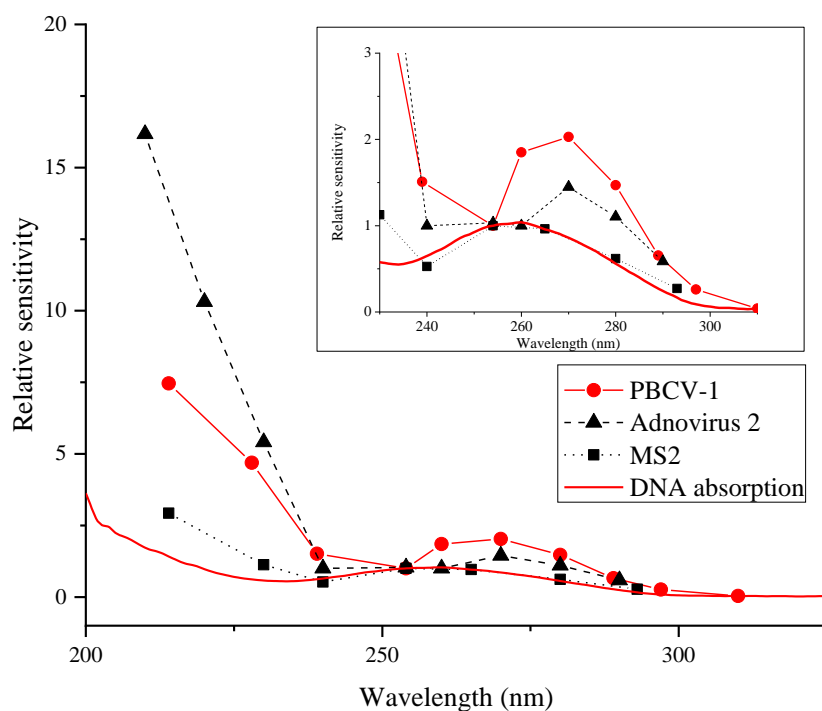


Figure 3-7. Normalized UV inactivation action spectrum for PBCV-1, MS2, Adenovirus 2, and DNA absorption.

The loss of infectivity at wavelengths above 240 nm followed the slope of the absorption spectrum of DNA, which had a peak in the vicinity of 260 nm. A possible explanation for this behavior has been discussed previously, i.e., UV induced damage to the virus genome is probably the main contributor to the loss of infectivity for wavelengths longer than 240 nm (Beck et al., 2013). However, the behavior of inactivation is quite different from the absorption spectrum of DNA at wavelengths below 240 nm. The inactivation constants of PBCV-1 at 214 nm and 228 nm are about 7.5-fold and 4.7-fold greater than that at 254 nm and were significantly larger than the maximum inactivation constant observed in the wavelength range between 260 nm to 280 nm. Action spectra of MS2 coliphage and Adenovirus 2 are included in Figure 3-7 as well. Similar patterns of action spectra for these viruses were observed at wavelengths above 240 nm due to the damage to DNA. However, PBCV-1 and Adenovirus were more sensitive at wavelengths below 240 nm, which is the wavelength range that has been associated with damage to proteins in other viruses. Therefore, it is possible that some essential proteins related to viral infection in both PBCV-1 and adenovirus may be sensitive to UV irradiation at wavelengths below 240 nm. Beck *et al.* also suggested that some protein-associated DNA can be damaged by UV irradiance at these wavelengths since the protein can absorb photon energy and transfer the energy to associated nucleic acids (Beck et al., 2013). MS2 did not show such sensitivity at these wavelengths, which may be because that MS2 is ssRNA virus while both PBCV-1 and adenovirus are dsDNA viruses. Further investigation is needed to reveal the mechanism of inactivation at wavelengths below 240 nm.

3.5 Conclusions

In this study, the collapse of *Chlorella sp.* culture caused by algal virus PBCV-1 was observed. At environmentally relevant level, the algal virus PBCV-1 was able to effectively prevent the growth of *Chlorella sp.*. Hence, UV₂₅₄ irradiation to inactivate algal virus was proposed to minimize the risk caused by potential viral infection during algal cultivation.

The UV₂₅₄ dose-response behavior of PBCV-1 indicated that roughly 5 log₁₀ units of inactivation was achieved by applying a UV₂₅₄ dose up to 120 mJ/cm². Considering the common concentration of PBCV-1 in the environment (below 100 PFU/mL), treatment with UV₂₅₄ doses larger than 60 mJ/cm² is able to inactivate most viable virus particles. UV₂₅₄ induced DNA damage was also

quantified by qPCR, which has been demonstrated to be a consistent method to measure the loss of infectivity based on nucleic acid lesions.

Investigation of the UV inactivation action spectrum for PBCV-1 has indicated that UV irradiance at lower wavelengths (below 240 nm) was more effective than longer UVC wavelengths to inactivate PBCV-1. The results illustrated that some important biomolecules other than nucleic acids may be sensitive to UV irradiance at wavelengths below 240 nm. The optimum inactivation of PBCV-1 was observed at wavelength of 214 nm, which is 7.5-fold more effective than that at the wavelength of 254 nm.

The data presented in this study showed that PBCV-1 can be inactivated by UV radiation from LP and MP lamps, which are commonly used in water and wastewater treatment processes. Future studies can be conducted to investigate UV-induced DNA damage at wavelengths other than 254 nm. Furthermore, additional research is needed to expand the knowledge of UV₂₅₄ dose-response as well as action spectrum to other types of algal viruses.

CHAPTER 4. NATURE-INSPIRED VIRAL DISRUPTION METHOD FOR COST-EFFECTIVE BIOFUEL PRODUCTION

4.1 Abstract

Algal biofuel has been advocated as a sustainable and environmentally friendly renewable energy source, but chemical usage and high energy consumption associated with cell disruption have been important barriers to this implementation. Various cell disruption methods have been developed to maximize lipid extraction efficiency, but most of them are economically infeasible due to the requirement of extreme conditions, complicated equipment, and high operation and maintenance costs. Viral infection of algae is a natural process that can lyse algal cells under ambient conditions without using chemicals or energy-intensive equipment. This study, for the first time, provides a comprehensive and in-depth evaluation of the feasibility of using viruses to assist algal lipid extraction. Detailed mechanistic studies were conducted to evaluate the infection behavior of *Chlorovirus* PBCV-1 on *Chlorella* sp., the impact of infection on the mechanical strength of the algal cell wall, lipid yield, and lipid distribution. Viral disruption with multiplicity of infection of 10^8 was able to disrupt concentrated algal biomass completely in six days. Our results indicated that viral disruption significantly reduced the mechanical strength of algal cells for lipid extraction. Lipid yield with viral disruption increased more than three times compared to no disruption control and was similar to that of ultrasonic disruption. Moreover, lipid composition analysis showed that the quality of extracted lipids was not affected by viral infection. The results showed that viral infection is a cost-effective technique to promote lipid extraction as extensive energy input and chemicals required by existing disruption methods are no longer needed. The results of this study provided new insights in the development of nature-inspired lipid extraction methods for cost-efficient biofuel production.

4.2 Introduction

Global industrialization and population growth have resulted in rapid depletion of fossil fuels and therefore have promoted research on sustainable and environmental friendly biofuels (Chisti, 2008). Microalgae with high growth rate, low arable land use, and high lipid content have shown many advantages over other energy crops (Alam et al., 2012; Brennan & Owende, 2010; H. Chen

et al., 2015; Kirrolia et al., 2013; Rawat et al., 2013). The precursor of biodiesel, microalgae lipids—serving as the main reservoir of energy in microalgae cells (Chen et al., 2012)—are enveloped in microalgae's cytoplasm and protected by rigid algal cell wall (D.-Y. Kim et al., 2016). Previous studies have shown that cell disruption and its associated chemical and energy usage contribute to most of the high extraction costs in lipid extraction (Coons et al., 2014; Halim et al., 2012; Nagarajan et al., 2013; Steriti et al., 2014). Therefore, there is a critical need to develop cell disruption processes to reduce chemical and energy usage.

Typical microalgal extraction processes are categorized into dry and wet extraction methods. Wet extraction is a potentially cost-effective approach (Lam & Lee, 2012; Lardon et al., 2009; Xu et al., 2011), as it avoids the energy intensive drying and dehydration process in the dry extraction process (Sander & Murthy, 2010). Cell disruption is a required pretreatment step in wet extraction to break the rigid algal cell wall and neutralize surface charge of algal cells to improve lipid yield (J. Kim et al., 2013; Steriti et al., 2014), but existing physical, chemical, and biological cell disruption methods are still costly (J. Kim et al., 2013; Shwetharani & Balakrishna, 2016). Physical disruption methods directly break cell walls and typical physical disruption methods include bead-beating, high pressure homogenization, ultrasonication, microwave, and electroporation (Chiaramonti et al., 2017; Greenly & Tester, 2015; Joannes et al., 2015; Lee et al., 2010). Chemical disruption methods utilize chemical reactions to lyse or break algal cell walls (Orr et al., 2015; Sathish & Sims, 2012; Yoo et al., 2012). Physical disruption methods require large amounts of energy for their thermal, electrical, or mechanical treatment processes. Although these energy-intensive processes are avoided in chemical disruption methods, large amounts of chemical usage, the need for chemical waste treatment and disposal, and equipment corrosion issues remain challenging in chemical disruption (J. Kim et al., 2013). Biological disruption methods based on enzymatic degradation of cell wall under mild reaction conditions have been developed (J. Kim et al., 2013). Various types of microalgae even with very resistant layers can be lysed by a specific mixture of enzymes (Chen et al., 2016; Taher et al., 2014). However, enzymatic cell disruption is also costly due to the high cost of enzymes (Chiaramonti et al., 2017). The combination of different disruption methods, such as thermal disruption and enzymatic disruption, could achieve higher lipid extraction efficiency (Chen et al., 2016), but the inherent constraints of high energy demand

and high enzyme cost still exist. Therefore, there is still a knowledge gap on cost-effective cell disruption techniques.

One potentially cost-effective approach is to use viruses for cell disruption to reduce energy consumption and chemical usage. Viruses are the most abundant biological entity in aquatic systems, but have been rarely studied for biofuel production (Cheng et al., 2013; Sanmukh et al., 2014). Algal viruses can lyse cyanobacteria and eukaryotic microalgae naturally (Van Etten, Burbank, et al., 1985; Van Etten, Burbank, Xia, et al., 1983; Van Etten, Van Etten, et al., 1985), and have been reported to play an important role in the decline of algal blooms (Fuhrman, 1999; Gachon et al., 2010; Van Etten & Dunigan, 2012), which shows their capability of treating large quantities of microalgae. A typical viral infection process involves attachment of viruses to algal cells, injection of viral DNA, reprogramming of algal transcription systems to produce and assemble new virus particles, and algal cell lysis and virus particle release (Meints et al., 1986; Van Etten & Dunigan, 2012). Similar to an autocatalytic reaction, a successful virus infection causes rapid lysis of an algal cell in a few hours and releases hundreds of newly assembled virus particles that are ready for subsequent infection. Even trace amounts of algal virus can trigger massive disruption of algal cells in the ambient environment without additional input of energy, chemicals, or enzymes. Algal viruses are also widely distributed throughout the world and relatively easy to acquire (Van Etten & Dunigan, 2012). Additionally, algal viruses are not likely to cause health problems to humans and the ecosystem as most algal viruses are host specific and decay rapidly in the environment in the absence of host cells (Gachon et al., 2010; Long & Short, 2016; Short, 2012; Yamada et al., 1991).

This study, for the first time, presents an evaluation of the feasibility of using viruses to assist algal lipid extraction. Detailed mechanistic experiments were conducted to evaluate the infection behavior of viruses, impact of infection on mechanical strength of the algal cell wall, lipid yield, and lipid distribution. The results showed that virus-assisted cell disruption of *Chlorella sp.* had similar performance as sonication—which is one of the most efficient, yet energy-intensive, disruption methods—on lipid extraction without using disruption chemicals and energy. The results of this study provide a new route to chemical-free cell disruption technique for highly cost-effective algal biofuel production.

4.3 Materials and Methods

4.3.1 Microalgae Cultivation and Quantification

The fresh water microalgal strain *Chlorella sp.* (ATCC 50258) was used in this study, as it is the host of widely spread *Chlorovirus* (Brussaard, 2004; Van Etten, Van Etten, et al., 1985) and has been frequently used in biodiesel production (Sawangkeaw et al., 2013; Valizadeh Derakhshan et al., 2014). A stock culture of *Chlorella sp.* was cultivated under a 14h light/10h dark cycle at 25 °C. Light was provided by an IPOWERS Super HPS 600 W lamp. *Chlorella sp.* was grown in ATCC medium 847, which contains 1.0 g Proteose Peptone, 250 mg NaNO₃, 25 mg CaCl₂, 75 mg MgSO₄, 75 mg K₂HPO₄, 175 mg KH₂PO₄, 25 mg NaCl, and a drop of 1.0% FeCl₃ solution in 1.0 L distilled water. Algal growth was quantified by a hemocytometer (Hausser Scientific) and a fluorescence microscope (Nikon Eclipse Ni). LIVE/DEAD® BacLight™ Bacterial Viability Kits were used to monitor viability of algal cells after viral infection. Additionally, dry algal biomass was obtained gravimetrically after drying at 105 °C for 12 h in an oven (Thermo Scientific).

4.3.2 Virus isolation and Quantification

A surface water sample with *Chlorovirus* was collected from a pond in the Celery Bog Nature Area, West Lafayette, IN. The collected water sample was filtered through a syringe filter with 0.2 µm PTFE membrane (Thermo Scientific) to remove non-viral particles. Then *Chloroviruses* in the filtrate were isolated by a modified plaque assay method, as previously described (Van Etten, Burbank, Kuczmariski, et al., 1983). A mixture of 100 µL diluted filtrate (approximately 50 PFU per 100 µL), 300 µL *Chlorella* cells (2×10^8 to 4×10^8 cells/mL), 100 µL erythromycin stock (1000 mg/L) and soft agar was poured into prepared agar plates. Agar medium (1.5%) and soft-agar medium (0.75%) were prepared by adding 15 g and 7.5 g agar in ATCC 847 medium, respectively. After incubation for a week at 25°C, viral plaque forming units (PFU) on agar plates were counted. *Chlorovirus* from a single plaque on the algal lawn was isolated and amplified in a host cell culture. To maintain algal viruses, 300 µL filtrate was added to 100 mL host microalgae culture (3×10^7 to 7×10^7 cells/mL). After incubation for three days, a new virus stock was prepared by filtering the viral suspension through a 0.2 µm syringe filter. Viral filtrate was stored at 4°C for future use.

Chlorovirus was identified by polymerase chain reaction (PCR) with four specific primer sets CVMs, PBCVs, ATCVs, CHLVs as previously described (Short et al., 2011). A freeze-thaw

pretreatment procedure consisting of three cycles of heating at 95°C for 2 mins and freezing to ice was used to release DNA. Each 50 μL PCR reaction contained 2 μL of pretreated sample, 10 μM virus specific PCR primers, 0.3 μL DreamTaq DNA Polymerase, 5 μL 10X DreamTaq green buffer, 1 μL dNTP mix dissolved, and 31.7 μL autoclaved nanopure water. A negative control with the same buffer solution and nanopore water instead of sample was used to evaluate potential contamination. All PCR reactions were performed in a Bio-Rad 1000-Series Thermal Cycler with denaturation at 95°C for 2 min, 39 cycles of heating at 95°C for 30s, annealing at primer-specific temperatures for 45s, and extension at 72°C for 1 min. At the end of cycling, all PCR reactions were subjected to a final extension step at 72°C for 30 min. After PCR, 8 μL of reaction product was loaded into 1.5% agarose gel stained with SYBR safe stain and subject to electrophoresis in a Bio-Rad electrophoresis cell. The electrophoresis images were captured with Bio-Rad Gel Doc™ XR+ and Image Lab™ software.

4.3.3 Viral Infection and Dynamics

Viral infection behavior under various initial viral concentrations was investigated. Algal cells at early stationary phase were centrifuged at 3220 \times G for 5 min in Eppendorf Centrifuge 5810 R and then resuspended in growth medium. Concentrated algal suspensions were inoculated with viral concentrations of 0 (no virus control), $1.66\pm 0.04\times 10^1$, $1.66\pm 0.04\times 10^3$, $1.66\pm 0.04\times 10^5$, and $1.66\pm 0.04\times 10^7$ PFU/mL. Then concentrations of living algal cells were measured twice a day for 6 days until no living algal cells could be observed. Concentrations of living cells were plotted as a function of incubation time to evaluate infection behaviors under different initial virus concentrations.

4.3.3.1 Transmission electron microscopy

To examine algal cell lysis under high resolution, healthy and infected algal cells were observed under a Tecnai T12 transmission electron microscope (TEM) in the Purdue Electron Microscopy Facility with a modified method as described previously (Greiner et al., 2009). Target algal suspensions were first centrifuged to obtain an algal pellet and then fixed with a cacodylate-buffered (pH 6.8) 2% glutaraldehyde and 2% formaldehyde solution. After washing in buffer, samples were post-fixed in the same buffer with 2% OsO₄. Subsequently samples were dehydrated in a series of acetone solutions and embedded in Embed 812 Resin. Finally, ultrathin sections of

samples were obtained with diamond knives and stained with uranyl acetate and lead citrate for TEM observation.

4.3.3.2 Impact of viral infection on algal cell strength

Ultrasonic treatment was employed to evaluate the effect of viral infection on the mechanical strength of algal cells. A low frequency (20 kHz) ultrasonic processor (FB-505, Fisher Scientific) equipped with a 1/8-inch diameter ultrasonic horn was operated at 100 W input power to treat algal cells until the absorbance measurements of supernatants were stabilized. The average of last three absorbance measurements was used as the maximum absorbance when all intracellular materials were released. The magnitude of cell disruption was evaluated with the absorbance of released intracellular material in the supernatants at 675 nm wavelength with a NanoDrop 2000c Spectrophotometer (Thermo Scientific) after centrifugation at 3220×G for 5 min. The efficiency of cell breakage at each sonication energy level was then calculated by dividing the absorbance reading by the maximum absorbance. All ultrasonication treatments were conducted in an ice water bath to minimize influence caused by temperature rise.

4.3.3.3 Lipid extraction after viral infection

The effect of viral infection on the improvement of lipid extraction of algal cells were evaluated with modified Bligh and Dyer method (Bligh et al., 1959; Teo et al., 2014). Concentrated algal suspensions were exposed to three experimental conditions: 1) no treatment, 2) 300 s of sonication, and 3) viral infection for 5 days with multiplicity of infection (MOI) of 0.01. MOI is the ratio of added number of viruses and number of algal cells. Then treated samples were centrifuged at 3220×G for 5 min and separated supernatants and pellets were both subject to lipid extraction. Supernatants and pellets were mixed with 2 mL chloroform and 1 mL methanol for solvent extraction. The chloroform layer was collected after 30 minutes of vortexing and centrifugation at 3220×G for 5 min. Such an extraction procedure was repeated two more times to ensure complete extraction. Crude lipid was obtained by blow drying with nitrogen gas in fume hood.

4.3.4 Lipid Transesterification and Quantification

The obtained lipids were transesterified and analyzed by GC-MS. Crude lipids obtained were transesterified with 2 mL methanol containing 5% sulfuric acid at 85°C for 2 h (Sathish & Sims, 2012). One mL hexane was added to each mL mixture to extract fatty acid methyl esters (FAMES).

The hexane layer was collected after 15 min of vortexing and 5 min of centrifugation at 3220×G. Two more rounds of hexane extractions were applied to improve overall extraction efficiency. The extracted FAMES were analyzed with a Shimadzu GC-2010 Plus equipped with a TQ8040 mass spectrometer and a Shimadzu AOC-5000 autosampler. The GC-MS was operated at a flow rate of 1.44 mL·min⁻¹ using Helium as carrier gas and the source temperature of MS was set at 200°C. Each analysis started with a liquid injection of 1 µL sample in a HP-5MS column (30 m × 0.25 mm × 0.25 µm, Agilent) using 1:10 split ratio. The oven program was held at 80°C for 4 min, ramped to 235°C at a rate of 10 °C·min⁻¹, then the rate was cut down to 5°C·min⁻¹ until the temperature reached 300°C. The oven temperature was held at 300°C for 3 min to drive out residues in the column. A Supelco 37 component FAMES standard mix was used to identify and quantify FAMES. Each sample was spiked with 7.52 mg·L⁻¹ heptadecanoic acid methyl ester (Ultra Scientific) as an internal standard for GC-MS analysis. MS peaks (fatty acids C 16:1 and C 17:1) that not were included in the standard mix were identified by the mass spectral database in the Shimadzu GC-MS and quantified according to their nearest eluting peaks in the standard mix. The total lipid yield reported was the sum of all detected FAMES contents.

4.3.5 Statistical Analysis

Triplicate experiments were conducted for each sample and average values and standard errors were calculated for each analysis. Total lipid yield and extracted fatty acids were compared using a one-way ANOVA at a significant level of $\alpha = 0.05$.

4.4 Results and Discussion

4.4.1 Virus isolation and Identification

As shown in Figure 3-1, clear plaques formed by *Chlorovirus* were observed on the algal lawn. To further identify the isolated virus, a single plaque was transferred and further identified by PCR analysis (Figure 3-2). The results of gel electrophoresis after PCR showed that the band targeting CHLVs, which was designed to target all three types of *Chloroviruses*, and the band target PBCVs both showed positive signals, while bands targeting CVMs and ATCVs were both negative. The observed amplicon sizes of CHLVs and PBCVs bands were consistent with theoretical amplicon sizes reported in the literature (Short et al., 2011), suggesting that the isolated virus was indeed PBCV-1.

4.4.2 Viral infection of *Chlorella* sp.

To evaluate the feasibility of viral disruption of algal cells for wet lipid extraction, wet algal biomass with approximately 99% water content was used, which could be easily obtained by inexpensive harvest methods, such as flocculation or sedimentation (Yoo et al., 2012). Although infection of *Chlorella* sp. cells by PBCV-1 virus had been previously reported (Meints et al., 1984; Meints et al., 1986), little information was available on infection behavior at high algal cell density that is needed for biofuel production. Therefore, the infection process and dynamics at high algal density were further investigated.

Algal suspensions were exposed to PBCV-1 at a MOI of 0.01 and samples were collected before infection, 43 h post infection, and 54 h post infection for TEM observation. Algal cell disruption was observed both macroscopically and microscopically (Figure 4-1). Before infection, *Chlorella* cells were intact and formed a pellet after centrifugation, leaving clear supernatant (Figure 4-1A). Healthy *Chlorella* cells with integrated nuclei and undamaged cell walls were observed before the addition of viruses (Figure 4-1B,C). After viruses were added for 43 h, the color of the supernatant turned to light green due to released intracellular components (Figure 4-1D). The majority of *Chlorella* cells were still intact during this stage (Figure 4-1E), but disorganized nuclei as well as virus capsids were observed in some cells (Figure 4-1F). Empty (indicated by white arrow) and assembled (indicated by black arrow) virus capsids in hexagonal shape with a diameter of approximately 100 nm were observed (Figure 4-1F), which were consistent with the reported characteristics of PBCV-1 (Meints et al., 1986). Usually cell wall lysis and release of virus particles would occur after all viral capsids were assembled (Meints et al., 1986; Van Etten & Dunigan, 2012). After viruses were added for 54 h (Figure 4-1G), the green color in supernatant became darker but the algae pellet appeared dark green, which indicated that only part of the chlorophyll was released into the aqueous environment, while most of the chlorophyll stayed with cell debris. On the contrary, intracellular materials released by ultrasonic disruption tended to stay in the supernatant rather than precipitating in the pellet after centrifugation (Figure C-1 in Appendix C), which was consistent with previous results (Gerde et al., 2012).

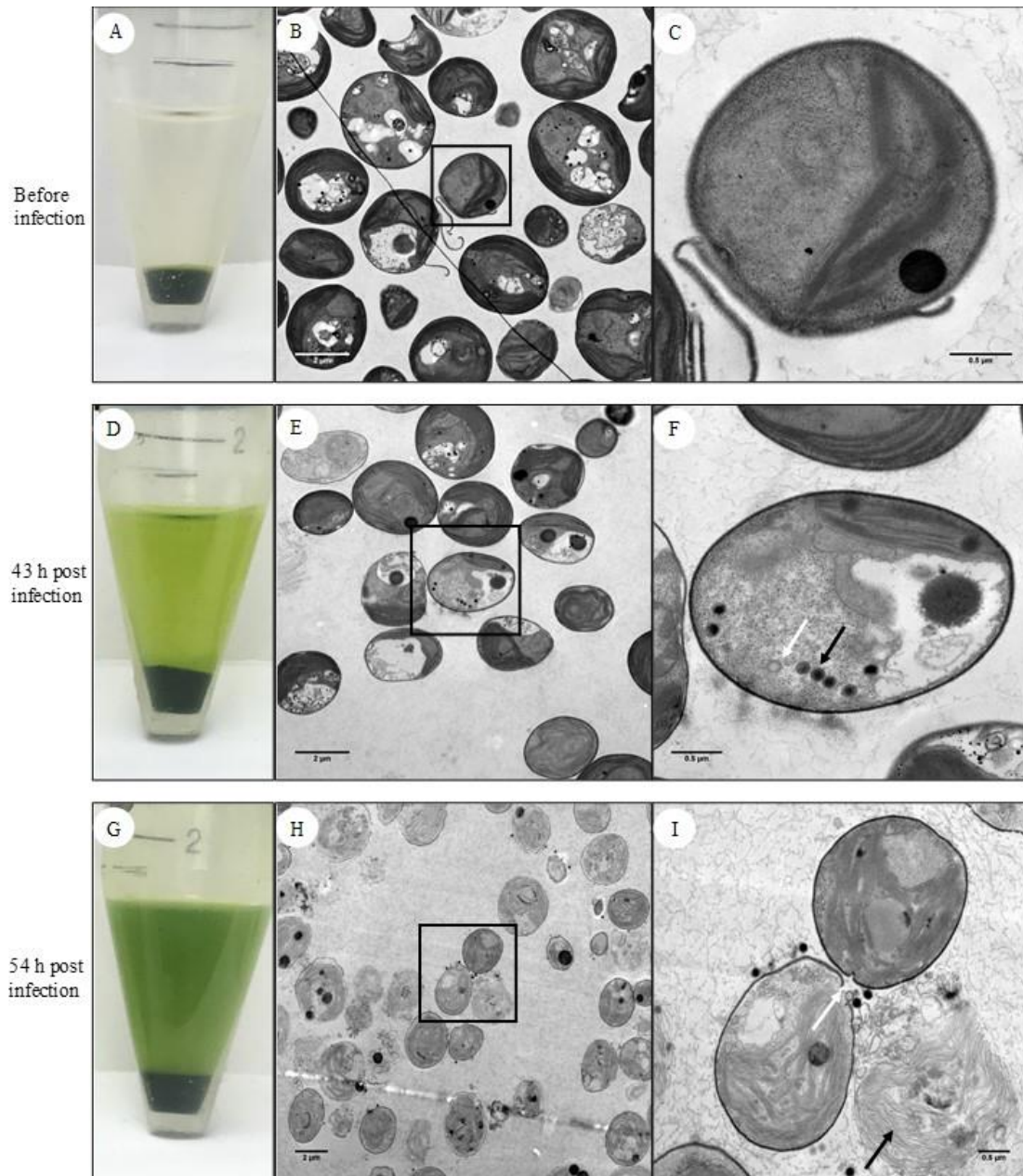


Figure 4-1. Pictures of *Chlorella* cells before and after viral infection. (A) Uninfected cells; (B) TEM picture of uninfected cells; (C) uninfected cell under high resolution; (D) Infected cells 43 h post infection; (E) TEM picture of infected cells 43 h post infection; (F) Infected cell 43 h post infection under high resolution showing assembled virus particles (black arrow) and empty virus capsids (white arrow); (G) Infected cells 54 h post infection; (H) TEM picture of infected cells 54 h post infection; (I) Infected cells 54 h post infection under high resolution showing highly deteriorated cell wall (black arrow) and empty virus capsid and degraded cell wall (white arrow).

As we zoomed into ultrastructural scale, it was observed that the majority of lysed cells grouped with intracellular components and cell debris, despite the fact that cell walls were highly deteriorated (Figure 4-1H). During this stage of infection, most *Chlorella* cells were lysed, and free viral particles were drifting in the solution. Cell walls were hardly recognizable, and intracellular components were clustered together. An empty virus capsid (white arrow) was found outside a fragment of degraded algal cell wall and a lysed algal cell (black arrow) was observed next to the empty capsid (Figure 4-1I), which was consistent with previous results that enzymes within the virus capsid were responsible for the digesting of algal cell wall (Meints et al., 1984). These results showed that the algal virus was able to effectively disrupt the algal cell wall to facilitate lipid extraction.

4.4.2.1 Infection dynamics under different MOI

MOI is an important factor for viral infection as high MOI increases efficiency of viral infection of algal cells and reduces infection time. However, high MOI adds preparation and operation costs, and therefore the characteristics of viral life cycle, such as replication time and virus burst size, should be considered to balance infection efficiency and cost. For example, fast viral replication and large viral burst size—the number of viruses released from each infected cell—can reduce the time used for virus accumulation, but these characteristics are affected by MOI and growth stage of host cells. Increasing MOI would reduce viral burst size and the growth stage of host cells would affect the speed of replication (Van Etten, Burbank, Xia, et al., 1983). PBCV-1 virus typically finishes one replication in 6-8 h and has a burst size of several hundred viruses (Van Etten & Dunigan, 2012), but these characteristics may be affected by MOI and algal cell concentrations. Therefore, the infection behaviors were investigated under various MOI. The concentrated algal suspensions were exposed to PBCV-1 concentrations between $1.66 \pm 0.04 \times 10^1$ and $1.66 \pm 0.04 \times 10^7$ PFU/mL. As shown in Figure 4-2, the concentration of live algal cells in the control sample (with no virus addition) remained stable throughout the experiment, while complete disruption (no live cells) was achieved in all viral infected samples. Complete algal cell disruption ranged from 105 h with highest MOI (1.46×10^{-2}) to 142 h with lowest MOI (1.46×10^{-8}). The increase of MOI by six orders of magnitude only saved 26% infection time used on complete cell disruption, which indicated that even low MOI is a good choice for algal cell disruption. In field applications of viral disruption, virus rich lysate after disruption could be recycled and fed back to a disruption tank to

further reduce disruption time and save costs on virus preparation. These results exemplified the advantages of using viruses for lipid extraction from algal cells as viruses can replicate by themselves without adding chemicals.

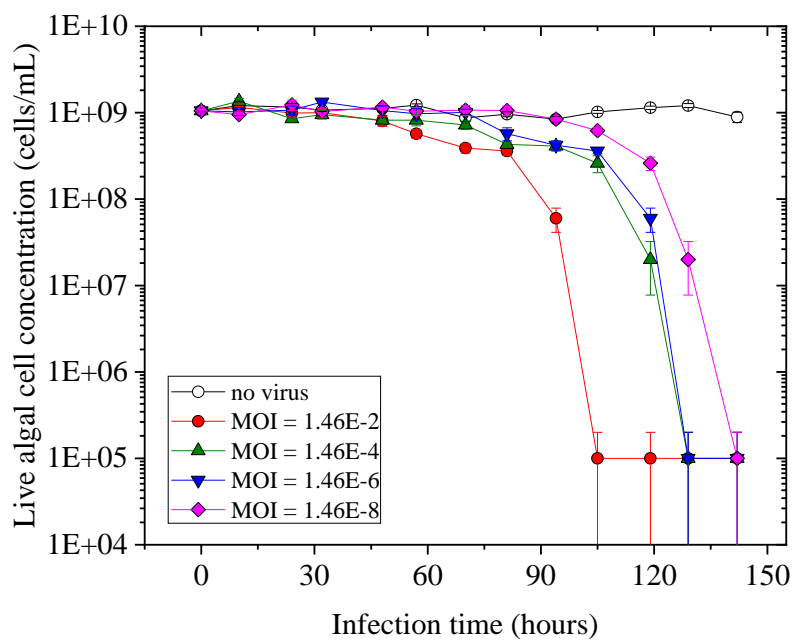


Figure 4-2. Infection of algal cells under different MOI

4.4.2.2 Reduction of algal cells' mechanical strength after viral infection

In addition to potentially replace existing cell disruption techniques, algal viruses can improve the efficiency of existing lipid extraction techniques by reducing algal cells' mechanical strength. As algal cells with reduced mechanical strength are more vulnerable to mechanical power, less energy is required for existing mechanical or chemical lipid extraction techniques to break algal cell walls and release intracellular lipids. In this study, sonication was employed to evaluate the effect of viral disruption on mechanical strength of algal cells, as sonication can break algal cells to release intracellular materials that tend to stay in the supernatant rather than precipitate in the pellet after centrifugation (Figure C-1). The release of intracellular materials has been used to evaluate the level of cell breakage for *C. reinhardtii* in a previous study (Gerde et al., 2012). The characteristic peak of chlorophyll with a secondary absorbance peak at 675 nm (Figure C-2) from released

intracellular materials was used to evaluate cell breakage after viral infection and the results are shown in Figure 4-3.

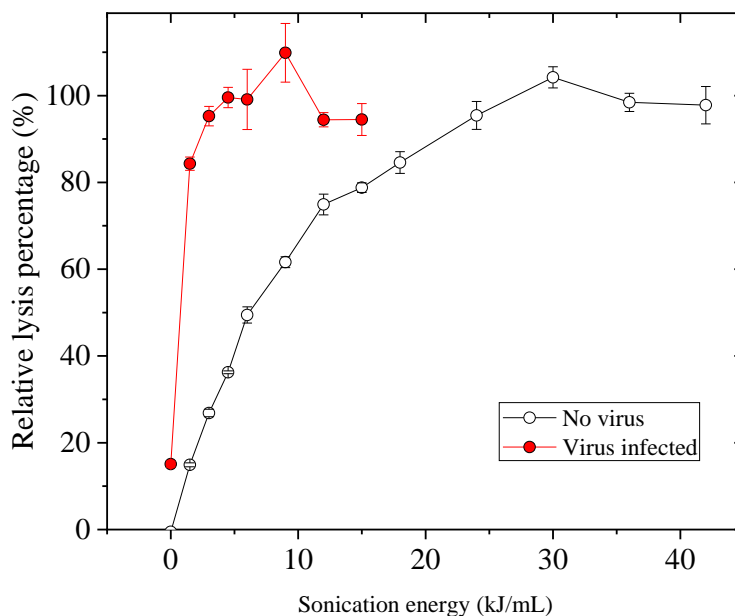


Figure 4-3. Improvement of cell lysis efficiency after viral infection.

For both untreated and virus disrupted samples, the efficiencies of cell breakage increased at low sonication energy levels and eventually levelled off under high sonication energy levels after all algal cells were disrupted. Much less sonication energy was needed to disrupt algal cells that was treated with viruses. To disrupt over 80% of algal cells, the consumed sonication energy for virus disrupted samples (1.5 kJ/mL) was 91.7% less than the sonication energy for untreated algal cells (18 kJ/mL). For complete cell breakage, the consumed sonication energy for virus disrupted samples (4.5 kJ/mL) was 85% less than the sonication energy for untreated samples (30 kJ/mL). The results also showed that algal cells after viral treatment were effectively disrupted even at low sonication energy levels. As shown in Figure 4-1H, algal cells after viral treatment were highly deteriorated and the crumbled cell walls could barely hold the intracellular materials. Viral disruption significantly reduced mechanical strength of algal cells and sonication effectively released intracellular materials in virus disrupted cells out of the damaged cell envelope, and as a result required energy or chemicals to break rigid cell walls in existing extraction techniques can be significantly reduced.

4.4.2.3 Lipid extraction after viral infection

The effects of treatment technologies on lipid extraction yield were compared to evaluate the effects of viral infection. Lipids from both cell pellets and supernatants were analyzed to evaluate distribution of lipids. Lipid yields in both viral infection (0.052 ± 0.004 mg/mg dry biomass) and sonication (0.049 ± 0.005 mg/mg dry biomass) were significantly higher than that of control without treatment (0.015 ± 0.003 mg/mg dry biomass), but no statistical difference was observed between viral infection and sonication (Figure 4-4). For the distribution of lipids, over 97% of the lipids with ultrasonic disruption were associated with supernatant, while 100% and 95% of the lipids extracted with no disruption and viral disruption, respectively, were associated with biomass pellet, which can be easily separated for further processing. The low lipid yield from undisrupted algal cells was likely due to surface charges of healthy algal cells that kept them within water phase and prevented sufficient contact with organic solvents (J. Kim et al., 2013). On the contrary, sonication ruptured algal cells into small pieces of cell debris, eliminated algal cell walls between intracellular materials and organic solvents, and improved lipid extraction yield. The Ultrasonic process broke algal cells into small pieces that were unable to be precipitated by centrifugation, and this suspended cell debris can trap released intracellular materials, such as lipids (Gerde et al., 2012; G. Wang et al., 2011), which explained the high lipid content observed in the supernatants of ultrasonic disrupted samples. Viral infection disrupted cells and improved contact between intracellular lipids and solvents. However, lipids were found mostly in the cell pellet after viral disruption rather than dispersed into the supernatant, as the majority of lysed cells after viral infection were clustered with intracellular components in the cell pellets (Figure 4-1H). The lipid rich biomass after viral infection could be concentrated and dehydrated to reduce water content, which could be beneficial for the downstream extraction processes. The similar performance of viral infection and sonication on cell disruption and the distribution of lipids after viral infection both suggest that viral infection is a promising technique to extract lipids from algal biofuel production.

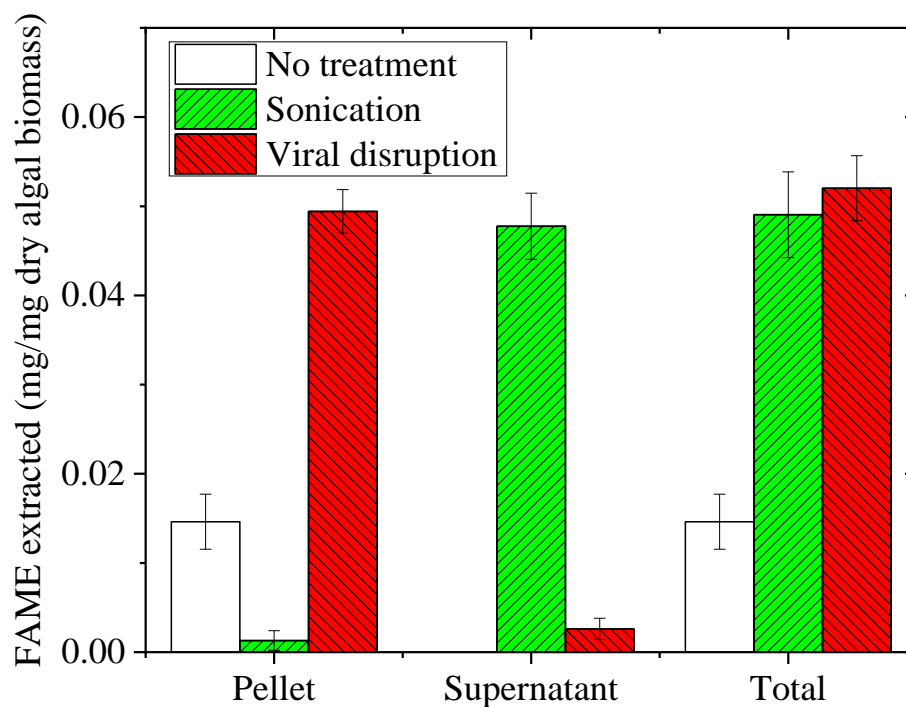


Figure 4-4. FAMEs extracted from algal cells with various disruption methods.

4.4.2.4 Effect of viral disruption on composition of fatty acids

Different from physical extraction techniques, viral infection can reprogram metabolic pathways of host algal cells and change the composition of lipids. For example, a marine algal virus *EhV* was reported to reprogram the metabolic pathway of its host *E. huxleyi* to synthesize more triglycerides (TAGs) after viral infection (Malitsky et al., 2016; Rosenwasser et al., 2014). Furthermore, algal viruses themselves are possible sources of lipids. PBCV-1 has been reported to contain a lipid membrane and virus *EhV* was reported to possess high content of TAGs (Malitsky et al., 2016; Van Etten & Dunigan, 2012). FAME profiles for each disruption method and their detailed compositions and yields are listed in Table 4-1.

Table 4-1. Composition and yield of fatty acids in extracted lipids

Fatty acids	Yield (10^{-3} mg FAME /mg dry biomass)		
	No treatment	Sonication	Viral disruption
C 15:0	1.21 \pm 0.09	2.71 \pm 0.02	2.77 \pm 0.07
C 16:0	2.33 \pm 0.65	9.24 \pm 1.36	9.27 \pm 0.46
C 16:1	4.11 \pm 0.06	11.33 \pm 0.32	11.98 \pm 0.38
C 17:0	1.80 \pm 0.66	5.99 \pm 0.65	7.65 \pm 1.21
C 17:1	1.30 \pm 0.01	4.17 \pm 0.10	4.72 \pm 0.36
C 18:2	1.30 \pm 0.69	4.97 \pm 1.01	4.79 \pm 0.20
C 18:3	2.58 \pm 0.95	10.64 \pm 0.98	10.84 \pm 0.60

The total yields for each type of fatty acids were compared using ANOVA and the results are summarized in Table 4-2. The results showed that yields of all types of fatty acids without disruption were much lower than the yields with disruption, which could be attributed to the low extraction efficiency caused by intact algal cell walls. On the other hand, similar fatty acid profiles were obtained from both ultrasonic and viral disruption, which indicated that viral disruption was as efficient as sonication to extract lipids without affecting the composition and yield of extracted lipids. It is worth noting that yields of fatty acids C16:0 ($p = 0.085$) and C17:0 ($p = 0.062$) obtained with viral disruption were higher than those obtained with ultrasonic disruption at an almost significant level ($p = 0.05$), showing that viral infection has the potential to improve lipid yields of specific fatty acids. However, the relatively low fatty acid yields associated with ultrasonic treatment may be due to sonication-induced lipid oxidation (Gerde et al., 2012). As there are still several fatty acids not identified in GC-MS analysis of fatty acids (Figure C-3), further studies are needed.

Table 4-2. Statistical analysis results of ANOVA analysis of individual fatty acids
p-value of ANOVA tests

Fatty acids	No treatment and sonication	No treatment and viral disruption	Sonication and viral disruption
C 15:0	0.002	0.002	0.217
C 16:0	<0.001	<0.001	0.085
C 16:1	0.001	<0.001	0.973
C 17:0	<0.001	<0.001	0.062
C 17:1	0.001	0.002	0.104
C 18:2	0.005	<0.001	0.773
C 18:3	<0.001	<0.001	0.778

4.4.3 Economical Aspects

In addition to highly efficient disruption performance, using viruses to disrupt wet algal biomass for lipid extraction has significant economic advantages over existing disruption methods that have been reported in the literature. Viral infection and lysis of algal biomass can be operated under room temperature and atmospheric pressure. Isolated viruses can be rapidly proliferated in a short time to meet the demand of scaled-up biofuel production. Viruses in lysate after disruption can be recycled and fed to the fresh wet biomass to save the time and cost on virus preparation. Purity of the virus suspension is not as important as that of disruption chemicals because viruses self-replicate and even a low number of viruses can proliferate quickly. Viral disruption does not require the extensive energy and chemicals that are needed in physical and chemical disruption methods (J. Kim et al., 2013). Additionally, algal viruses can be acquired and maintained with minimal costs as compared to high costs of enzymes for cell wall degradation (Sierra et al., 2017). These advantages have made viral disruption a promising technique for lipid extraction in large-scale biofuel production.

4.5 Conclusions

In this study, viral infection has been examined as an efficient and cost-effective disruption method for lipid extraction from algal cells. Unlike other conventional disruption methods that are chemical and energy intensive, trace numbers of viruses can disrupt algal cells in a short time under room temperature and normal pressure. With significantly less energy input, viral disruption exhibited comparable performance to sonication for algal cell disruption. Moreover, viral disruption significantly reduced mechanical strength and increased solvent permeability of algal cells, which could be applied with existing extraction methods to reduce their biofuel production costs.

Although viral disruption did not show significant impact on the content of extracted lipids, more in-depth investigations of the effects of viral infection on metabolic pathways should be conducted to identify the optimal conditions for biofuel production. Promising results were obtained from the *Chlorella sp.*-PBCV system and it is worth expanding the investigation to other algal viruses, especially those that can infect algal species with high lipid content. With optimized host-virus systems and optimized infection conditions, cost-effectiveness and sustainability of algal biofuel can be further improved.

CHAPTER 5. CONCLUSIONS AND FUTURE WORK

5.1 Conclusions

The development of stable and cost-effective microalgal biofuel production still faces many challenges. This dissertation focused on some of the challenges of algal cultivation caused by invading organisms and the high cost of lipid extraction. Also included was an examination of the effectiveness of UV irradiation as a process to inactivate invading viral parasites that can threaten algal cultivation. On the other hand, a nature-inspired virus-assisted algal cell disruption method was examined for a reduced cost on lipid extraction.

Tetraselmis measured with MPN assay and PBCV-1 measured with plaque assay turned out to be well-suited for UV system validation studies. Both *Tetraselmis* and PBCV-1 are resistant to UVC radiation when compared to other organisms that are environmentally-relevant or that are used in validation of UV-based systems that are designed for other endpoints. Importantly, both the MPN assay and the plaque assay are culture-based methods, which represent relevant measurement endpoints for quantification of the responses of microbes to UV exposure. The UV_{254} dose-response behavior of both *Tetraselmis* and PBCV-1 followed a single-event (i.e., 1st order) kinetic model to the point where the limit of detection for the detection limit of their culture-based quantification methods was reached. Both challenge organisms showed roughly five \log_{10} units of inactivation for UV_{254} doses over 120 mJ/cm^2 . Measured inactivation action spectra for both *Tetraselmis* and PBCV-1 showed local maxima in the vicinity of 260 nm, which indicated that UV-induced damage to DNA played an important role in the inactivation near this wavelength. However, PBCV-1 is also quite sensitive to UV exposure at wavelengths below approximately 240 nm, indicating that a MP UV reactor may represent a good choice to remove this type of algal virus from water. As such, there may be merit to apply UV sources that emit in the wavelength range of 254 nm - 280 nm for the inactivation of *Tetraselmis* and below 240 nm for the inactivation of PBCV-1.

Viral infection has been examined as an efficient and cost-effective cell disruption method for lipid extraction from algal cells. Viruses at very low concentration can disrupt algal cells in a short

period of time at ambient conditions, which can eliminate the need for the energy and chemical intensive steps required in conventional cell disruption methods. On the other hand, viral disruption method was shown to demonstrate comparable performance to sonication, which is one of the most effective, although not cost-effective, methods for cell disruption. Furthermore, viral infection illustrated great potential for reducing the mechanical strength and increasing solvent permeability of algal cell walls, which could be used as a pretreatment for existing extraction methods to reduce their processing cost. Therefore, promising results were obtained to apply microalgal host-virus systems in the establishment of cost-effective algal biofuel production.

Overall, this dissertation provides demonstration and insights for the development of robust and cost-efficient biofuel production by using photochemical and biological approaches, which could be beneficial for researchers and scientists in algal biofuel studies

5.2 Future Work

It is important to reiterate that this dissertation focused entirely on the behavior of *Tetraselmis* and PBCV-1 as target organisms. Additional research is needed to expand the knowledge base associated with the responses of other invading organisms to UVC radiation and their action spectra. Furthermore, both *Tetraselmis* measured with MPN and PBCV-1 measured with a plaque assay, as tools for validation of UV reactors, need to be applied to a full-scale UV system for water treatment in algal cultivation system.

The action spectrum of PBCV-1 were measured by a plaque assay, which is a culture-based method and thus the calculated inactivation constants represented the loss of infectivity due to UV irradiation. It will be interesting to measure the action spectrum of PBCV-1 based on damage to DNA, which could be accomplished by qPCR. We have examined the loss of infectivity due to damage to DNA for a wavelength at 254 nm, so it is possible to expand this measurement to other wavelengths. The results will contribute to the understanding the mechanism of UV inactivation for PBCV-1.

Although viral disruption did not show significant impact on the content of extracted lipids, more in-depth investigations of the effects of viral infection on metabolic pathways should be conducted

to identify the optimal conditions for biofuel production. Promising results were obtained from *Chlorella sp.*-PBCV system and it is worth expanding the investigation to other algal viruses, especially those that can infect algal species with high lipid content. With optimized host-virus systems and optimized infection conditions, cost-effectiveness and sustainability of algal biofuel can be further improved.

APPENDIX A. SUPPORTING INFORMATION FOR CHAPTER 2

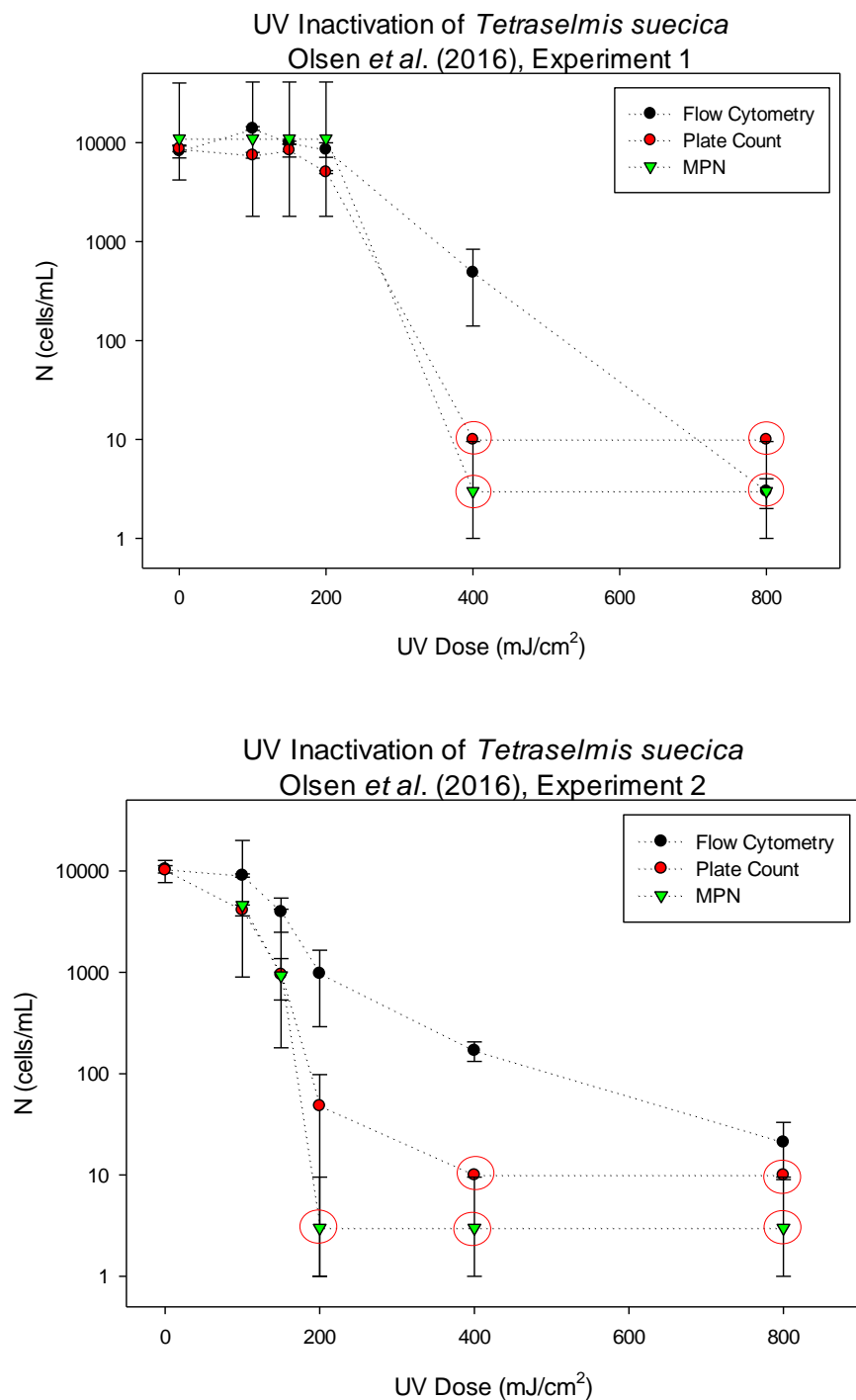


Figure A-1. Investigation of UV dose-response behavior of *Tetraselmis suecica* by Olsen *et al.* (Olsen *et al.*, 2015; Olsen *et al.*, 2016).

Olsen *et al.* developed and applied a flow cytometry method for quantification of the response of *Tetraselmis suecica* to UVC radiation (Olsen et al., 2015; Olsen et al., 2016). The UV source they applied in their experiments was the collimated output of a medium-pressure mercury lamp. The flow cytometry method involved staining of *T. suecica* cells with 5-carboxyfluorescein diacetate acetomethoxy ester (CDFA-AM), which indicates esterase activity in cells. They compared their results with parallel applications of culture-based methods: plate count and MPN.

The results of two UV dose-response experiments based on this approach were reported and are summarized graphically below. For these experiments, the results of the flow cytometry and plate count assays are presented below as a mean \pm one standard deviation, whereas for the MPN assay, the results are presented as the mean and the corresponding 95% confidence interval. Data points that are circled in red were reported as less than the value indicated on the graph.

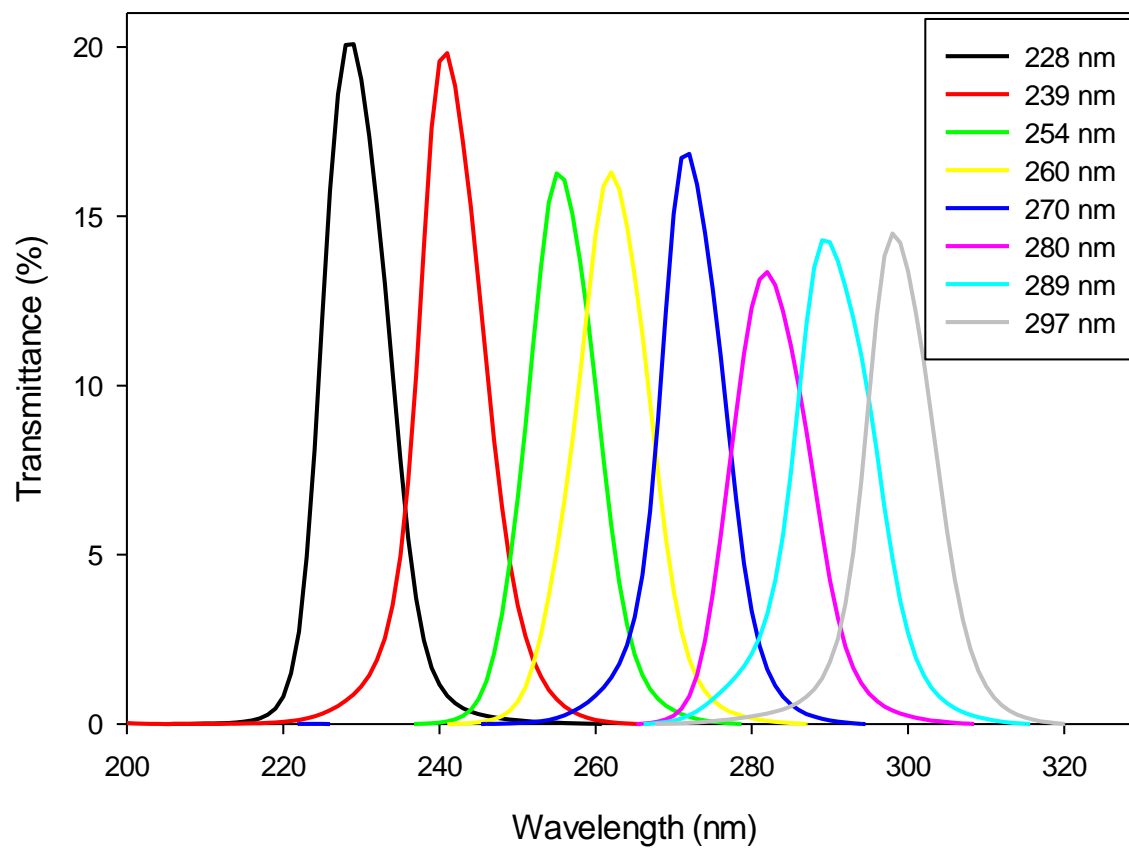


Figure A-2. Transmittance spectra of narrow bandpass optical filters

Each optical filter was characterized by a transmittance spectrum; filters were identified by the nominal wavelength corresponding to maximum transmittance.

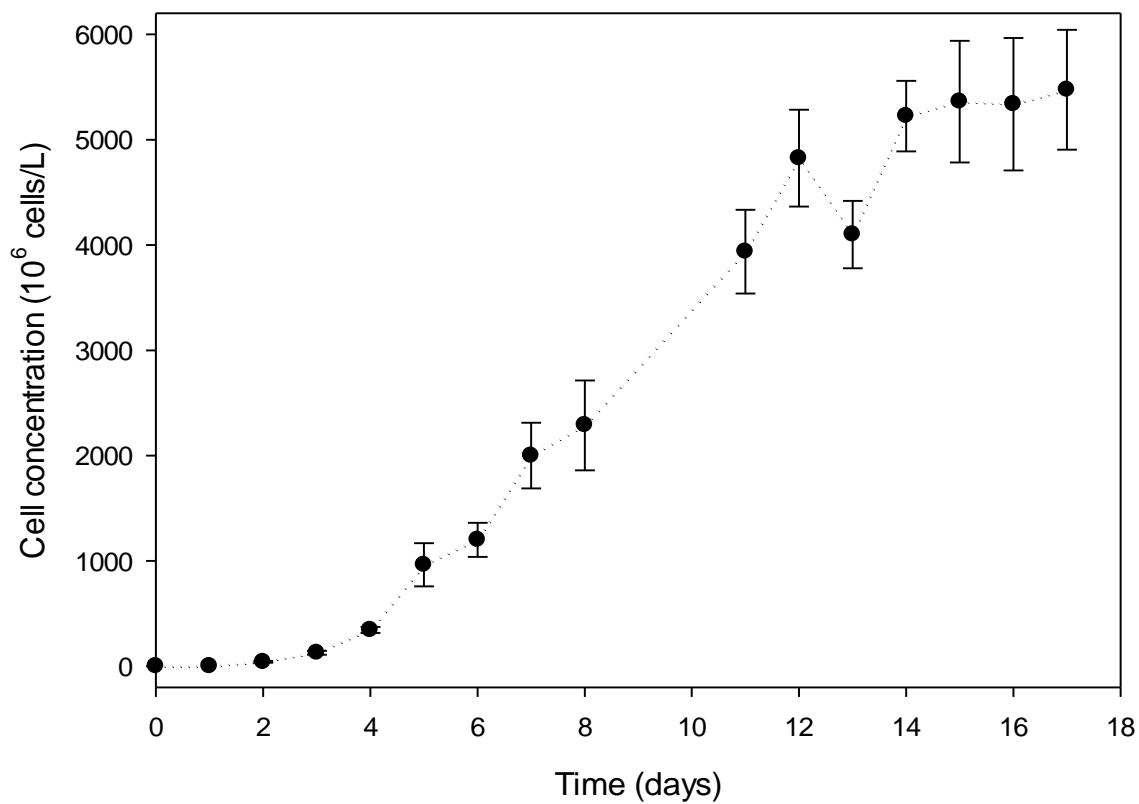


Figure A-3. Growth behavior of *Tetraselmis sp.*: Dynamics of *Tetraselmis* growth for incubation in ATCC Medium 1747 at 25°C with a 14 hour/10 hour light dark cycle. Symbols represent the mean; error bars represent the 95% confidence interval, as determined by the MPN assay.

Table A-1. Sample fluorescence was used as a surrogate measure for the concentration of *Tetraselmis* cells.

Fluorescence Counts (430/680)										
47	61	72	44	81	53	54	47	59	67	66
Mean			59.0			lower 99.9% CI		6.0		
Standard deviation			11.6			upper 99.9% CI		112.4		

As a means of defining the baseline for these measurements, the fluorescence signal for the ATCC Medium 1747 without inoculation was measured on 11 samples. The 99.9% confidence interval of fluorescence was also calculated from these replicate measurements. From these calculations, a fluorescence signal of 112.4 (arbitrary units) was defined as the upper 99.9% CI for the fluorescence measurements of ATCC Medium 1747 without inoculation. This value was used as the fluorescence signal to discriminate positive (cell growth) from negative (no growth) samples.

It is important to recognize that fluorescence is measured on an arbitrary scale. The magnitude of a fluorescence signal will depend on the intensity of the radiation source used to excite the fluorophore and other features that are likely to be instrument-specific. Since the output power of the lamps that are used in fluorometers is variable, the magnitude of fluorescence will also vary among fluorometers. Therefore, the numerical value of the threshold fluorescence signal will vary among instruments, but the method described above can be applied generally to determine this value.

Table A-2. UV₂₅₄ dose-response behavior of *Tetraselmis* cells, as measured with collimated beam reactor.

	Cell concentration (cells/L)					
UV ₂₅₄ Dose (mJ/cm ²)	0	80	160	240	320	400
Exposure time (s)	0	239	478	718	957	1196
MPN	1.86E+07	1.86E+05	<6.00E+02	<6.00E+02	8.00E+02	<6.00E+02
Lower 95% CI	3.00E+06	3.00E+04	<1.00E+02	<1.00E+02	1.00E+02	<1.00E+02
Higher 95% CI	7.60E+07	7.60E+05	<1.80E+03	<1.80E+03	4.00E+03	<1.80E+03
MPN	4.60E+07	4.60E+04	3.00E+03	<6.00E+02	<6.00E+02	<6.00E+02
Lower 95% CI	8.00E+06	8.00E+03	6.00E+02	<1.00E+02	<1.00E+02	<1.00E+02
Higher 95% CI	2.40E+08	2.40E+05	8.80E+03	<1.80E+03	<1.80E+03	<1.80E+03
MPN	3.00E+07	8.60E+04	4.60E+03	8.00E+02	8.00E+02	1.80E+03
Lower 95% CI	6.00E+06	1.40E+04	8.00E+02	1.00E+02	1.00E+02	2.00E+02
Higher 95% CI	8.80E+07	4.20E+05	2.40E+04	4.00E+03	4.00E+03	7.20E+03
UV ₂₅₄ Dose (mJ/cm ²)	0	40	120	200	280	360
Exposure time (s)	0	110	330	552	773	994
MPN	8.60E+07	4.60E+05	8.00E+02	1.80E+03	<6.00E+02	<6.00E+02
Lower 95% CI	1.40E+07	8.00E+04	1.00E+02	2.00E+02	<1.00E+02	<1.00E+02
Higher 95% CI	4.20E+08	2.40E+06	4.00E+03	7.20E+03	<1.80E+03	<1.80E+03
MPN	8.60E+06	8.60E+05	4.20E+03	1.80E+03	8.00E+02	<6.00E+02
Lower 95% CI	1.40E+06	1.40E+05	8.00E+02	2.00E+02	1.00E+02	<1.00E+02
Higher 95% CI	4.20E+07	4.20E+06	9.40E+03	7.20E+03	4.00E+03	<1.80E+03
MPN	1.86E+07	8.60E+05	8.00E+02	1.80E+03	<6.00E+02	<6.00E+02
Lower 95% CI	3.00E+06	1.40E+05	1.00E+02	2.00E+02	<1.00E+02	<1.00E+02
Higher 95% CI	7.60E+07	4.20E+06	4.00E+03	7.20E+03	<1.80E+03	<1.80E+03

Numerical values in italics and shaded indicate observations below the detection limit. Note that the full range of UV₂₅₄ doses was applied in two separate exposure experiments, with the first experiment comprising UV₂₅₄ doses of 0, 80, 160, 240, 320, and 400 mJ/cm², while the second experiment comprised UV₂₅₄ doses of 0, 40, 120, 200, 280, and 360 mJ/cm². A cell suspension with an initial cell concentration (counted by hemocytometer) of 2.12×10^7 cells/L \pm 6.11×10^6 cells/L (95% CI) was prepared for the first experiment. A cell suspension with an initial cell concentration (counted by hemocytometer) of 1.93×10^7 cells/L \pm 7.43×10^6 cells/L (95% CI) was prepared for the second experiment.

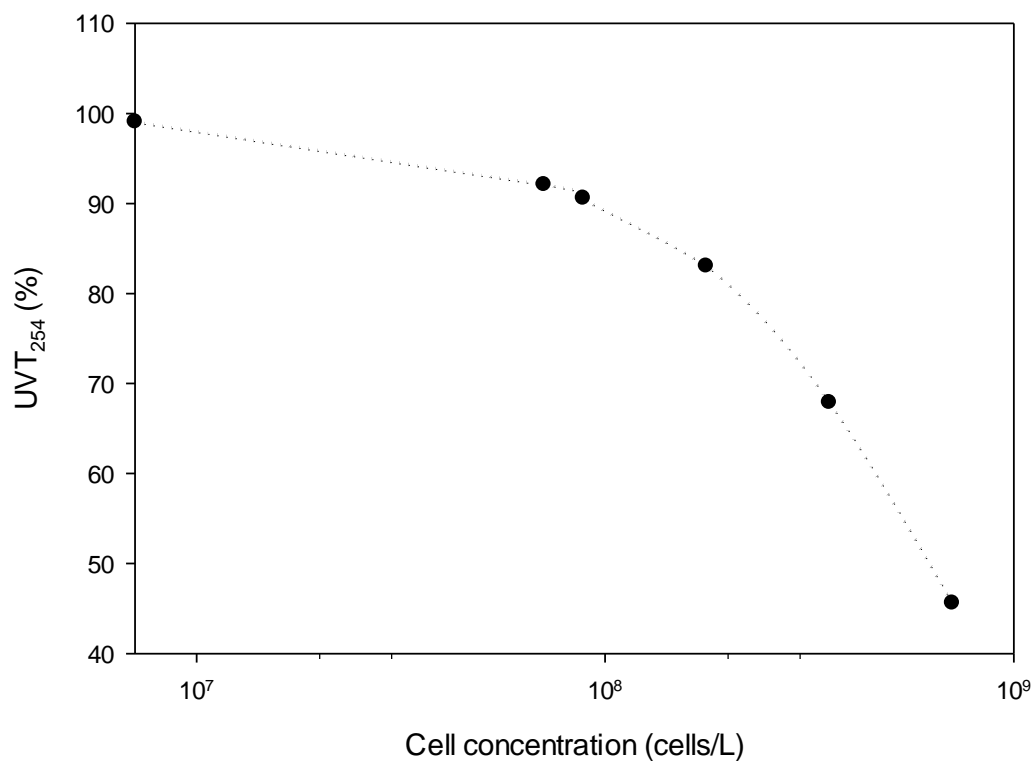


Figure A-4. UVT₂₅₄ as a function of *Tetraselmis* cell concentration.

The cell concentration of the undiluted *Tetraselmis* suspension was $7.07 \times 10^8 \pm 4.47 \times 10^7$ cells/L (95% CI) counted by hemocytometer. The suspension was diluted with DI water by 2, 4, 8, 10, and 100 times. Then UVT₂₅₄ (1.0 cm optical path length) of all suspensions were measured by a CARY 300 Bio UV-Visible Spectrophotometer.

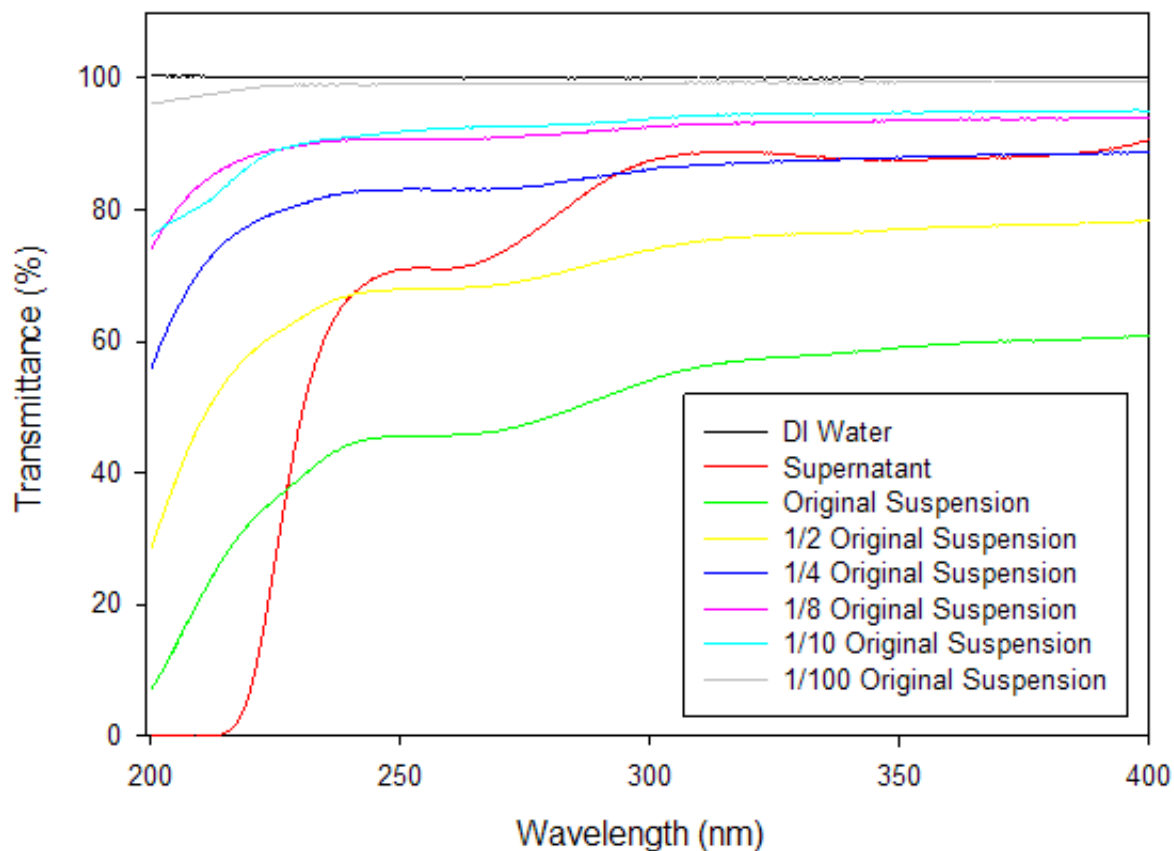


Figure A-5. Transmittance scans ($200 \text{ nm} \leq \lambda \leq 400 \text{ nm}$) of *Tetraselmis* suspension at different concentrations and supernatant after centrifugation.

The original suspension was prepared with a concentration of $7.07 \times 10^8 \text{ cells/L} \pm 4.47 \times 10^7 \text{ cells/L}$ (95% CI) counted by hemocytometer. The supernatant was prepared by centrifuging the original suspension at $3250 \times g$ for 5 minutes, then the upper layer supernatant was collected for measurement. The other suspensions were prepared by diluting original suspension with DI water by 2, 4, 8, 10, and 100 times.

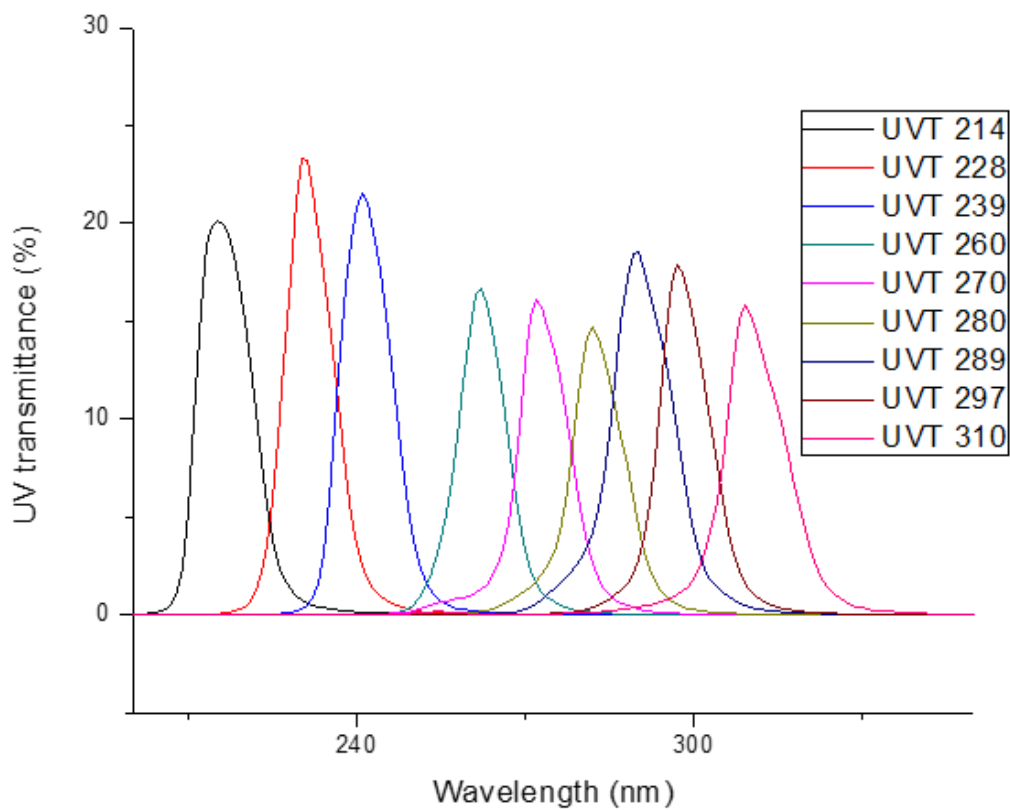
APPENDIX B. SUPPORTING INFORMATION FOR CHAPTER 3

Figure B-1. Transmittance spectra of narrow bandpass optical filters. Each optical filter was characterized by a transmittance spectrum; filters were identified by the nominal wavelength corresponding to maximum transmittance.

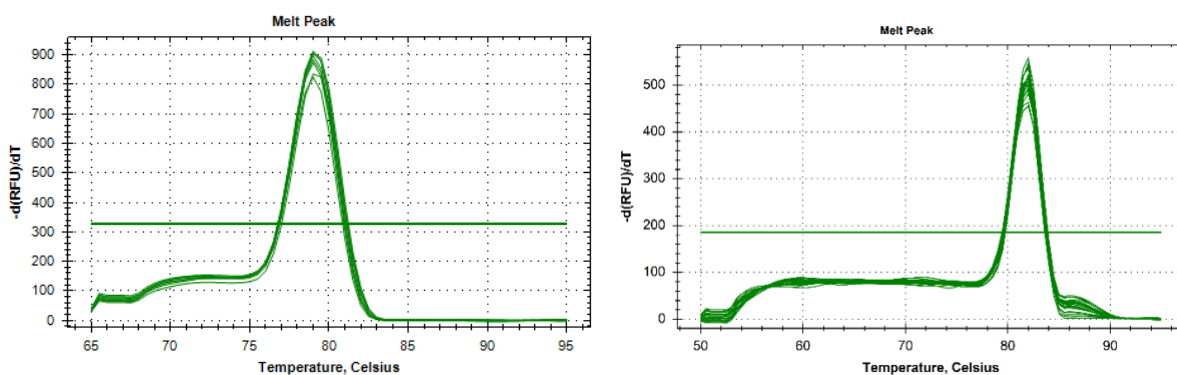
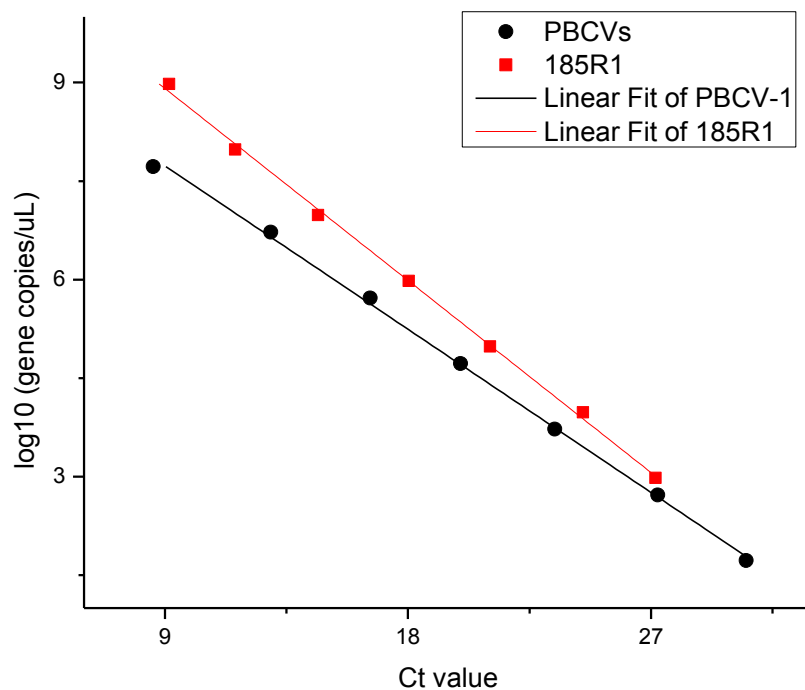


Figure B-2. Standard curve and melting curves for PBCVs and 185R1

The qPCR standard curves of primer sets PBCVs and 185R1 are:

$$\text{PBCVs: } \log_{10} \left(\frac{\text{gene copies}}{\mu\text{L}} \right) = -0.2782 \times \text{Ct value} + 10.247 \quad (R^2 = 0.9986)$$

$$\text{185R1: } \log_{10} \left(\frac{\text{gene copies}}{\mu\text{L}} \right) = -0.3244 \times \text{Ct value} + 11.825 \quad (R^2 = 0.9986)$$

The single peak in melting curves of primer sets 185R1 (left) and PBCVs (right) indicated that the binding between these primer sets and target genes were specific.

Table B-1. UV254 dose-response behavior of PBCV-1

Table B-1. UV254 dose-response behavior of PBCV-1						
	Dose	Concentration	Standard	Dose	Concentration	Standard
	(mJ/cm ²)	(PFU/mL)	deviation (PFU/mL)	(mJ/cm ²)	(PFU/mL)	deviation (PFU/mL)
Results of Plaque assay	0	3.67E+07	9.07E+06	0	3.20E+07	3.61E+06
	40	4.63E+05	2.19E+05	20	1.80E+06	7.37E+05
	80	1.70E+04	6.56E+03	60	2.70E+04	4.36E+03
	120	1.80E+03	7.81E+02	100	4.32E+03	1.19E+03
	160	<i>1.00E+02</i>	<i>0.00E+00</i>	140	<i>1.00E+02</i>	<i>0.00E+00</i>
	200	<i>1.00E+02</i>	<i>0.00E+00</i>	180	<i>1.00E+02</i>	<i>0.00E+00</i>
	240	<i>1.00E+02</i>	<i>0.00E+00</i>			
	280	<i>1.00E+02</i>	<i>0.00E+00</i>			
	Dose	Concentration	Standard	Dose	Concentration	Standard
	(mJ/cm ²)	(gene copies/mL)	deviation (gene copies/mL)	(mJ/cm ²)	(gene copies/mL)	deviation (gene copies/mL)
Results of qPCR	0	1.35E+07	3.97E+06	0	2.43E+07	4.78E+06
	40	3.84E+06	1.82E+06	20	1.15E+07	2.07E+06
	80	2.30E+06	6.67E+05	60	2.98E+06	9.18E+05
	120	8.77E+05	6.10E+05	100	1.20E+06	6.84E+05
	160	2.30E+05	9.20E+04	140	1.14E+06	3.27E+05
	200	2.24E+05	1.32E+05	180	5.62E+05	1.37E+05
	240	2.23E+05	1.09E+05			
	280	1.35E+05	7.86E+04			

UV₂₅₄ dose-response behavior of PBCV-1, as measured with both plaque assay and qPCR using primer set of PBCVs. Numerical values in italics and shaded indicate observations below the detection limit. Note that the full range of UV₂₅₄ doses was applied in two separate exposure experiments, with the first experiment comprising UV₂₅₄ doses of 0, 40, 80, 120, 160, 200, 240, and 280 mJ/cm², while the second experiment comprised UV₂₅₄ doses of 0, 20, 60, 100, 140, and 180 mJ/cm².

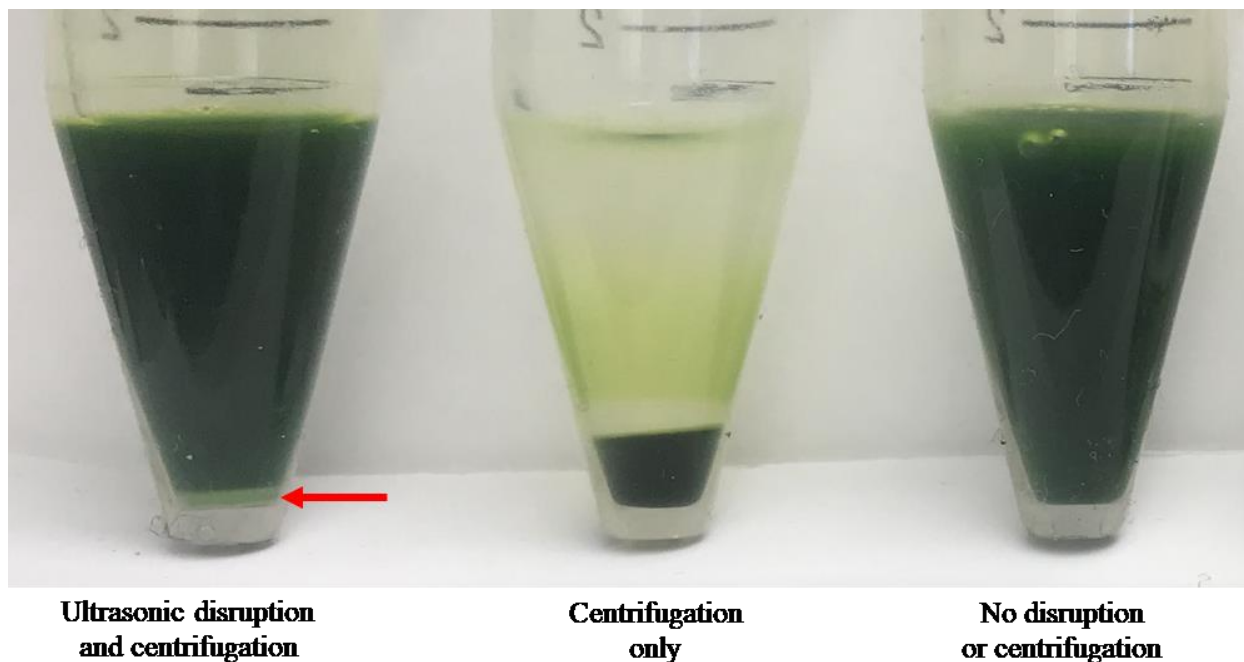
APPENDIX C. SUPPORTING INFORMATION FOR CHAPTER 4

Figure C-1. Release of intracellular materials after sonication treatment.

The white pellet (indicated by red arrow) in left vial indicated that intracellular materials were mostly released after sonication as undisrupted pellet showed green color (mid vial).

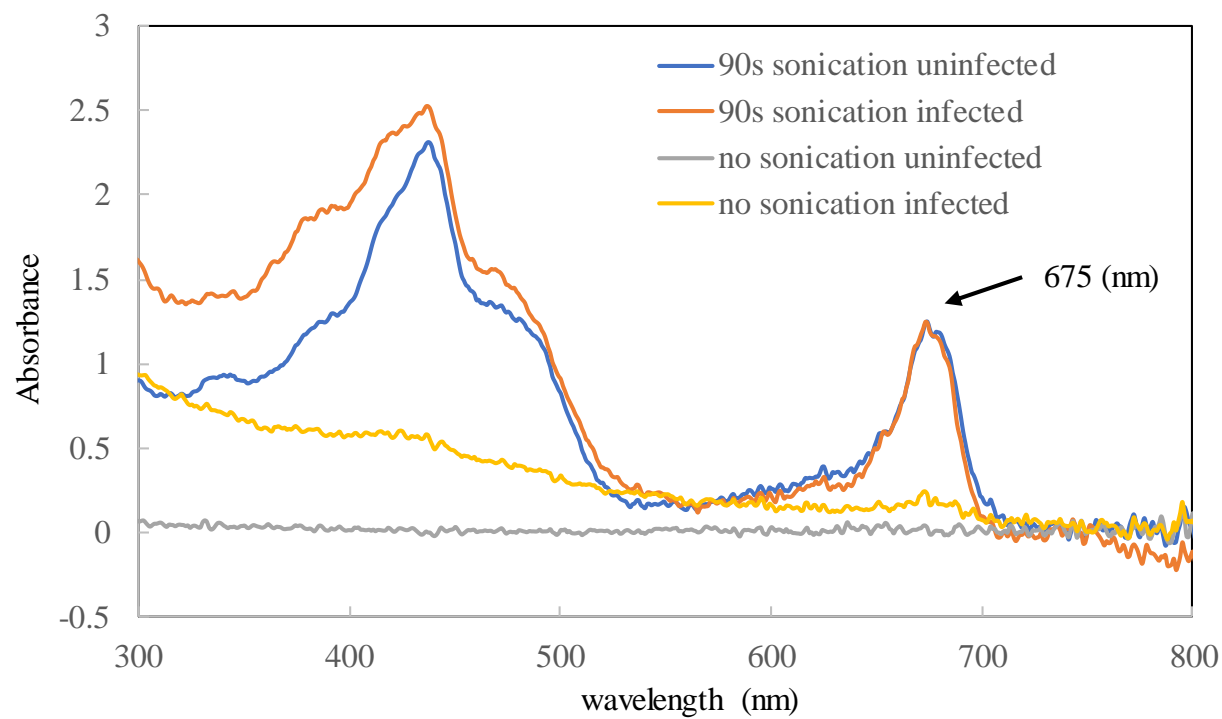


Figure C-2. Absorbance spectrum of supernatant after different treatments.

The peak at 675 nm was used to quantify chlorophyll released from algal cells.

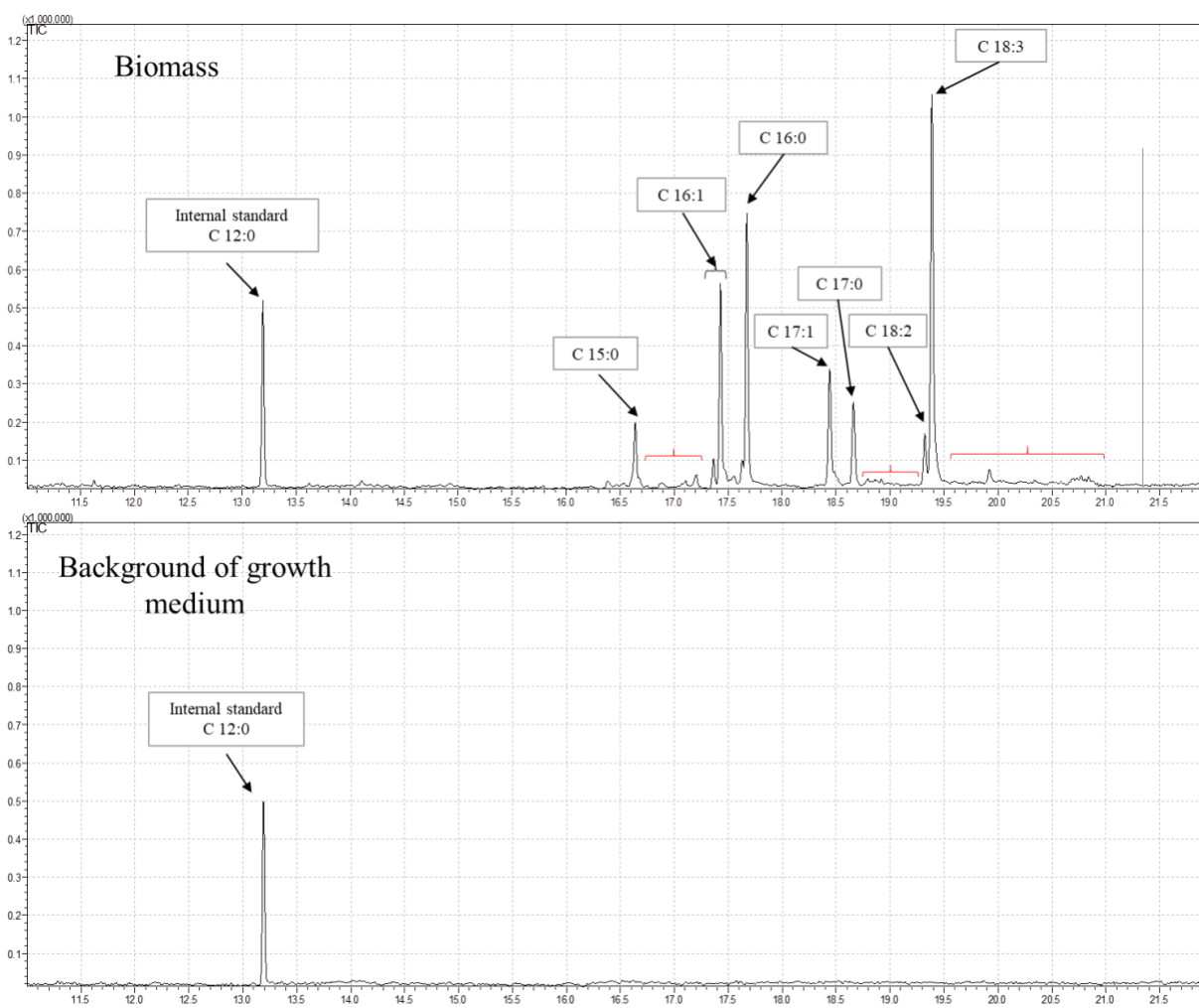


Figure C-3. Mass spectrum of fatty acids extracted from biomass and background of growth medium.

Peaks attributed to the internal standard and the detected FAME compounds are shown with black arrows, while red brackets indicate unidentified FAMES.

REFERENCES

- Adam, F., Abert-Vian, M., Peltier, G., & Chemat, F. (2012). "Solvent-free" ultrasound-assisted extraction of lipids from fresh microalgae cells: A green, clean and scalable process. *Bioresource Technology*, *114*, 457-465
- Al-lwayzy, S. H., Yusaf, T., & Al-Juboori, R. A. (2014). Biofuels from the fresh water microalgae *Chlorella vulgaris* (fwm-cv) for diesel engines. *Energies*, *7*(3), 1829-1851
- Alam, F., Date, A., Rasjidin, R., Mobin, S., Moria, H., & Baqui, A. (2012). Biofuel from algae-is it a viable alternative? *Procedia Engineering*, *49*, 221-227
- Bartley, M. L., Boeing, W. J., Corcoran, A. A., Holguin, F. O., & Schaub, T. (2013). Effects of salinity on growth and lipid accumulation of biofuel microalga *Nannochloropsis salina* and invading organisms. *Biomass and Bioenergy*, *54*, 83-88
- Baudoux, A. C., & Brussaard, C. P. (2005). Characterization of different viruses infecting the marine harmful algal bloom species *Phaeocystis globosa*. *Virology*, *341*(1), 80-90
- Beck, S. E., Rodriguez, R. A., Linden, K. G., Hargy, T. M., Larason, T. C., & Wright, H. B. (2013). Wavelength dependent uv inactivation and DNA damage of adenovirus as measured by cell culture infectivity and long range quantitative pcr. *Environmental Science & Technology*, *48*(1), 591-598
- Becker, E. W. (1994). *Microalgae: Biotechnology and microbiology* (Vol. 10): Cambridge University Press.
- Belay, A. (1997). Mass culture of spirulina outdoors—the earthrise farms experience. *Spirulina Platensis*, 131-158
- Belosevic, M., Guy, R., Taghi-Kilani, R., Neumann, N., Gyürék, L., Liyanage, L., . . . Finch, G. (1997). Nucleic acid stains as indicators of *Cryptosporidium parvum* oocyst viability. *International Journal for Parasitology*, *27*(7), 787-798
- Besaratinia, A., Yoon, J.-i., Schroeder, C., Bradforth, S. E., Cockburn, M., & Pfeifer, G. P. (2011). Wavelength dependence of ultraviolet radiation-induced DNA damage as determined by laser irradiation suggests that cyclobutane pyrimidine dimers are the principal DNA lesions produced by terrestrial sunlight. *The FASEB Journal*, *25*(9), 3079-3091
- Blatchley, E. R. (1997). Numerical modelling of uv intensity: Application to collimated-beam reactors and continuous-flow systems. *Water Research*, *31*(9), 2205-2218

- Blatchley, E. R., Dumoutier, N., Halaby, T., Levi, Y., & Lane, J. (2001). Bacterial responses to ultraviolet irradiation. *Water Science and Technology*, 43(10), 179-186
- Bligh, E. G., & Dyer, W. J. (1959). A rapid method of total lipid extraction and purification. *Canadian Journal of Biochemistry and Physiology*, 37(8), 911-917
- Bohrerova, Z., Shemer, H., Lantis, R., Impellitteri, C. A., & Linden, K. G. (2008). Comparative disinfection efficiency of pulsed and continuous-wave uv irradiation technologies. *Water Research*, 42(12), 2975-2982
- Bolton, J. R., & Linden, K. G. (2003). Standardization of methods for fluence (uv dose) determination in bench-scale uv experiments. *Journal of Environmental Engineering*, 129(3), 209-215
- Bratbak, G., Egge, J. K., & Heldal, M. (1993). Viral mortality of the marine alga *emiliana huxleyi* (haptophyceae) and termination of algal blooms. *Marine Ecology Progress Series*
- Brennan, L., & Owende, P. (2010). Biofuels from microalgae—a review of technologies for production, processing, and extractions of biofuels and co-products. *Renewable and Sustainable Energy Reviews*, 14(2), 557-577
- Brussaard, C. P. (2004). Viral control of phytoplankton populations—a review. *Journal of Eukaryotic Microbiology*, 51(2), 125-138
- Carlton, J., Reid, D., & van Leeuwen, H. (1993). The role of shipping in the introduction of non-indigenous organisms to the coastal waters of the united states and the analysis of control options. *National Sea Grant Project R/ES6 USA*, 213
- Cervero-Aragó, S., Sommer, R., & Araujo, R. M. (2014). Effect of uv irradiation (253.7 nm) on free legionella and legionella associated with its amoebae hosts. *Water Research*, 67, 299-309
- Chen, H., Zhou, D., Luo, G., Zhang, S., & Chen, J. (2015). Macroalgae for biofuels production: Progress and perspectives. *Renewable and Sustainable Energy Reviews*, 47, 427-437
- Chen, L., Li, R., Ren, X., & Liu, T. (2016). Improved aqueous extraction of microalgal lipid by combined enzymatic and thermal lysis from wet biomass of *nannochloropsis oceanica*. *Bioresource Technology*, 214, 138-143
- Chen, L., Liu, T., Zhang, W., Chen, X., & Wang, J. (2012). Biodiesel production from algae oil high in free fatty acids by two-step catalytic conversion. *Bioresource Technology*, 111, 208-214

- Chen, Z., Zhang, B., Zhang, J., Lei, X., Zhang, H., Li, Y., . . . Boughner, L. A. (2015). A lytic bacterium's potential application in biofuel production through directly lysing the diatom *Phaeodactylum tricornerum* cell. *Algal Research*, *12*, 197-205
- Cheng, Y.-S., Zheng, Y., Labavitch, J. M., & VanderGheynst, J. S. (2013). Virus infection of *Chlorella variabilis* and enzymatic saccharification of algal biomass for bioethanol production. *Bioresource Technology*, *137*, 326-331
- Chevrefils, G., Caron, É., Wright, H., Sakamoto, G., Payment, P., Barbeau, B., & Cairns, B. (2006). Uv dose required to achieve incremental log inactivation of bacteria, protozoa and viruses. *IUVA News*, *8*(1), 38-45
- Chiamonti, D., Prussi, M., Buffi, M., Rizzo, A. M., & Pari, L. (2017). Review and experimental study on pyrolysis and hydrothermal liquefaction of microalgae for biofuel production. *Applied Energy*, *185*, 963-972
- Chisti, Y. (2007). Biodiesel from microalgae. *Biotechnology Advances*, *25*(3), 294-306
- Chisti, Y. (2008). Biodiesel from microalgae beats bioethanol. *Trends in Biotechnology*, *26*(3), 126-131
- Chiu, K., Lyn, D. A., Savoye, P., & Blatchley III, E. R. (1999). Integrated uv disinfection model based on particle tracking. *Journal of Environmental Engineering*, *125*(1), 7-16
- Clauß, M. (2006). Higher effectiveness of photoinactivation of bacterial spores, uv resistant vegetative bacteria and mold spores with 222 nm compared to 254 nm wavelength. *Acta Hydrochimica et Hydrobiologica*, *34*(6), 525-532
- Clesceri, L. S. G., Eaton, A. E., Rice, A. D., Franson, E. W., & Mary Ann, H. (2005). *Standard methods for the examination of water and wastewater*.
- Coons, J. E., Kalb, D. M., Dale, T., & Marrone, B. L. (2014). Getting to low-cost algal biofuels: A monograph on conventional and cutting-edge harvesting and extraction technologies. *Algal Research*, *6*, 250-270
- Day, J. G., Slocumbe, S. P., & Stanley, M. S. (2012). Overcoming biological constraints to enable the exploitation of microalgae for biofuels. *Bioresource Technology*, *109*, 245-251
- Doucha, J., Straka, F., & Lívanský, K. (2005). Utilization of flue gas for cultivation of microalgae (*Chlorella* sp.) in an outdoor open thin-layer photobioreactor. *Journal of Applied Phycology*, *17*(5), 403-412

- Etten, J. L. V. (2003). Unusual life style of giant chlorella viruses. *Annual Review of Genetics*, 37(1), 153-195
- Fuhrman, J. A. (1999). Marine viruses and their biogeochemical and ecological effects. *Nature*, 399(6736), 541-548
- Gachon, C. M., Sime-Ngando, T., Strittmatter, M., Chambouvet, A., & Kim, G. H. (2010). Algal diseases: Spotlight on a black box. *Trends in Plant Science*, 15(11), 633-640
- Gastrich, M. D., Leigh-Bell, J. A., Gobler, C. J., Roger Anderson, O., Wilhelm, S. W., & Bryan, M. (2004). Viruses as potential regulators of regional brown tide blooms caused by the alga, *aureococcus anophagefferens*. *Estuaries*, 27(1), 112-119
- Gerde, J. A., Montalbo-Lomboy, M., Yao, L., Grewell, D., & Wang, T. (2012). Evaluation of microalgae cell disruption by ultrasonic treatment. *Bioresource Technology*, 125, 175-181
- Gilcreas, F. (1966). Standard methods for the examination of water and waste water. *American Journal of Public Health and the Nations Health*, 56(3), 387
- Gonzalez, L. E., & Bashan, Y. (2000). Increased growth of the microalga *chlorella vulgaris* when coimmobilized and cocultured in alginate beads with the plant-growth-promoting bacterium *azospirillum brasilense*. *Applied and Environmental Microbiology*, 66(4), 1527-1531
- Greenly, J. M., & Tester, J. W. (2015). Ultrasonic cavitation for disruption of microalgae. *Bioresource Technology*, 184, 276-279
- Greiner, T., Frohns, F., Kang, M., Van Etten, J. L., Käsmann, A., Moroni, A., . . . Thiel, G. (2009). *Chlorella* viruses prevent multiple infections by depolarizing the host membrane. *Journal of General Virology*, 90(8), 2033-2039
- Gupta, P. L., Lee, S.-M., & Choi, H.-J. (2016). Integration of microalgal cultivation system for wastewater remediation and sustainable biomass production. *World Journal of Microbiology and Biotechnology*, 32(8), 1-11
- Häder, D.-P. (2011). Ultraviolet effects on phytoplankton. Retrieved from <http://photobiology.info/Hader.html>
- Halim, R., Danquah, M. K., & Webley, P. A. (2012). Extraction of oil from microalgae for biodiesel production: A review. *Biotechnology Advances*, 30(3), 709-732
- Hargy, T. M., Clancy, J. L., Bukhari, Z., & Marshall, M. M. (2000). Shedding uv light on the cryptosporidium threat. *Journal of Environmental Health*, 63(1), 19

- Harm, W. (1980). Biological effects of ultraviolet radiation.
- Harrison, S. T. (1991). Bacterial cell disruption: A key unit operation in the recovery of intracellular products. *Biotechnology Advances*, 9(2), 217-240
- Hijnen, W., Beerendonk, E., & Medema, G. J. (2006). Inactivation credit of uv radiation for viruses, bacteria and protozoan (oo) cysts in water: A review. *Water Research*, 40(1), 3-22
- IMO. (2008). Guidelines for approval of ballast water management systems (g8). In: International Maritime Organization, London, UK.
- Joannes, C., Sipaut, C. S., Dayou, J., Yasir, S. M., & Mansa, R. F. (2015). The potential of using pulsed electric field (pef) technology as the cell disruption method to extract lipid from microalgae for biodiesel production. *International Journal of Renewable Energy Research (IJRER)*, 5(2), 598-621
- Karentz, D., McEuen, F. S., Land, M. C., & Dunlap, W. C. (1991). Survey of mycosporine-like amino acid compounds in antarctic marine organisms: Potential protection from ultraviolet exposure. *Marine Biology*, 108(1), 157-166
- Katsanevakis, S., Zenetos, A., Belchior, C., & Cardoso, A. C. (2013). Invading european seas: Assessing pathways of introduction of marine aliens. *Ocean & Coastal Management*, 76, 64-74
- Kim, B.-H., Ramanan, R., Cho, D.-H., Oh, H.-M., & Kim, H.-S. (2014). Role of rhizobium, a plant growth promoting bacterium, in enhancing algal biomass through mutualistic interaction. *Biomass and Bioenergy*, 69, 95-105
- Kim, D.-Y., Vijayan, D., Praveenkumar, R., Han, J.-I., Lee, K., Park, J.-Y., . . . Oh, Y.-K. (2016). Cell-wall disruption and lipid/astaxanthin extraction from microalgae: *Chlorella* and *haematococcus*. *Bioresource Technology*, 199, 300-310
- Kim, J., Yoo, G., Lee, H., Lim, J., Kim, K., Kim, C. W., . . . Yang, J.-W. (2013). Methods of downstream processing for the production of biodiesel from microalgae. *Biotechnology Advances*, 31(6), 862-876
- Kirrolia, A., Bishnoi, N. R., & Singh, R. (2013). Microalgae as a boon for sustainable energy production and its future research & development aspects. *Renewable and Sustainable Energy Reviews*, 20, 642-656
- Lam, M. K., & Lee, K. T. (2012). Microalgae biofuels: A critical review of issues, problems and the way forward. *Biotechnology Advances*, 30(3), 673-690

- Lammers, P. J., Huesemann, M., Boeing, W., Anderson, D. B., Arnold, R. G., Bai, X., . . . Brown, J. (2017). Review of the cultivation program within the national alliance for advanced biofuels and bioproducts. *Algal Research*, 22, 166-186
- Lardon, L., Helias, A., Sialve, B., Steyer, J.-P., & Bernard, O. (2009). Life-cycle assessment of biodiesel production from microalgae. *Environmental Science & Technology*, 43(17), 6475-6481
- Larsen, J. B., Larsen, A., Thyraug, R., Bratbak, G., & Sandaa, R.-A. (2008). Response of marine viral populations to a nutrient induced phytoplankton bloom at different pCO₂ levels. *Biogeosciences*, 5(2), 523-533
- Lawrence, J. E. (2008). Furtive foes: Algal viruses as potential invaders. *Ices Journal of Marine Science*, 65(5), 716-722
- Lee, J.-Y., Yoo, C., Jun, S.-Y., Ahn, C.-Y., & Oh, H.-M. (2010). Comparison of several methods for effective lipid extraction from microalgae. *Bioresource Technology*, 101(1), S75-S77
- Lehahn, Y., Koren, I., Schatz, D., Frada, M., Sheyn, U., Boss, E., . . . Vardi, A. (2014). Decoupling physical from biological processes to assess the impact of viruses on a mesoscale algal bloom. *Current Biology*, 24(17), 2041-2046
- Li, Q., Du, W., & Liu, D. (2008). Perspectives of microbial oils for biodiesel production. *Applied Microbiology and Biotechnology*, 80(5), 749-756
- Liltved, H., Vogelsang, C., Modahl, I., & Dannevig, B. (2006). High resistance of fish pathogenic viruses to uv irradiation and ozonated seawater. *Aquacultural Engineering*, 34(2), 72-82
- Long, A. M., & Short, S. M. (2016). Seasonal determinations of algal virus decay rates reveal overwintering in a temperate freshwater pond. *The ISME journal*, 10(7), 1602-1612
- MacIntyre, H. L., & Cullen, J. J. (2016). Classification of phytoplankton cells as live or dead using the vital stains fluorescein diacetate and 5-chloromethylfluorescein diacetate. *Journal of Phycology*
- Malayeri, A. H., Mohseni, M., Cairns, B., Bolton, J. R., Chevrefils, G., Caron, E., . . . Linden, K. G. (2016). Fluence (uv dose) required to achieve incremental log inactivation of bacteria, protozoa, viruses and algae. *IUVA News*, 18(3), 4-6
- Malitsky, S., Ziv, C., Rosenwasser, S., Zheng, S., Schatz, D., Porat, Z., . . . Vardi, A. (2016). Viral infection of the marine alga *emiliana huxleyi* triggers lipidome remodeling and induces the production of highly saturated triacylglycerol. *New Phytologist*, 210(1), 88-96

- Mamane-Gravetz, H., Linden, K. G., Cabaj, A., & Sommer, R. (2005). Spectral sensitivity of bacillus subtilis spores and ms2 coliphage for validation testing of ultraviolet reactors for water disinfection. *Environmental Science & Technology*, 39(20), 7845-7852
- Mbonimpa, E. G., Vadheim, B., & Blatchley, E. R. (2012). Continuous-flow solar uvb disinfection reactor for drinking water. *Water Research*, 46(7), 2344-2354
- McCrary, M. H. (1915). The numerical interpretation of fermentation-tube results. *The Journal of Infectious Diseases*, 183-212
- McGuigan, K. G., Conroy, R. M., Mosler, H.-J., du Preez, M., Ubomba-Jaswa, E., & Fernandez-Ibanez, P. (2012). Solar water disinfection (sodis): A review from bench-top to roof-top. *Journal of Hazardous Materials*, 235, 29-46
- McKinney, C. W., & Pruden, A. (2012). Ultraviolet disinfection of antibiotic resistant bacteria and their antibiotic resistance genes in water and wastewater. *Environmental Science & Technology*, 46(24), 13393-13400
- Mead, A., Carlton, J. T., Griffiths, C. L., & Rius, M. (2011). Revealing the scale of marine bioinvasions in developing regions: A south african re-assessment. *Biological Invasions*, 13(9), 1991-2008
- Meints, R. H., Lee, K., Burbank, D. E., & Van Etten, J. L. (1984). Infection of a chlorella-like alga with the virus, pbcv-1: Ultrastructural studies. *Virology*, 138(2), 341-346
- Meints, R. H., Lee, K., & Van Etten, J. L. (1986). Assembly site of the virus pbcv-1 in a chlorella-like green alga: Ultrastructural studies. *Virology*, 154(1), 240-245
- Meng, X., Yang, J., Xu, X., Zhang, L., Nie, Q., & Xian, M. (2009). Biodiesel production from oleaginous microorganisms. *Renewable Energy*, 34(1), 1-5
- Milano, J., Ong, H. C., Masjuki, H., Chong, W., Lam, M. K., Loh, P. K., & Vellayan, V. (2016). Microalgae biofuels as an alternative to fossil fuel for power generation. *Renewable and Sustainable Energy Reviews*, 58, 180-197
- Mitchell, S., & Richmond, A. (1987). The use of rotifers for the maintenance of monoalgal mass cultures of spirulina. *Biotechnology and Bioengineering*, 30(2), 164-168
- Moreno-Garrido, I., & Cañavate, J. P. (2001). Assessing chemical compounds for controlling predator ciliates in outdoor mass cultures of the green algae dunaliella salina. *Aquacultural Engineering*, 24(2), 107-114

- Nagarajan, S., Chou, S. K., Cao, S., Wu, C., & Zhou, Z. (2013). An updated comprehensive techno-economic analysis of algae biodiesel. *Bioresource Technology*, *145*, 150-156
- Ng, W.-O., & Pakrasi, B. H. (2001). DNA photolyase homologs are the major uv resistance factors in the cyanobacterium *synechocystis* sp. Pcc 6803. *Molecular and General Genetics MGG*, *264*(6), 924-931
- NWRI, N. W. R. I. (2012). *Ultraviolet disinfection: Guidelines for drinking water and reuse*. Retrieved from
- Olsen, R. O., Hess-Erga, O.-K., Larsen, A., Thuestad, G., Tobiesen, A., & Hoell, I. A. (2015). Flow cytometric applicability to evaluate uv inactivation of phytoplankton in marine water samples. *Marine Pollution Bulletin*, *96*(1), 279-285
- Olsen, R. O., Hoffmann, F., Hess-Erga, O.-K., Larsen, A., Thuestad, G., & Hoell, I. A. (2016). Ultraviolet radiation as a ballast water treatment strategy: Inactivation of phytoplankton measured with flow cytometry. *Marine Pollution Bulletin*, *103*(1-2), 270-275
- Orr, V. C., Plechkova, N. V., Seddon, K. R., & Rehmann, L. (2015). Disruption and wet extraction of the microalgæ *chlorella vulgaris* using room-temperature ionic liquids. *ACS Sustainable Chemistry & Engineering*
- Ou, H., Gao, N., Deng, Y., Qiao, J., & Wang, H. (2012). Immediate and long-term impacts of uv-c irradiation on photosynthetic capacity, survival and microcystin-lr release risk of *microcystis aeruginosa*. *Water Research*, *46*(4), 1241-1250
- Ou, H., Gao, N., Deng, Y., Wang, H., & Zhang, H. (2011). Inactivation and degradation of *microcystisaeruginosa* by uv-c irradiation. *Chemosphere*, *85*(7), 1192-1198
- Pan, J., Muppaneni, T., Sun, Y., Reddy, H. K., Fu, J., Lu, X., & Deng, S. (2016). Microwave-assisted extraction of lipids from microalgae using an ionic liquid solvent [bmim][hso 4]. *Fuel*, *178*, 49-55
- Pecson, B. M., Ackermann, M., & Kohn, T. (2011). Framework for using quantitative pcr as a nonculture based method to estimate virus infectivity. *Environmental Science & Technology*, *45*(6), 2257-2263
- Pecson, B. M., Martin, L. V., & Kohn, T. (2009). Quantitative pcr for determining the infectivity of bacteriophage ms2 upon inactivation by heat, uv-b radiation, and singlet oxygen: Advantages and limitations of an enzymatic treatment to reduce false-positive results. *Applied and Environmental Microbiology*, *75*(17), 5544-5554

- Post, F., Borowitzka, L., Borowitzka, M., Mackay, B., & Moulton, T. (1983). The protozoa of a western australian hypersaline lagoon. *Hydrobiologia*, *105*(1), 95-113
- Rawat, I., Kumar, R. R., Mutanda, T., & Bux, F. (2013). Biodiesel from microalgae: A critical evaluation from laboratory to large scale production. *Applied Energy*, *103*, 444-467
- Reitan, K. I., Rainuzzo, J. R., & Olsen, Y. (1994). Effect of nutrient limitation on fatty acid and lipid content of marine microalgae. *Journal of Phycology*, *30*(6), 972-979
- Richmond, A. (2008). *Handbook of microalgal culture: Biotechnology and applied phycology*: John Wiley & Sons.
- Rodolfi, L., Chini Zittelli, G., Bassi, N., Padovani, G., Biondi, N., Bonini, G., & Tredici, M. R. (2009). Microalgae for oil: Strain selection, induction of lipid synthesis and outdoor mass cultivation in a low-cost photobioreactor. *Biotechnology and Bioengineering*, *102*(1), 100-112
- Rosenwasser, S., Mausz, M. A., Schatz, D., Sheyn, U., Malitsky, S., Aharoni, A., . . . Feldmesser, E. (2014). Rewiring host lipid metabolism by large viruses determines the fate of emiliania huxleyi, a bloom-forming alga in the ocean. *The Plant Cell*, tpc. 114.125641
- Sakai, H., Katayama, H., Oguma, K., & Ohgaki, S. (2011). Effect of photoreactivation on ultraviolet inactivation of microcystis aeruginosa. *Water Science and Technology*, *63*(6), 1224-1229
- Sander, K., & Murthy, G. S. (2010). Life cycle analysis of algae biodiesel. *The International Journal of Life Cycle Assessment*, *15*(7), 704-714
- Sanmukh, S. G., Khairnar, K., Chandekar, R. H., & Paunekar, W. N. (2014). Increasing the extraction efficiency of algal lipid for biodiesel production: Novel application of algal viruses. *African Journal of Biotechnology*, *13*(15)
- Santos, A. L., Moreirinha, C., Lopes, D., Esteves, A. C., Henriques, I., Almeida, A., . . . Cunha, A. n. (2013). Effects of uv radiation on the lipids and proteins of bacteria studied by mid-infrared spectroscopy. *Environmental Science & Technology*, *47*(12), 6306-6315
- Sathish, A., & Sims, R. C. (2012). Biodiesel from mixed culture algae via a wet lipid extraction procedure. *Bioresource Technology*, *118*, 643-647
- Satyanarayana, K., Mariano, A., & Vargas, J. (2011). A review on microalgae, a versatile source for sustainable energy and materials. *International Journal of Energy Research*, *35*(4), 291-311

- Sawangkeaw, R., & Ngamprasertsith, S. (2013). A review of lipid-based biomasses as feedstocks for biofuels production. *Renewable and Sustainable Energy Reviews*, *25*, 97-108
- Shoaf, W. T., & Lium, B. W. (1976). Improved extraction of chlorophyll a and b from algae using dimethyl sulfoxide. *Limnology and Oceanography*, *21*(6), 926-928
- Short, S. M. (2012). The ecology of viruses that infect eukaryotic algae. *Environmental Microbiology*, *14*(9), 2253-2271
- Short, S. M., Rusanova, O., & Staniewski, M. A. (2011). Novel phycodnavirus genes amplified from canadian freshwater environments. *Aquatic Microbial Ecology*, *63*(1), 61-67
- Shunyu, S., Yongding, L., Yinwu, S., Genbao, L., & Dunhai, L. (2006). Lysis of aphanizomenon flos-aquae (cyanobacterium) by a bacterium bacillus cereus. *Biological Control*, *39*(3), 345-351
- Shwetharani, R., & Balakrishna, R. G. (2016). Efficient algal lipid extraction via photocatalysis and its conversion to biofuel. *Applied Energy*, *168*, 364-374
- Sierra, L. S., Dixon, C. K., & Wilken, L. R. (2017). Enzymatic cell disruption of the microalgae chlamydomonas reinhardtii for lipid and protein extraction. *Algal Research*, *25*, 149-159
- Sommer, R., Cabaj, A., Haider, T., & Hirschmann, G. (2004). Uv drinking water disinfection—requirements, testing and surveillance: Exemplified by the austrian national standards m 5873-1 and m 5873-2. *IUVA News*, *6*(4), 27-35
- Steichen, J. L., Windham, R., Brinkmeyer, R., & Quigg, A. (2012). Ecosystem under pressure: Ballast water discharge into galveston bay, texas (USA) from 2005 to 2010. *Marine Pollution Bulletin*, *64*(4), 779-789
- Steriti, A., Rossi, R., Concas, A., & Cao, G. (2014). A novel cell disruption technique to enhance lipid extraction from microalgae. *Bioresource Technology*, *164*, 70-77
- Sun, Z., & Blatchley III, E. R. (2017). Tetraselmis as a challenge organism for validation of ballast water uv systems. *Water Research*, *121*, 311-319
- Suttle, C. A., & Chan, A. M. (1994). Dynamics and distribution of cyanophages and their effect on marine synechococcus spp. *Applied and Environmental Microbiology*, *60*(9), 3167-3174
- Taher, H., Al-Zuhair, S., Al-Marzouqi, A. H., Haik, Y., & Farid, M. (2014). Effective extraction of microalgae lipids from wet biomass for biodiesel production. *Biomass and Bioenergy*, *66*, 159-167

- Tanzi, C. D., Vian, M. A., & Chemat, F. (2013). New procedure for extraction of algal lipids from wet biomass: A green clean and scalable process. *Bioresource Technology*, *134*, 271-275
- Teo, C. L., Jamaluddin, H., Zain, N. A. M., & Idris, A. (2014). Biodiesel production via lipase catalysed transesterification of microalgae lipids from tetraselmis sp. *Renewable Energy*, *68*, 1-5
- Tica, S., Filipović, S., Živanović, P., & Milovanović, B. (2010). Test run of biodiesel in public transport system in belgrade. *Energy Policy*, *38*(11), 7014-7020
- Tsolaki, E., & Diamadopoulos, E. (2010). Technologies for ballast water treatment: A review. *Journal of Chemical Technology and Biotechnology*, *85*(1), 19-32
- USEPA. (2006). Ultraviolet disinfection guidance manual for the final long term 2 enhanced surface water treatment rule. In: US Environmental Protection Agency Washington, DC.
- Valizadeh Derakhshan, M., Nasernejad, B., Dadvar, M., & Hamidi, M. (2014). Pretreatment and kinetics of oil extraction from algae for biodiesel production. *Asia-Pacific Journal of Chemical Engineering*, *9*(5), 629-637
- Van Etten, J. L., Burbank, D. E., Kuczmarski, D., & Meints, R. H. (1983). Virus infection of culturable chlorella-like algae and development of a plaque assay. *Science*, *219*(4587), 994-996
- Van Etten, J. L., Burbank, D. E., Schuster, A. M., & Meints, R. H. (1985). Lytic viruses infecting a chlorella-like alga. *Virology*, *140*(1), 135-143
- Van Etten, J. L., Burbank, D. E., Xia, Y., & Meints, R. H. (1983). Growth cycle of a virus, pbcv-1, that infects chlorella-like algae. *Virology*, *126*(1), 117-125
- Van Etten, J. L., & Dunigan, D. D. (2012). Chloroviruses: Not your everyday plant virus. *Trends in Plant Science*, *17*(1), 1-8
- Van Etten, J. L., Van Etten, C. H., Johnson, J., & Burbank, D. (1985). A survey for viruses from fresh water that infect a eucaryotic chlorella-like green alga. *Applied and Environmental Microbiology*, *49*(5), 1326-1328
- Villacorte, L. O., Tabatabai, S. A. A., Anderson, D. M., Amy, G. L., Schippers, J. C., & Kennedy, M. D. (2015). Seawater reverse osmosis desalination and (harmful) algal blooms. *Desalination*, *360*, 61-80
- Walker, T. L., Purton, S., Becker, D. K., & Collet, C. (2005). Microalgae as bioreactors. *Plant cell reports*, *24*(11), 629-641

- Wang, G., & Wang, T. (2011). Lipid and biomass distribution and recovery from two microalgae by aqueous and alcohol processing. *Journal of the American Oil Chemists' Society*, 89(2), 335-345
- Wang, M., Yuan, W., Jiang, X., Jing, Y., & Wang, Z. (2014). Disruption of microalgal cells using high-frequency focused ultrasound. *Bioresource Technology*, 153, 315-321
- Ware, M. W., Augustine, S. A., Erisman, D. O., See, M. J., Wymer, L., Hayes, S. L., . . . Villegas, E. N. (2010). Determining uv inactivation of toxoplasma gondii oocysts by using cell culture and a mouse bioassay. *Applied and Environmental Microbiology*, 76(15), 5140-5147
- Wilson, B. (1992). *Coliphage ms-2 as a uv water disinfection efficacy test surrogate for bacterial and viral pathogens*. Paper presented at the Proc. of the AWWA Water Quality Technology Conference. Toronto, Ont., AWWA, 1992.
- Xin, L., Hong-ying, H., Ke, G., & Ying-xue, S. (2010). Effects of different nitrogen and phosphorus concentrations on the growth, nutrient uptake, and lipid accumulation of a freshwater microalga *scenedesmus* sp. *Bioresource Technology*, 101(14), 5494-5500
- Xu, L., Brillman, D. W. W., Withag, J. A., Brem, G., & Kersten, S. (2011). Assessment of a dry and a wet route for the production of biofuels from microalgae: Energy balance analysis. *Bioresource Technology*, 102(8), 5113-5122
- Yamada, T., Higashiyama, T., & Fukuda, T. (1991). Screening of natural waters for viruses which infect *chlorella* cells. *Applied and Environmental Microbiology*, 57(12), 3433-3437
- Yoo, G., Park, W.-K., Kim, C. W., Choi, Y.-E., & Yang, J.-W. (2012). Direct lipid extraction from wet *chlamydomonas reinhardtii* biomass using osmotic shock. *Bioresource Technology*, 123, 717-722
- Yun, M., Oh, Y.-K., Praveenkumar, R., Seo, Y.-S., & Cho, S. (2017). Contaminated bacterial effects and qpcr application to monitor a specific bacterium in *chlorella* sp. Kr-1 culture. *Biotechnology and Bioprocess Engineering*, 22(2), 150-160
- Zhang, Q., Zhan, J.-j., & Hong, Y. (2015). The effects of temperature on the growth, lipid accumulation and nutrient removal characteristics of *chlorella* sp. Hq. *Desalination and Water Treatment*, 1-6